UC Santa Barbara

UC Santa Barbara Electronic Theses and Dissertations

Title

Cosmogenic S-35 as an Intrinsic Hydrologic Tracer for Young Groundwater in Mountain Basins and Managed Aquifer Recharge Facilities

Permalink

https://escholarship.org/uc/item/4fq8b5jk

Author

Uriostegui, Stephanie Haydee

Publication Date

2015

Peer reviewed|Thesis/dissertation

UNIVERSITY OF CALIFORNIA

Santa Barbara

Cosmogenic ^{35}S as an Intrinsic Hydrologic Tracer for Young Groundwater in Mountain

Basins and Managed Aquifer Recharge Facilities

A dissertation submitted in partial satisfaction of the

requirements for the degree Doctor of Philosophy

in Geological Sciences

by

Stephanie Haydeé Urióstegui

Committee in charge:

Professor Jordan F. Clark, Chair

Professor Oliver Chadwick

Professor Christina Tague

Dr. Bradley Esser

March 2015

The dissertation of Stephanie Haydeé Urióstegui is approved.

_____

Oliver Chadwick

_____

Christina Tague

_____

Bradley Esser

_____

Jordan F. Clark, Committee Chair

December 2015

Cosmogenic ^{35}S as an Intrinsic Hydrologic Tracer for Young Groundwater in Mountain

Basins and Managed Aquifer Recharge Facilities

Copyright © 2015

by

Stephanie Haydeé Urióstegui

ACKNOWLEDGEMENTS

VITA OF STEPHANIE HAYDEÉ URIÓSTEGUI
December 2015

EDUCATION

May 2008   Bachelor of Science in Biology, Minor in Chemistry,
California State University, Fullerton

March 2015 Doctor of Philosophy in Geological Sciences,
(expected)   University of California, Santa Barbara

PROFESSIONAL EMPLOYMENT

Summer   Glen T. Seaborg Nuclear Forensics Summer Internship, Lawrence
2010, 2011   Livermore National Laboratory (LLNL)

2009-2012   Graduate Research Assistant and Teaching Assistant, Department of
Earth Science, University of California, Santa Barbara (UCSB)

2012-2015   Lawrence Graduate Scholar, LLNL

PUBLICATIONS

Urióstegui SH, Bibby RK, Esser BK, Clark JF (2015) Analytical method for measuring ^{35}S in natural waters. *Analytical Chemistry*, 87: 6064-6070.

Urióstegui SH, Bibby RK, Esser BK, Clark JF (In Review) Quantifying annual groundwater recharge and storage in the central Sierra Nevada using naturally-occurring ^{35}S.

Urióstegui SH, Bibby RK, Esser BK, Clark JF (In Review) Quantifying groundwater travel time near managed aquifer recharge operations using ^{35}S as an intrinsic tracer.

AWARDS

2011   Fugro West Scholarship, UCSB

2010-2012   LUCE Environmental Science to Solutions Fellowship, UCSB

2014   Best Poster: Biennial Symposium on Managed Aquifer Recharge

2012-2015   Lawrence Graduate Scholar Program, LLNL

FIELDS OF STUDY

Major Field: Geology

Studies in Tracer Hydrology with Professor Jordan Clark

Studies in Environmental Radiochemistry with Dr. Bradley Esser (LLNL)

ABSTRACT

Cosmogenic ^{35}S as an Intrinsic Hydrologic Tracer for Young Groundwater in Mountain

Basins and Managed Aquifer Recharge Facilities

by

Stephanie Haydeé Urióstegui

The current drought crisis in California highlights the vulnerability of freshwater

resources, particularly groundwater reservoirs, which supply up to 60% of California's water

during drought years. Understanding the potential impacts of climate change on

groundwater recharge and storage is critical as drought periods become more frequent in the

state. Groundwater residence times provide insight into groundwater recharge and transport

mechanisms and storage capacities. This study developed and evaluated a new intrinsic

tracer method to quantify groundwater recharge and transport using the occurrence of the

naturally-produced radioisotope sulfur-35 (^{35}S, half-life 87.5 days) in water as dissolved

sulfate ($^{35}SO_4$). Improvements made to established analytical techniques expand the

analytical range of $^{35}SO_4$, which broadens the utility of $^{35}SO_4$ as a hydrologic tracer. The

$^{35}SO_4$ tracer method was applied to two distinct hydrologic settings: 1) high-elevation Sierra

Nevada basins, and 2) low-elevations basins containing managed aquifer recharge (MAR)

facilities.

In the Sierra Nevada study, the new $^{35}SO_4$ method was used to empirically constrain annual groundwater recharge in Sagehen Creek Basin (SCB) and Martis Valley Groundwater Basin (MVGB). Compared to relatively high $^5SO_4$ activity in seasonal snowmelt (5.5 ± 0.3 to 52.9 ± 3.4 mBq/L), groundwater and surface water consistently yielded low $^{35}SO_4$ activities resulting in a calculated percent new snowmelt (PNS) of <30%. The consistently low PNS suggests that recent (<1 year old) snowmelt represents only a small fraction of the larger aquifer system. As snowpack continues to decline due to climate change, streamflow and springs may respond in a two phase manner: rapid response in discharge followed by more gradual decreases over decades due to declines in groundwater recharge.

The MAR study used $^{35}SO_4$ to quantify groundwater travel times near MAR operations. MAR sites divert excess surface water, imported water, and reclaimed wastewater into surface-spreading ponds or direct injection wells to replenish groundwater in heavy-usage areas. Identifying groundwater travel times near MAR facilities is critical for determining the fate and transport of potential contaminants, especially for facilities that incorporate a significant portion of reclaimed wastewater. Successful application of the $^{35}SO_4$ tracer method near MAR sites is dependent on careful characterization of the $^{35}SO_4$ activity in source waters. Relative to established deliberate tracer experiments, which require extensive field and laboratory effort, the less intensive $^{35}SO_4$ technique showed comparable groundwater travel times at two MAR facilities located in southern California. Both the Sierra Nevada and MAR studies demonstrate that $^{35}SO_4$ is a valuable, yet underutilized tracer in hydrologic studies.

TABLE OF CONTENTS

LIST OF FIGURES

LIST OF TABLES

I. Introduction

Physical and geochemical techniques are commonly used to investigate groundwater processes such as recharge rate and residence times, which is important for effectively managing groundwater basins. Physical approaches rely on direct measurements of hydrologic parameters and use mathematical representations of concepts and processes. Geochemical techniques use chemical or isotopic substances to obtain information such as groundwater flow, reactive processes, and groundwater age for various timescales (Clark and Fritz, 1997; Cook and Herczeg, 2000). Advances in geochemical techniques, in particular hydrologic tracers, have expanded our understanding of groundwater processes.

A. Background of Hydrologic Tracers used for Investigating Groundwater Recharge, Storage, and Transport

Geochemical age tracers have been utilized for decades to investigate groundwater recharge, storage, and transport in both high-elevation basins and lowland aquifers (Davis *et al.*, 1980; Clark and Fritz, 1997; Cook and Herczeg, 2000; Glynn and Plummer, 2005). Ideal tracers are soluble, mobile, and behave conservatively (i.e., are non-reactive and do not sorb readily to aquifer material). Two main categories of groundwater age tracers are 1) deliberate tracers (e.g., Davis *et al.*, 1980) and 2) intrinsic tracers (e.g. Phillips and Castro, 2003; Glynn and Plummer, 2005). Deliberate tracers are constituents that are added to water bodies at the surface or subsurface. Intrinsic tracers are present in the environment such as atmospherically-derived radionuclides or stable constituents present in the recharged water with known patterns of age with time.

1

Deliberate tracer experiments require the physical injection of a tracer. Noble gas isotopes of helium, neon, and xenon, and the nonreactive synthetic gas sulfur hexafluoride (SF_6), have frequently been used to resolve groundwater ages on timescales of less than one year in low elevation basins dominated by Managed Aquifer Recharge (MAR) operations (e.g., Clark *et al*., 2004; Moran and Halliwell, 2003; Massman *et al*., 2008; McDermott *et al*., 2008). MAR is the practice of artificially storing water in groundwater basins that have been depleted by local production. Deliberate tracers have also been used in high elevation streams to quantify oxygen reaeration rates in rivers (e.g., Wanninkhof *et al*., 1993; Reid *et al*., 2007; Clark *et al*., 2014). Significant disadvantages to deliberate tracer studies include 1) high analysis costs and 2) extensive fieldwork and laboratory effort. Moreover, while SF_6 has been extensively used in previous deliberate tracer studies, its emission is regulated in California because it is a strong greenhouse gas.

Intrinsic groundwater tracers, such as dissolved gases and isotopic tracers, are useful for characterizing young (<50 year old) groundwater and investigating the vulnerability of aquifers to climate change. Dissolved noble gas concentrations (Ne, Ar, Kr, and Xe) combined with tritium-helium ($^3H/^3He$), chlorofluorocarbons (CFCs), and passive SF_6 age dating have been useful in determining apparent ages of young groundwater in several high-elevation basins including the Central Sierra Nevada (e.g. Rademacher *et al*., 2001; Segal *et al*. 2014; Singleton and Moran, 2010; Manning *et al.*, 2012) and Rocky Mountain Range (Manning and Caine, 2007). These approaches have also been used in a variety of low elevation groundwater basins (e.g., Schlosser *et al.*, 1988; Busenberg and Plummer, 1992, 2000; Ekwurzel *et al.*, 1994; Stute *et al.*, 2007) including a few studies near MAR operations (e.g., Clark *et al.*, 2004; Massmann *et al.,* 2008). Due to analytical uncertainties being greater than or equal to one year for these commonly utilized intrinsic tracers (Clark *et al.*,

2004; Singleton and Moran, 2010; Manning *et al*., 2012), groundwater ages of less than one year cannot be resolved by current methods.

New tracer methods are needed to resolve groundwater recharge and transport on annual timescales due to the high cost of current deliberate tracer methods and analytical limitations of current intrinsic tracer techniques. This study developed and evaluated a new intrinsic tracer method using the cosmogenic radionuclide sulfur-35 (^{35}S) in water as dissolved sulfate (^{35}SO$_4$) to investigate groundwater recharge and transport in two distinct hydrologic settings: 1) high-elevation Sierra Nevada basins, and 2) low-elevations basins containing MAR facilities. In Chapter II, existing analytical techniques are refined to expand the analytical range of ^{35}SO$_4$. The new ^{35}SO$_4$ method was used to empirically determine annual groundwater recharge in snow-dominated Sierra Nevada basins (Chapter III). In Chapter IV, ^{35}SO$_4$ was used to quantify groundwater residence times in low-elevation basins dominated by MAR operations.

B. ^{35}S as a Hydrologic Tracer

Cosmic ray spallation of atmospheric argon continually produces ^{35}S in the upper atmosphere. ^{35}S eventually enters the hydrologic cycle as dissolved ^{35}SO$_4$ through precipitation (Tanaka and Turekian, 1991), and ^{35}SO$_4$ activities in precipitation range from <0.7 to 63 mBq/L (Cooper *et al*., 1991; Michel *et al*., 2000, 2002; Plummer *et al*., 2001; Novak *et al*., 2004; Shanely *et al*., 2005; Böhlke and Michel 2009; Singleton *et al*., 2014). Previous hydrologic studies have demonstrated that naturally-occurring ^{35}SO$_4$ is a useful intrinsic tracer for measuring shallow groundwater residence times of both water and SO$_4$ (e.g. Cooper *et al*., 1991; Michel *et al*., 2000, 2002; Plummer *et al*., 2001; Novak *et al*., 2004; Shanely *et al*., 2005). The 87.5-day half-life of ^{35}S makes it useful for investigating

residence times of SO_4 and shallow groundwater on timescales of up to 1.2 years (5 half-lives).

To date, hydrologic studies using $^{35}SO_4$ as an intrinsic tracer have focused on low-sulfate waters from alpine and subalpine basins where biogeochemical cycling and water/rock interactions are minimal and the hydrologic sulfate budget is dominated by atmospheric inputs (e.g. Cooper *et al*., 1991; Sueker *et al*., 1999; Michel *et al*., 2000, 2002; Plummer *et al*., 2001; Singleton *et al*., 2014).

C. New Analytical Method for Measuring ^{35}S

The application of $^{35}SO_4$ as an intrinsic tracer has been limited to environmental waters containing low SO_4 concentrations because only small amounts of SO_4 can be analyzed using current liquid scintillation counting (LSC) techniques. Chapter II describes a new analytical method for measuring $^{35}SO_4$ activities in natural waters. Compared to previous published methods (Hong and Kim, 2005; Brothers *et al*., 2010), the significant advances to the method include larger sample loading capacity for LSC analysis while maintaining high counting efficiency, sample purification, mitigation of counting interferences from reagent impurities, and optimization of LSC counting parameters. The new technique expands the analytical range of $^{35}SO_4$ in environmental waters containing a wide range of SO_4 concentrations, which broadens the capabilities of $^{35}SO_4$ as a hydrologic tracer.

D. Quantifying Annual Groundwater Recharge from Snowmelt in the Central Sierra Nevada using ^{35}S

Groundwater is critical to water supply in snow-dominated regions of the western U.S. because it serves as a buffer against the impacts of drought by storing and releasing

snowmelt to streams as baseflow. Snowmelt is an important component of groundwater recharge and storage in high-elevation basins (e.g. Earman *et al*., 2006), therefore spatial and temporal changes in snow dynamics due to a climate warming will likely change the amount and timing of water availability.

Uncertainties in the impact of climate change to groundwater recharge in snow-dominated Sierra Nevada basins is of particular concern in California where the majority of surface waters and groundwater are derived from Sierra Nevada snowpack. Groundwater supplies about 40% of California's total water supply during an average year, and as much as 60% during dry years when groundwater pumping increases to make up for the lack of surface runoff (California Department of Water Resources, 2014, 2015). With groundwater playing an ever-increasing role in meeting the State's water demands under a warming climate, understanding the storage and transport of groundwater becomes critically important.

Quantifying groundwater recharge and storage on annual timescales provides unique information for examining basin vulnerability to changing recharge conditions resulting from short-term fluctuations in climate. Integrated hydrologic modeling that simulates both groundwater and surface water flow and age has shown that changes in recharge have the largest effect on short (<1 year) timescale components (Engdahl and Maxwell, 2015). As snowpack continues to decline due to a warming climate, identifying the annual groundwater recharge derived from snowmelt is useful for evaluating the storage capacity of groundwater systems.

In the Sierra Nevada study (Chapter III), $^{35}SO_4$ was used to quantify the percentage of annual snowmelt in groundwater and surface waters in two Central Sierra Nevada basins.

Minimal contribution of snowmelt to surface waters during primary snowmelt period in both study basins indicates significant annual groundwater recharge and a relatively large aquifer system, which may be critical for mitigating the impacts of climate change to streamflow in these snow-dominated basins.

E. Quantifying Groundwater Travel Time near Managed Aquifer Recharge Operations using ^{35}S

Growing demands on groundwater resources have made the MAR operations increasingly important for supplementing public water supplies. MAR sites divert excess surface water, imported water, and reclaimed wastewater into surface-spreading ponds or direct injection wells to replenish groundwater in heavy-usage areas. Direct injection wells are also used to minimize the effects of seawater intrusion in many coastal groundwater basins in Southern California. In populated semi-arid regions such as southern California where groundwater and imported water are in short supply, the use of reclaimed water to replenish groundwater basins provides a safe, reliable, and drought resistant source for MAR operations; however, water quality concerns are raised when recycled wastewater is a portion MAR source waters. Understanding flow characteristics of recharged water is critical for protecting public and environmental health.

Quantifying groundwater travel times near MAR facilities is important for determining the fate and transport of potential contaminants, especially for facilities that incorporate a significant portion of reclaimed wastewater. In California, regulations for Groundwater Replenishment Reuse Projects (GRRP) require specific subsurface residence times prior to extraction for potable reuse (Johnson, 2009; California Division of Drinking Water, 2015). Depending on the degree of above ground treatment technologies before recharge, minimum

time for tertiary-treated recycled water can be as little as 2 months if the minimum pathogen removal is achieved above ground via above ground treatment processes, or could exceed 6 months if tertiary recycled water is surface spread. The travel time is also based on the method used for its determination with added or deliberate tracers being considered the most reliable and Darcy's Law calculations the least (California Division of Drinking Water, 2015).

The MAR study described in Chapter IV used $^{35}SO_4$ to quantify groundwater travel times near two MAR facilities in southern California. Due to seasonal variability of $^{35}SO_4$ activity in MAR source waters, careful characterization of $^{35}SO_4$ in source waters is important for the successful application of the $^{35}SO_4$ tracer method near MAR sites. Relative to established deliberate tracer experiments, comparable groundwater travel times for the less intensive $^{35}SO_4$ technique at two southern California MAR facilities demonstrates the usefulness of $^{35}SO_4$ in these shallow aquifer systems.

II. Analytical Method for Measuring Cosmogenic ^{35}S in Natural Waters

A. Abstract

Cosmogenic sulfur-35 in water as dissolved sulfate ($^{35}SO_4$) has successfully been used as an intrinsic hydrologic tracer in low-SO_4, high-elevation basins. Its application in environmental waters containing high SO_4 concentrations has been limited because only small amounts of SO_4 can be analyzed using current liquid scintillation counting (LSC) techniques. This chapter presents a new analytical method for analyzing large amounts of $BaSO_4$ for ^{35}S. Efficiency gains when suspending $BaSO_4$ precipitate in Inta-Gel Plus cocktail were quantified, $BaSO_4$ precipitate was purified to remove dissolved organic matter, interference of radium-226 and its daughter products was mitigated by selection of high purity barium chloride, and LSC counting parameters were optimized for ^{35}S determination in larger masses of $BaSO_4$. Using this improved procedure, counting efficiencies are comparable to published LSC techniques despite a 10-fold increase in the SO_4 sample load. $^{35}SO_4$ was successfully measured in high SO_4 surface waters and groundwaters containing low ratios of ^{35}S activity to SO_4 mass demonstrating that this new analytical method expands the analytical range of $^{35}SO_4$ and broadens the utility of $^{35}SO_4$ as an intrinsic tracer in hydrologic settings.

B. Introduction

Hydrologic tracer applications using sulfur-35 in water as dissolved sulfate ($^{35}SO_4$) have been limited due to high minimal detectable activity (MDA) values and low SO_4 loading capabilities of established methods. Previous methods include preconcentration of approximately 100 mg SO_4 followed by low-level liquid scintillation counting (LSC). Based

on the 100 mg limit of SO_4, low-SO_4 waters have typically been concentrated by passing 20 L of water through a column packed with an ion-exchange resin (Amberlite-400) using gravity filtration or a peristaltic pump (Sueker *et al.*, 1999; Michel *et al.*, 2000; 2002; Shanley *et al.*, 2005; Böhlke and Michel, 2009; Priyadarshi *et al.*, 2014). After eluting SO_4 off the resin, samples have been prepared for LSC by precipitating SO_4 as $BaSO_4$ collected onto glass fiber filters (Hong and Kim, 2005) or converting SO_4 to Na_2SO_4 crystals that are dissolved and the solution counted in a scintillation cocktail (Brothers *et al.*, 2010). While these methods have been successful for low-SO_4 waters (<5 mg/L), high-SO_4 waters (5-150 mg/L) contain low ^{35}S relative to the mass of SO_4 which necessitates analyzing a larger mass of $BaSO_4$ to achieve accurate measurements of $^{35}SO_4$. The LSC technique using glass fiber filters is inherently limited because of the difficulty in mounting SO_4 masses >100 mg onto the filters.

A secondary technique of counting dissolved Na_2SO_4 is problematic because the charge and large size of the SO_4 anion impedes formation of a stable microemulsion in liquid scintillation cocktail and can cause phase instability (PerkinElmer, 2014). Concentrations as low as $0.1M$ Na_2SO_4 (96 mg of SO_4 in 10 ml of water) are not recommended due to no or very little sample capacity for the common cocktails ULTIMA Gold AB, ULTIMA Gold LLT, and Insta-Gel Plus (PerkinElmer, 2014). Currently there are no cocktails available that could handle counting dissolved Na_2SO_4 for a sample load ≥ 1000 mg of SO_4.

In order to expand the analytical range of $^{35}SO_4$ in high-SO_4 systems, a new analytical method was developed for $^{35}SO_4$ by improving preconcentration of the SO_4, selecting high purity $BaCl_2$ reagents to mitigate counting interferences, purifying the $BaSO_4$ precipitate, and optimizing LSC counting parameters.

C. Experimental Section

1. Preconcentration of Sulfate

Environmental waters contain a wide range of SO_4 concentrations, therefore a batch method was used to preconcentrate $^{35}SO_4$ (Figure 1), with the goal of processing between 100 and 2000 mg of SO_4 per sample. The batch method was selected rather than the published column methods because samples collected in the field can be brought to the laboratory where multiple samples can be processed at the same time.
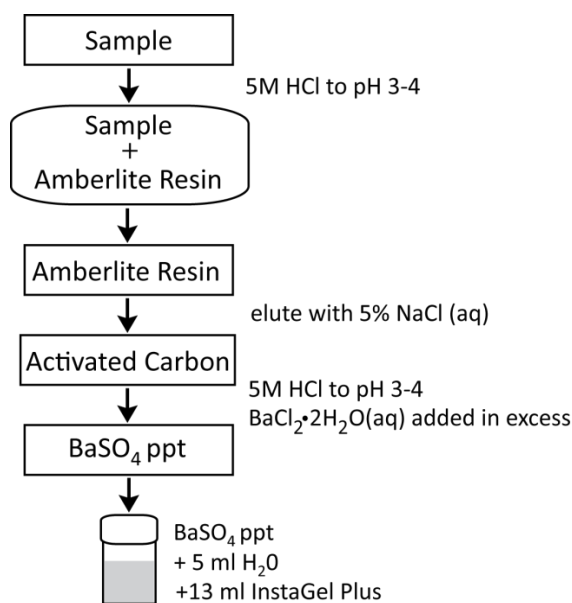
Figure 1. Schematic diagram of $^{35}SO_4$ preconcentration, purification, and mounting for LSC.

A laboratory sample matrix was created by dissolving anhydrous Na_2SO_4 containing no ^{35}S in 20 L of deionized water (DI) to obtain SO_4 concentrations of 5, 50, and 100 mg/L. The samples were transferred to buckets lined with plastic bags. During the method

development work, anion exchange resin (Amberlite, IRA-400) efficiency was found to be independent of pH for natural waters with relatively neutral pH; however, samples were acidified to pH 3-4 with 5M HCl prior to adding 20 g of resin to ensure that SO_4 is in solution. An industrial spinner was used to suspend 20 g of an anion exchange resin (Amberlite, IRA-400) in the sample for 2 hours, binding the SO_4 to the resin. To establish the spin time for SO_4 sorption, sample aliquots were collected every 15 min for 2 hours and the percent recovery was determined based on the SO_4 concentrations measured by ion chromatography (IC). After 2 hours of resin suspension, laboratory samples with 5, 50, and 100 mg/L of SO_4 had SO_4 recoveries of 90%, 88%, and 70%, respectively (Figure 2). Using five industrial spinners and a 2 hour-spin time per sample allows for the analysis of at least 10 samples in an average work day.

The resin was then transferred to a column and SO_4 was eluted off the resin with 250 ml of 5% NaCl solution. For 20 g of resin loaded with up to 1000 mg of SO_4, greater than 96% recovery of SO_4 was achieved with 250 ml of 5% NaCl (aq). The samples were then acidified to pH 3-4 with 5M HCl, heated, and Ba was added in excess (as dissolved $BaCl_2 \cdot 2H_2O$) to form a $BaSO_4$ precipitate. The $BaSO_4$ precipitate was allowed to settle overnight, then decanted and transferred to a 50 ml centrifuge tube. The $BaSO_4$ was triple rinsed with DI water.

.
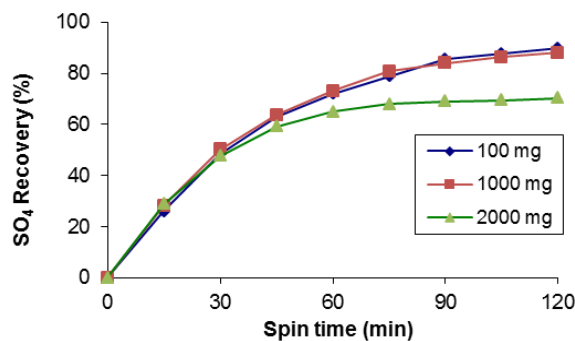
Figure 2. Percent recovery of SO_4 over 120 min for laboratory solutions containing 100, 1000, and 2000 mg of dissolved SO_4.

2. Sample Mounting for LSC

Samples containing 100 mg or less of SO_4 were transferred to 20 ml plastic scintillation vials (PerkinElmer) using 5 ml of DI water. Since more than 5 ml of water is needed to transfer larger masses of SO_4 to scintillation vials, samples containing 100 to 2000 mg of SO_4 were transferred to glass scintillation vials, dried overnight in a 100°F drying oven, and the dry weight of the $BaSO_4$ precipitate was recorded.

3. LSC Analysis

For this study, ^{35}S was analyzed as $BaSO_4$ in Insta-Gel Plus (PerkinElmer) scintillation cocktail. Insta-Gel Pus forms a stable gel that suspends particulates for counting. The stability of the gel phase is dependent on temperatures being between 5 and 27°C and the percentage sample load of water to cocktail being ≥20% (PerkinElmer, 2014). In this method, 5 ml of DI water was added to the dried $BaSO_4$ precipitate and the vial was shaken to completely suspend the precipitate in the DI water. Two 6.5 ml aliquots of Insta-Gel Plus were added and shaken in between to ensure even distribution of the precipitate and to create

12

a 28% sample load in the vial. Samples were refrigerated for 30 min prior to loading onto a Quantulus 1220 Ultra-Low Level Liquid Scintillation Spectrometer (LSS) equipped with a chiller.

4. Optimization of Counting Windows

The optimal counting region for LSC on a Quantulus 1220 was determined by counting a sample containing 100 mg of SO_4 precipitated as $BaSO_4$ that was spiked with a NIST-traceable ^{35}S standard. For both glass and plastic scintillation vials, the optimal window setting was determined by the figure of merit (FOM), a ratio of signal to noise that is the square of the counting efficiency divided by the background, E^2/B. Backgrounds and counting efficiencies were determined using various window settings and the high-energy beta default setting on the Quantulus 1220. The theoretical maximum energy of ^{35}S is 167 keV with the average being 53 keV, however, the ^{35}S counting region for the Quantulus 1220 has a maximum energy of 39 keV.

Based on the FOM, the ideal counting region is window setting 148 to 415 (4 to 31 keV) for both the glass and plastic scintillation vials. Backgrounds in this narrower window setting are 0.83 and 1.33 counts per minute (CPM) for plastic and glass vials, respectively. Counting efficiencies for window 148 to 415 are 53.0±0.1% for the plastic vial and 56.5±0.1% for the glass vial, which are approximately double the detection efficiencies reported by the Hong and Kim (2005) (Table 1). To ensure the efficiency gain is due to the suspension of $BaSO_4$ in Insta-Gel Plus rather than differences between a Quantulus LSS and the more frequently used TriCarb LSS, 100 mg of SO_4 spiked with ^{35}S standard was counted on both instruments. For glass vials, the counting efficiencies for window setting 4 to 167 keV was 58.1% on the Quantulus 1220 and 60.3% on the TriCarb 3100 (Table 1), which

suggests that the efficiency gain using this method is primarily due to the suspension of

$BaSO_4$ in Insta-Gel Plus.

Table 1. Summary of counting conditions for 100 mg of SO_4 in plastic and glass scintillation vials using various window settings.

Vial type	Window setting (keV)	Window setting (channel)	Bkg (CPM)	Efficiency (%)[a]	FOM (E^2/B)[a]
Quantulus 1220					
Plastic	4-167	148-658	2.94	53.9±0.1	989±5
Plastic	4-39	148-450	0.98	53.9±0.1	2960±14
Plastic	4-31	148-415	0.83	53.0±0.1	3379±12
Glass	4-167	148-658	4.71	58.1±0.1	716±4
Glass	4-39	148-450	1.63	57.9±0.1	2058±10
Glass	4-31	148-415	1.33	56.5±0.1	2396±10
TriCarb 3100					
Plastic	4-167	148-658	1.65	57.0±0.1	1969±5
Glass	4-167	148-658	1.62	60.3±0.2	2245±13
Hong and Kim (2005)[b]					
Plastic	4-167	148-658	1.87	25.2±1.2	340±24
Glass	4-167	148-658	2.18	21.9±1.2	221±17

[a] Uncertainties are standard deviations.
[b] Hong and Kim (2005) backgrounds were prepared using GF/B filters and Ultima Gold LLT cocktail and counted on a Packard Tri-Carb 3170 TR/SL.

5. Reagent Purity

Expanding the analysis beyond the l00 mg of SO_4 established in previous studies

necessitates counting a larger mass of SO_4 for environmental waters which contain high SO_4

concentrations (5-150 mg/L) with low ^{35}S activity The additional $BaCl_2$ reagent

($BaCl_2 \cdot 2H_2O$) needed to precipitate SO_4 requires identifying reagent impurities that result in

higher background count rates. Chemical separation of the SO_4 from other anions by

precipitation in an acidic environment with Ba highly purifies the sample prior to counting.

One concern is the isotope ^{133}Ba, a radionuclide that emits gamma radiation with an energy that overlaps with the ^{35}S counting region. ^{133}Ba is a fission product with a 10.7 year half-life and is not found in nature so its presence should be low in the reagent; to verify this, the amount of ^{133}Ba in various $BaCl_2$ lots obtained from different manufacturers was experimentally determined. Approximately 20 g of $BaCl_2 \cdot 2H_2O$ from the five lots were counted by gamma spectroscopy. For each lot, the ^{133}Ba activity per gram of Ba was below the MDA (Table 2) indicating that ^{133}Ba is not present in amounts that would significantly contribute to background count rates in the ^{35}S region of interest.

During the method development work, however, ^{226}Ra was found in every $BaCl_2$ lot. ^{226}Ra is a long-lived radionuclide (1600 year half-life) in the ^{238}U decay series and is the predominant species of radium isotope. The daughter products of ^{226}Ra include short-lived alpha-emitting (^{222}Rn, ^{218}Po, ^{214}Po, ^{210}Po) and beta-emitting (^{214}Pb, ^{210}Pb, ^{214}Bi, ^{210}Bi) radionuclides, most of which have half-lives on the order of minutes to days. Because of the very similar chemistry between barium and radium, separation of the two elements is difficult and, given the amount of barium needed per sample to form the $BaSO_4$ precipitation, it was not feasible to perform large scale separation chemistry.

^{226}Ra activity in the $BaCl_2$ lots was experimentally determined by dissolving 3.8 g of $BaCl_2 \cdot 2H_2O$ from each lot in 10 ml of DI water in glass scintillation vials, and 10 ml of High Efficiency Mineral Oil (PerkinElmer) was added to each vial. The samples were sealed and stored for 19 days prior to analysis on the Quantulus 1220 LSS to allow for ^{226}Ra and its daughter products to reach equilibrium. The ^{226}Ra activity varied between 21 and 1,145 mBq

mBq with the lowest activity observed for the high-purity $\geq 99.999\%$ trace metal basis

reagent (Table 2). The ^{226}Ra activity per gram of Ba ranged from 9.85 to 533.28 mBq/g.

Of secondary concern would be the presence of ^{228}Ra (5.75 year half-life), which could

also contribute to higher background count rates. The maximum beta emission for ^{228}Ra is

below the counting region for ^{35}S; however, its daughter product ^{228}Ac (6.15 hour half-life),

does emit a gamma ray energy which could affect the ^{35}S counting region. Since ^{228}Ac also

emits a gamma ray at 911.1 keV, gamma spectroscopy was used to determine the amount of

^{228}Ra in 20 g of $BaCl_2 \cdot 2H_2O$ from the five $BaCl_2$ lots. Similar to the results for ^{133}Ba, ^{228}Ra

was below the MDA (Table 2) indicating that very little ^{228}Ra is present in the $BaCl_2$ lots.

Table 2. Summary of ^{226}Ra and ^{133}Ba activity in $BaCl_2$ reagent batches obtained from different manufacturers.

Batch ID	Vendor	Grade	Lot Number	^{226}Ra/ $BaCl_2 \cdot 2H_2O$ (mBq/g)	^{226}Ra/Ba (mBq/g)	^{228}Ra/Ba (mBq/g)	^{133}Ba/Ba (mBq/g)
Batch 1	BDH	ACS	129517	80.40	143.01	<15.11	<3.67
Batch 2	BDH	ACS	3174C512	27.44	48.81	<15.93	<4.38
Batch 3	BDH	ACS	3174C512	26.38	46.93	<16.57	<5.32
Batch 4	Aldrich	$\geq 99.999\%$ trace metal basis	MKBK5701V	5.54	9.85	<11.84	<3.26
Batch 5	Aldrich	NA	05519PF	299.81	533.28	<17.23	<8.29

NA= Not available

6. Background Reduction from Optimization of Instrument Parameters

Unless the Quantulus 1220 is calibrated correctly, ^{226}Ra and its daughter products lead to

higher backgrounds in the ^{35}S counting region. Specifically, alpha emissions of ^{226}Ra, ^{222}Rn,

^{218}Po, ^{214}Po, ^{210}Po can be interpreted as beta events, particularly for reagent lots containing

higher amounts of ^{226}Ra. Additionally, the background contribution would increase over time as the ^{226}Ra daughter products reach equilibrium. Finally, larger masses of $BaSO_4$ have higher quench resulting in a shift of alpha emissions into the ^{35}S counting region that also lead to higher backgrounds.

To mitigate the increased background count rate from the ingrowth of ^{226}Ra, two software selectable parameters were optimized on the Quantulus 1220 LSS: the Pulse Shape Analyzer (PSA) and the Pulse Amplitude Comparator (PAC). The PSA discriminator setting provides a means to separate pure beta emissions from pure alpha emissions. Unless the PSA setting is on, alpha events will be interpreted as beta events.

The optimal PSA setting was determined using a NIST-traceable ^{241}Am standard, which is a pure alpha emitter. The solution was prepared with PerkinElmer Ultima Gold LLT cocktail and counted under various PSA setting ranging from 40 to 65. PSA 40 was the optimum setting because it was the lowest PSA that achieved 100% alpha counting efficiency in the alpha counting region (channel 500-900), minimizing spillover of alpha counts into the ^{35}S beta counting region (channel 148-415) and thus reducing the background count rate in the ^{35}S region.

Optimization of the PAC further reduced the background. The PAC rejects optical cross talk between photomultiplier tubes (PMTs) by comparing the amplitude of the pulses from each PMT and determining the amount of pulse amplitude variation that may be tolerated. Because higher PAC settings lower both background count rates and counting efficiency, the optimum PAC setting was determined by the FOM so as to lower the background without significantly reducing counting efficiency. Approximately 1000 mg of SO_4 as $BaSO_4$ was suspended in Insta-Gel Plus and counted under the following PAC settings: 1 (Default), 50,

100, 150, 175, 200, and 225. The largest FOM occurred at PAC 150 followed by PAC 100 (Table 3), indicating that a PAC setting between 100 and 150 is the optimal setting for measuring low-level beta emission from ^{35}S. A PAC setting of 120 was used for sample analyses in this study.

Table 3. Background count rate and counting efficiencies for 1000 mg of SO_4 under various Pulse Amplitude Comparator (PAC) settings.

PAC Setting	Bkg (CPM)	Efficiency (%)	FOM
1	1.50	66	1901
50	1.47	67	2481
100	1.42	63	2781
150	1.28	61	2907
175	1.29	59	2709
200	1.33	54	2432
225	1.21	49	2389

After both the PAC and PSA settings were optimized, background count rates were quantified by precipitating 1500 mg of SO_4 with each of the five $BaCl_2$ lots. Samples were counted after seven days under PAC 1 and PSA OFF (Default); PAC 1 and PAC 40; and PAC 120 and PAC 40 settings. As expected, the highest background was observed for samples precipitated with the Batch 5 reagent which contained the highest amount of ^{226}Ra activity (Table 4). Using the optimized PAC 120 and PSA 40 settings reduced the background count rate by at least 30% for all five $BaCl_2$ lots.

Table 4. $^{35}SO_4$ background count rates for 1500 mg of SO_4 precipitated with different $BaCl_2$ reagent batches under various PAC and PSA settings.

Batch ID	Bkg (CPM)		
	Default	PAC 1, PSA 40	PAC 120, PSA 40
Batch 1	7.54	5.80	3.69
Batch 2	3.12	2.63	1.85
Batch 3	3.25	2.53	1.75
Batch 4	1.72	1.38	0.98
Batch 5	32.30	26.05	18.22

Optimization of PSA and PAC settings and use of higher-purity $BaCl_2$ reagent significantly reduces but does not eliminate background count rates in the ^{35}S region of interest. Background count rates are positively correlated with the amount of SO_4 precipitated as $BaSO_4$; however, the optimal PAC 120 and PSA 40 settings lower the slope of background to SO_4 relative to the Default setting (Figure 3).

Ingrowth of ^{226}Ra daughter products results in a time dependent background, particularly under the Default setting where alpha emissions are interpreted as ^{35}S beta events. Once Insta-Gel Plus is added and the sample vials are sealed, ^{226}Ra decays to the short-lived radionuclide ^{222}Rn (half-life 3.8 days), which is a gas that becomes trapped in the cocktail and potentially in the vial headspace. Over the course of several weeks, ingrowth of ^{222}Rn and its daughters occurs until ^{226}Ra reaches secular equilibrium with its daughters. For illustration, 1500 mg of SO_4 was precipitated with the low purity Batch 5 $BaCl_2$ reagent (533.28 mBq of ^{226}Ra per gram of Ba) and counted repeatedly over an eight-day period. The background count rate at approximately one week (170 hours) after vials were sealed was 37.38 cpm under the Default setting, which was reduced to 25.10 cpm under the optimized PAC 120 and PSA settings. The lower rate of increase under the optimized setting indicates

that potential ingrowth of ^{226}Ra daughter products into the ^{35}S counting region was

mitigated.
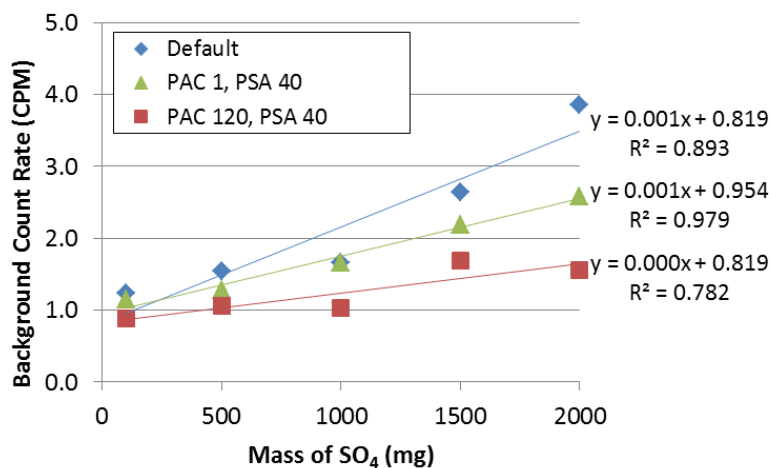
Figure 3. Background count rate for varying masses of SO$_4$ precipitated with Batch 2 BaCl$_2$ reagent containing 48.81 mBq of ^{226}Ra per gram of Ba under the following settings: PAC 1 and PSA OFF (Default); PAC 1 and PSA 40; PAC 120 and PSA 40. Count rate generally increases with increasing mass of SO$_4$ for all settings, however, PAC 120 and PSA 40 setting resulted in lower background count rates, particularly for SO$_4$ masses ≥1000 mg.
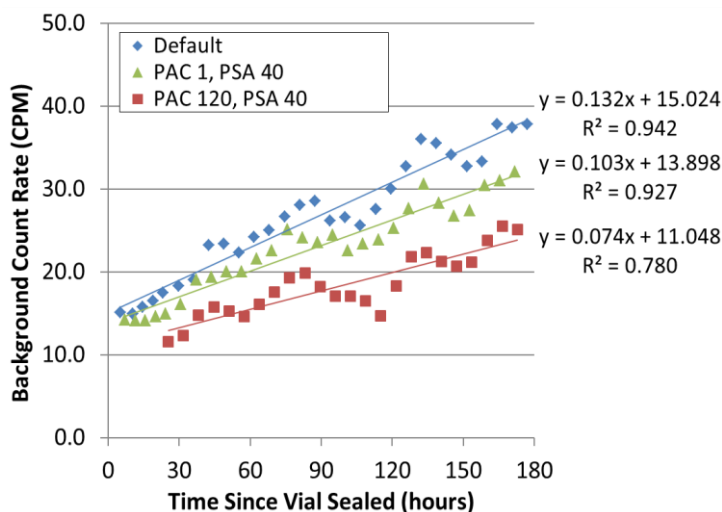
Figure 4. Background count rates for 1500 mg of SO_4 precipitated with Batch 5 $BaCl_2$ reagent containing 533.28 mBq of ^{226}Ra per gram of Ba. After the vial was sealed, the sample was counted under various PAC and PSA settings over approximately 170 hours.

Based on the time-dependent ingrowth of ^{226}Ra daughter products, the samples were counted as quickly as possible to minimize the background count rate in the ^{35}S region of interest. Waiting 20 days to count the sample allows for full ingrowth of ^{226}Ra daughters; however, the background count rate will necessarily be higher due to ^{226}Ra spilling into the ^{35}S counting region. Additionally, there will be significant decay of ^{35}S over the 20-day period (~14%) due to its 87.5-day half-life. This limits the effectiveness of the decay analysis and, it should be noted, ^{226}Ra ingrowth would affect any procedure that counts $BaSO_4$ directly.

7. Counting Configurations for Sample Analysis

Given that ^{226}Ra impurities exist in all $BaCl_2$ lots, which affect the background count rates in the ^{35}S counting region, care should to be taken with respect to the activity of ^{226}Ra, mass of SO_4 counted as $BaSO_4$, and time that elapses between when sample vials are sealed

21

and counted. For this study, the $BaCl_2$ reagent used for $BaSO_4$ precipitation was limited to those lots containing ^{226}Ra concentrations of <50 mBq per mg of $BaSO_4$. Samples were counted within 36 hours of being sealed to minimize the increased background count rate due to ingrowth of ^{226}Ra in the ^{35}S region of interest and to minimize the decay of ^{35}S. Using high purity $BaCl_2$ reagent and counting samples within 36 hours of being sealed, the optimized PAC and PSA instrument parameters reduced the background from 1.65 cpm to 1.04 cpm for 1000 mg of SO_4 (Figure 5).
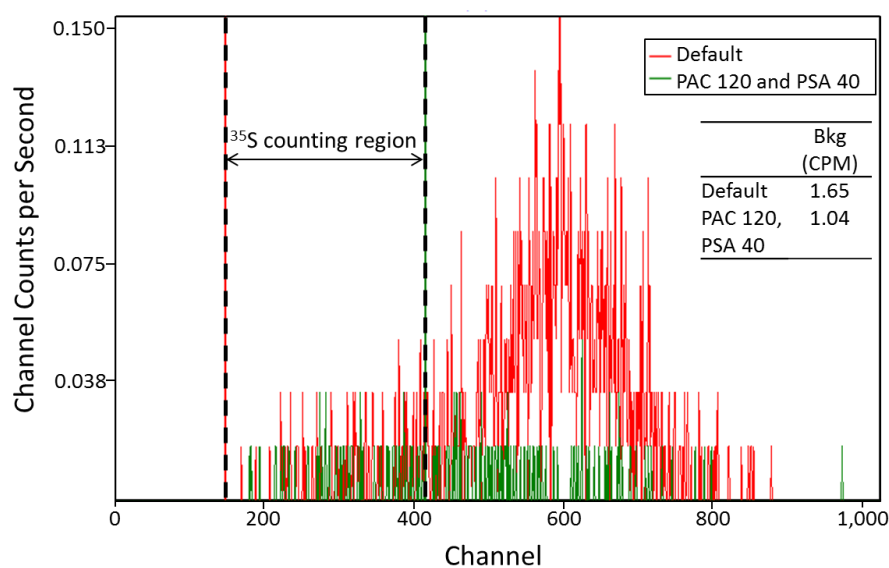
Figure 5. $^{35}SO_4$ energy spectra and background counts for 1000 mg of ^{35}S-free SO_4 precipitated with Batch 2 $BaCl_2$ reagent containing 48.81 mBq of ^{226}Ra per gram of Ba. Relative to the Default setting background count rate of 1.65 cpm, the optimized PAC 120 and PSA 40 settings reduced the background to 1.04 cpm.

For environmental samples, a $BaSO_4$ mass-dependent background subtraction was created based on the generally observed linear relationship between increasing SO_4 mass and increasing background count rate (Figure 3), and this subtraction was used to calculate net count rate and sample activity. Using ^{35}S-dead $BaSO_4$ in the same matrix as the sample itself (e.g. same $BaSO_4$ mass, same cocktail, same vial type, and same count time) for the mass-dependent background subtraction accounts for any potential counting interferences due to radionuclides such as [133]Ba or Ra isotopes from the $BaCl_2$ reagent, or [40]K that may be present in the glass vial.

Using optimized instrument settings, the effect of $BaSO_4$ mass on counting efficiency was determined. A series of ^{35}S standards were prepared in glass scintillation vials by spiking varying masses of SO_4 with a NIST-traceable ^{35}S standard prior to precipitation with Ba. An attenuation curve of the counting efficiency versus the mass of SO_4 demonstrates that counting efficiency decreases linearly as SO_4 mass increases (Figure 6). For 1000 mg of SO_4, the 19.0±0.1% counting efficiency is similar to the 21.4±1.2 % efficiency for 100 mg of SO_4 reported by Hong and Kim (2005) despite an order of magnitude increase in the mass of SO_4.

With the correct ratio of water to Insta-Gel Plus cocktail and maintaining the samples at the recommended Insta-Gel temperature range (5-27 ℃; PerkinElmer, 2014), counting efficiency is expected to remain stable due to minimal gravimetric settling of $BaSO_4$ in the vial. Gravimetric settling of $BaSO_4$ would lead to a decrease in counting efficiency over time. To examine how efficiency changed over time, 1000 mg of SO_4 was spiked with ^{35}S standard, suspended in Insta-Gel Plus, and counted at day 1 and again 12 days later. The counting efficiency at day 1 was 19.0±0.1% and at day 12 was 19.5±0.1%, indicating that

gravimetric settling of $BaSO_4$ is minimal due to a uniform and stable mixture of sample and Insta-Gel Plus.
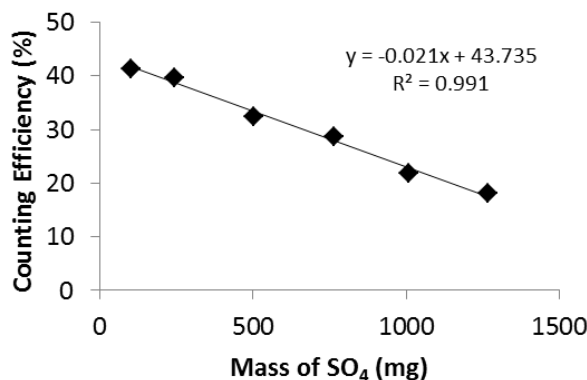
Figure 6. Counting efficiency for various masses of SO_4 precipitated as $BaSO_4$. Efficiency decreased as the SO_4 mass increased.

D. Method Application to Natural Waters

1. Sample Purification

In analysis of natural waters, dissolved organic materials result in colored impurities that lead to color quenching and higher background count rates during LSC. Two techniques were tested to remove organics and mitigate sample quenching; an activated carbon treatment prior to $BaSO_4$ precipitation and a wet ashing treatment post $BaSO_4$ precipitation. For the activated carbon treatment, after eluting the resin with NaCl, samples were passed through a column containing 4.0 g of 20-40 mesh activated carbon. The samples were then acidified to pH 3-4 with 5M HCl, heated, and precipitated as $BaSO_4$. For the wet ashing

treatment, the $BaSO_4$ is transferred to a centrifuge tube with 25 ml of DI water, heated in a

hot water bath, and treated with concentrated HCl and H_2O_2.

To evaluate the effectiveness of activated carbon and wet ashing at mitigating color

quenching in environmental waters using surface waters collected from Del Valle Reservoir

in Alameda County, CA that contained 6.1 mg/L of dissolved organic carbon. Five-liter

sample volumes of Del Valle water were filtered through a 0.45 micron high-capacity filter,

acidified to pH 3-4 with 5M HCl, then gravity feed through 20 g of anion exchange resin.

After elution of the sample with 250 ml of 5% NaCl (aq), samples were either passed

through a column containing 2.0 g of activated carbon, wet ashed following $BaSO_4$

precipitation, or both treated with activated carbon and wet ashed. Table 5 summarizes the

experimental conditions for the Del Valle waters.

The 1220 Quantulus used in this study has a standard quench parameter (SQP) that

quantifies quenching of a sample by subtracting the spectrum of the sample alone from that

of an external standard with the sample in the counting chamber. The SQP value is

analogous to the transform Spectral Index of the External Standard (tSIE) parameter on the

Tri-Carb LSS. SQP values decrease depending on the amount of quenching; higher

quenching correlates with lower SQP values. Compared to laboratory background,

progressively cleaning up the Del Valle sample resulted in a SQP closer to the background

reference value of 726.98 (Table 5). Environmental samples are treated uniformly with

activated carbon. If any color is present after the activated carbon treatment, wet ashing is

performed.

Table 5. Summary of standard quench parameters (SQP) for Del Valle surface water treated with activated carbon and/or wet ashing.

Treatment	SQP
Background[a]	726.98
No treatment	701.27
Activated carbon treatment	717.39
Wet ashing	717.40
Activated carbon and wet ashing	722.81

[a] Background contained 120 mg of ^{35}S-free SO_4, which is similar to the mass recovered for Del Valle samples.

2. Sample Analysis and Measurement Precision

A subset of environmental waters from Orange County, California, was used to evaluate the method. The surface waters and groundwater ranged in SO_4 concentration from 0.8 to 215 mg/L. Samples were collected by filtering up to 20 L of water through a 0.45 μm high-capacity filter into polypropylene containers. All samples were processed and analyzed following the method outlined in this study.

$^{35}SO_4$ activity and one sigma counting errors for Orange County surface waters and groundwater are provided in Table 6. In the case of field duplicates, samples were not homogenized prior to sample processing. The results were yield-corrected by determining the total amount of SO_4 in the samples (concentration determined by IC multiplied by the volume of water analyzed) relative to the gravimetric recovery of SO_4 as $BaSO_4$ prior to the addition of Insta-Gel Plus. Samples were decay-corrected to the collection date. Total recovery of SO_4 typically ranged between 30 and 98%, with samples containing SO_4 concentrations of >100 mg/L resulting in SO_4 recovery of <40%. Reproducibility of the

measurements was evaluated through comparison of field duplicates using the relative error

ratio (RER):

$$RER = \left| \frac{S-D}{\sqrt{\sigma_S{}^2 + \sigma_D{}^2}} \right| \qquad (1)$$

where S is the sample $^{35}SO_4$ activity (mBq/L); D is the field duplicate $^{35}SO_4$ activity

(mBq/L); and $\sigma_S{}^2$ and $\sigma_D{}^2$ are one sigma counting errors for the sample and field duplicate

(mBq/L), respectively.

Field replicates with RER ratios at or below 3.0 are considered reproducible. All but two

the 19 total RER ratios were below 3.0, with the two outliers having RER ratios of 3.5 and

5.4. For duplicates with RER ratios below 3.0, the mean RER value was 1.3, indicating that

good precision was achieved for the majority of the environmental samples.

Table 6. $^{35}SO_4$ activities and one sigma counting errors for Orange County groundwater and surface water samples.

Site ID	Collection Date	SO$_4$ (mg/L)	$^{35}SO_4\pm1\sigma$ (mBq/L)	Field Duplicate $^{35}SO_4\pm1\sigma$ (mBq/L)	RER
Surface water					
SAR	05-Feb-2013	137	8.3±1.9	19.0±2.4	3.5
SAR	02-Apr-2013	133	16.2±1.7	NA	
WB	04-Feb-2013	110	14.9±1.7	20.6±2.0	2.2
WB	01-Apr-2013	125	22.0±1.8	NA	
LJ	04-Feb-2013	117	13.6±1.8	16.0±2.0	0.9
LJ	01-Apr-2013	215	16.0±2.3	15.0±2.3	0.3
AL	05-Feb-2013	119	8.6±1.6	18.5±2.1	2.7
MB	02-Apr-2013	0.8	1.5±0.2	1.2±0.2	0.9
KB	05-Feb-2013	109	17.1±1.7	19.4±1.9	0.9
KB	01-Apr-2013	188	28.4±2.5	11.1±2.0	5.4
Groundwater					
KBS-3/1	05-Feb-2013	112	15.9±1.8	11.3±1.8	1.8
KBS-3/1	02-Apr-2013	177	5.4±1.8	NA	
AM-7/1	05-Feb-2013	17.3	4.5±0.4	3.4±0.5	1.7
AM-7/1	16-Apr-2013	46.3	3.1±0.4	2.4±0.5	0.6
AM-8/1	05-Feb-2013	15.7	3.0±0.4	2.8±0.3	0.5
AM-8/1	16-Apr-2013	20.7	2.4±0.3	2.1±0.3	0.9
AM-48/1	05-Feb-2013	25.2	3.9±0.5	4.2±0.6	0.2
AM-48/1	04-Apr-2013	44.3	2.7±0.4	4.3±0.6	2.3
AMD-12/1	05-Feb-2013	17.9	2.9±0.3	3.8±0.5	1.5
AMD-12/1	16-Apr-2013	9.1	1.7±0.2	2.6±0.3	2.8
AMD-12/2	05-Feb-2013	136	4.8±1.6	10.3±1.8	2.3
AMD-12/2	16-Apr-2013	142	0.8±1.2	NA	
PW1	05-Feb-2013	27.8	4.3±0.5	4.4±0.6	0.1

NA= Field duplicate was not available

E. Conclusions

This study developed a robust analytical technique for measuring $^{35}SO_4$ in environmental waters that contain a wide range of SO$_4$ concentrations. Compared to previous published methods (Hong and Kim, 2005; Brothers *et al*., 2010), the advances include (1) significant improvements to loading large masses of BaSO$_4$ precipitate in Insta-Gel Plus cocktail for counting while maintaining high counting efficiency comparable to published techniques

despite a 10-fold increase in the SO_4 sample load; (2) purification of $BaSO_4$ by the removal of dissolved organic matter which eliminates color quenching in liquid scintillation counting; (3) identification of ^{226}Ra impurity in $BaCl_2$ reagents which affect ^{35}S determination; (4) mitigation of the ingrowth from ^{226}Ra daughter products by optimization of instrument parameters; (5) utilizing a batch method to decrease sample analysis time and increase throughput. These improvements allowed for successful analysis high SO_4 surface waters and groundwater, which has not been previously attempted. Additionally, compared to published techniques, these advancements significantly improve ^{35}S determination in low-SO_4 waters as well.

III. Quantifying Annual Groundwater Recharge from Snowmelt in the Central Sierra Nevada using Naturally-Occurring ^{35}S

A. Abstract

Identifying basin vulnerability to climate change is of vital importance in the Sierra Nevada and other snow-dominated basins where groundwater systems are essential to water supply. Quantifying the component of new (current year's) snowmelt in groundwater and surface water is useful in evaluating basin vulnerability because significant annual recharge may indicate that streamflow will respond rapidly to annual variability in precipitation, followed by more gradual decreases in recharge as recharge declines over decades. Hydrologic models have shown that changes in recharge affect short (<1 year) timescale components; however, field studies that identify this young component are rare. The goal of this study was to utilize the short-lived, naturally-occurring cosmogenic isotope sulfur-35 (^{35}S) to quantify new snowmelt contribution to groundwater and surface waters in Sagehen Creek Basin (SCB) and Martis Valley Groundwater Basin (MVGB) located within the Tertiary volcanics of the central Sierra Nevada, California. Activities of ^{35}S were measured in dissolved sulfate (^{35}SO$_4$) in SCB and MVGB snowpack, groundwater, springs, and streamflow. The percent of new snowmelt (PNS) in SCB streamflow ranged from 0.2 ± 6.6% during baseflow conditions to 14.0 ± 3.4% during high flow periods of snowmelt. Similar to SCB, the PNS in MVGB groundwater and streamflow was typically <30% with the largest fractions occurring in late spring or early summer following peak streamflow. The consistently low PNS suggests that a significant fraction of annual snowmelt in SCB

and MVGB recharges groundwater, and groundwater contributions to streamflow in these systems has the potential to mitigate climate change impacts on runoff.

B. Introduction

Groundwater vulnerability to climate change in high-elevation basins has widespread implications for ecosystem health and water supply (Earman and Dettinger, 2011; Earman *et al*., 2015). In the mountains of the western United States, groundwater is a major component of streamflow, even during peak snowmelt conditions (Genereux and Hooper, 1998; Liu *et al*., 2004). Spatial and temporal changes in snow dynamics, such as declines in snowpack accumulation (Mote 2003; Mote *et al*., 2005) and earlier onset of snowmelt (Hamlet *et al.*, 2005; Mote *et al*., 2005; Knowles *et al.*, 2006), is of particular concern for Sierra Nevada basins because groundwater recharge is mainly derived from snowpack for most of the southwest (Winograd *et al*., 1998; Earman *et al*., 2006). Groundwater in the Sierra Nevada and other high-elevation basins is critical for water supply (Frisbee *et al*., 2011) and ecosystem health, yet the impact of climate change on groundwater recharge is poorly understood (Earman and Dettinger, 2011; Viviroli *et al*., 2011; Earman *et al*., 2015).

Understanding climate change impacts on groundwater resources in the Sierra Nevada and other high-elevation basins is difficult due to a weak understanding of direct and indirect effects of climate change on mountain recharge processes (Earman and Dettinger 2011; Earman *et al*., 2015). Current forecasts of the effects of climate change vary widely. In snow-dominated basins that are predicted to experience a shift in precipitation from snow to rain, groundwater recharge may decrease because snow is a more efficient recharging agent than rain (Winograd *et al*., 1998; Earman *et al*., 2006; Meixner *et al*., submitted). However, reductions in snowpack or shifts from snow to rain may have little effect on

groundwater recharge in fractured-rock aquifers that are permeability limited (Manning *et al*. 2012). Under either condition, investigating groundwater response times would reduce the uncertainty of how mountain basins respond to changing precipitation patterns.

Groundwater residence time is useful in evaluating groundwater sensitivity to climate change because it provides insight into recharge processes, storage capacity, and flow characteristics of groundwater reservoirs. Shallow groundwater basins are likely to have lower buffering capacity and greater sensitivity to climate change (Singleton and Moran, 2010). Short residence times indicate shallow groundwater reservoirs and relatively small storage capacities. Because groundwater storage capacity and residence time in high-elevation basins like the Sierra Nevada can elucidate groundwater vulnerability to climate change, an accurate basin study typically requires the use of groundwater tracer techniques.

Intrinsic groundwater tracers, such as dissolved gases and isotopic tracers, are useful for characterizing groundwater residence times in high-elevation basins (e.g. Manning and Solomon, 2005; Plummer *et al*., 2001; Manning *et al*., 2012; Segal *et al*., 2014). In the Sierra Nevada, dissolved noble gas concentrations (Ne, Ar, Kr, and Xe) combined with tritium-helium ($^3H/^3He$) age dating have been useful in determining groundwater ages of <50 years in various basins such as Martis Valley Groundwater Basin (MVGB) and Olympic Valley Basin (Segal *et al*. 2014; Singleton and Moran, 2010). For the nearby Sagehen Creek Basin (SCB), Manning *et al*. (2012) used time series measurements of chlorofluorocarbons (CFCs), sulfur hexafluoride (SF_6), and tritium (^3H) to determine apparent groundwater ages of springs and found that most springs are best characterized by a bimodal mixture of <1 year old water and water recharged after 1950. Recharge studies using CFCs, SF_6, and $^3H/^3He$ tracer methods have determined groundwater ages of <1 year;

however, the uncertainties of these methods are typically greater than or equal to 1 year (Singleton and Moran, 2010; Manning *et al*., 2012).

Integrated hydrologic modeling has shown that changes in recharge have the largest effect on short (<1 year) timescale components, which in turn drive changes in the composite ages of the hydrologic system (Engdahl and Maxwell, 2015); however, field-based studies that identify this young component are rare. The development and application of groundwater tracer methods which can resolve seasonal fluxes of precipitation on <1 year timescales would improve our understanding of groundwater residence times and storage capacities in mountain basins.

An infrequently utilized intrinsic tracer that captures the timescale of <1 year is the radioisotope sulfur-35 (^{35}S). The half-life of 87.5 days (Lal and Peters, 1967) is ideal for investigating groundwater recharge and cycling of $^{35}SO_4$ on timescales of <1.2 years (5 half-lives). Hydrologic studies in high-elevation basins such as the Rocky Mountain Range have successfully used $^{35}SO_4$ to determine mean residence times of SO_4 and groundwater in basins where the hydrologic SO_4 budget is dominated by atmospheric inputs, and biogeochemical cycling and water/rock interactions are minimal (Cooper *et al*., 1991; Michel *et al*., 2000; Shanley *et al*., 2005; Sueker *et al*., 1999). Because of its short half-life, the $^{35}SO_4$ tracer can be used to characterize basins that have a significant component of total streamflow derived from the current year's snowmelt (hereon referred to as "new" snowmelt), which would be an important tool in evaluating the vulnerability of water resources to changing precipitation patterns.

This study utilized intrinsic $^{35}SO_4$ to determine the annual flux of new snowmelt being stored or discharged from two central Sierra Nevada Basins: SCB and MVGB. The $^{35}SO_4$

33

tracer method is used to quantify the fraction of surface water and groundwater derived from new snowmelt to constrain the new snowmelt contribution to groundwater recharge.

C. Study Site Description

SCB and MVGB are located on the eastern slope of the central Sierra Nevada, CA, near the crest of the Sierran divide, northwest of Lake Tahoe (Figure 7). MVGB has an area of approximately 148 km^2, which is over five times the 27 km^2 area for SCB. Both SCB and MVGB cover a similar elevation range; 1940-2600 m and 1740-2700 m for SCB and MVGB, respectively. The large difference in surface area allows for the investigation of how groundwater recharge from new snowmelt is affected by larger surface area and storage volume.

Both basins have a mean annual precipitation of approximately 80 cm per year, 80% of which falls as snow during the winter months (Snowpack Telemetry (SNOTEL) Site #834 in MVGB and Site #539 located within 2.0 km of SCB; http://www.wcc.nrcs.usda.gov/snow/). Peak snowmelt typically occurs in early April, and surface flows are controlled by melting snowpack with peak stream discharge occurring in the late spring to early summer. SCB is drained by Sagehen Creek, which flows from west to east as a tributary to the Truckee River (Figure 7). Several surface water bodies within MVGB also eventually flow into the Truckee River including Martis Lake and Donner Creek (Figure 8B). Daily mean streamflow values for Sagehen Creek were obtained from a U.S. Geological Survey (USGS) gauging station located near the outlet of SCB.

SCB and MVGB basins are underlain by Cretaceous granites and granodiorites typical of the Sierra Nevada batholith. However, Miocene to Pleistocene volcanics comprised mainly of andesitic flows, breccias, and basalts are the predominant rock type in both basins

(Sylvester, 2008; California Department of Water Resources, 2006). Surficial Quaternary alluvium, colluvium, and glacial deposits derived from the Tertiary aged volcanic rocks overlie and interfinger with the volcanic sequences. The alluvial and glacial deposits have higher specific storage than the volcanic and basement rocks and likely support surficial aquifers in this region.

$^{35}SO_4$ is useful for studying groundwater recharge and transport in basins where biogeochemical or sorption processes are minimal. Sorption of newly recharged $^{35}SO_4$ anion in a groundwater basin, accompanied by exchange with older SO_4 in which ^{35}S has decayed away, could complicate the interpretation of new snowmelt contribution to groundwater recharge. Sorption of $^{35}SO_4$ typically occurs in soils with low pH and an abundance of minerals containing iron and aluminum oxyhydroxides (Chao *et al*., 1964; Parfitt, 1978), conditions that are rarely found in the Sierra Nevada. Based on the limited SO_4 adsorption capacities found in other high-elevation Sierra Nevada catchments (Williams *et al*., 2001), sorption of $^{35}SO_4$ in SCB and MVGB soils is not expected to affect the transport of $^{35}SO_4$ in these groundwater basins.

Groundwater residence times and recharge processes in SCB and MVGB have been studied extensively using noble gas and environmental tracer techniques. Based on CFCs and $^3H/^3He$ data, Rademacher *et al*. (2001) found that the apparent groundwater ages of springs in SCB ranged from <2 to 36 years using the simplified piston-flow model. In MVGB, Segal *et al*. (2014) used $^3H/^3He$ and dissolved noble gases to determine groundwater ages and recharge temperatures at various wells throughout MVGB. They found that groundwater recharge generally occurred at lower elevations, and that long screened wells were a mixture of groundwater with ages of 50 to over 1000 years. These

studies have characterized the residence time of water on the scale of greater than 2 years, but the uncertainty inherent in the analytical techniques limit its application on the <1 year timescale making them unsuitable for investigating the transport and storage of new snowmelt. Application of the $^{35}SO_4$ tracer technique will improve our understanding of groundwater residence times and storage capacities in mountain basins on seasonal timescales.
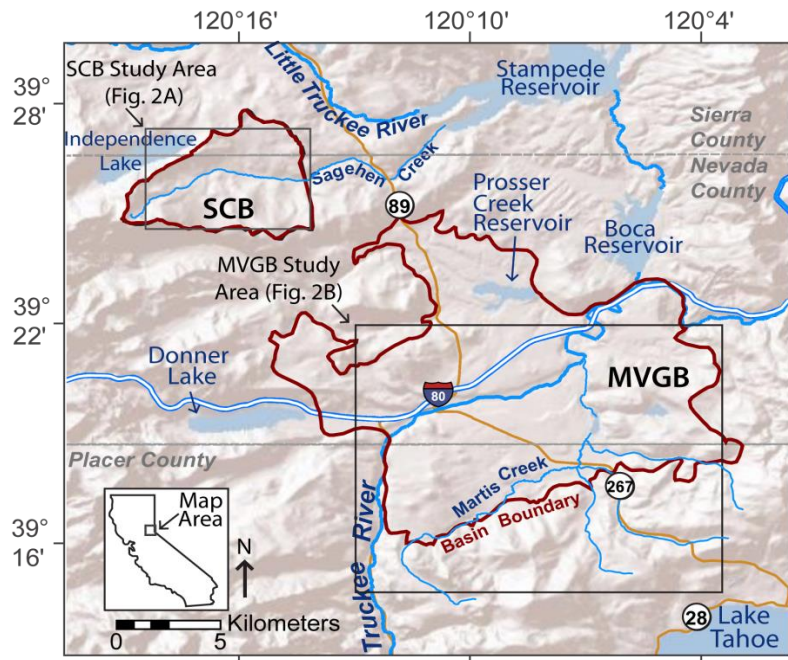
Figure 7. Location of Sagehen Creek Basin (SCB) and Martis Valley Groundwater Basin (MVGB) in California. Source: USGS National Hydrography Data Set and California Department of Water Resources.
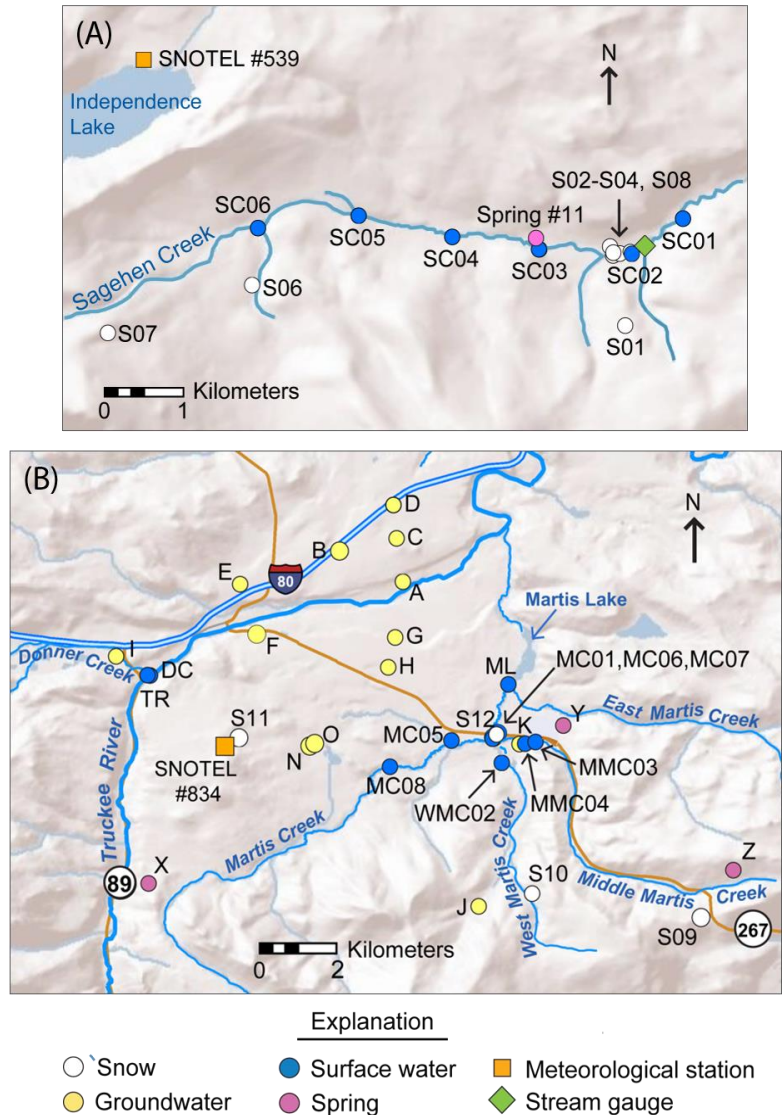
Figure 8. $^{35}SO_4$ sampling locations in (A) SCB and (B) MVGB. Source: USGS National Hydrography Data Set and California Department of Water Resources.

D. Methods

1. Snow Sampling

SCB snowpacks were collected in winter 2009/2010 and 2010/2011 by shoveling full-depth vertical snow pits until an impermeable layer (i.e. ice layer or ground surface) was

reached. Snow was allowed to melt in plastic containers, yielding between 13 and 20 L of melt water per sample. A total of 15 snowpack composite samples were collected on three sampling dates (one in winter 2009/2010 and two in winter 2010/2011) from eight sites within SCB (Figure 8A). The sites range in elevation from 1844 m near the basin floor to 2373 m on the western slope of SCB.

Snow collection techniques were modified for MVGB to better characterize temporal and spatial difference of $^{35}SO_4$ snow activity within a season. In November 2011, prior to the first major water year (WY) 2012 winter precipitation event, 210 L containers were placed at four MVGB sampling locations (Figure 8B), which cover the MVGB range in elevation. The contents of each container were transferred into 20 L buckets on four sample collection dates in winter 2011/2012 with the goal of obtaining 20 L of melt water per sampling event. If less than 20 L was obtained over a collection period, the uppermost layers of the surrounding snow, which is representative of the most recent snowfall, was added to the sample container to achieve approximately 20 L of melt water. The May 2, 2012 sampling event yielded between 2.0 and 13.5 L of melt water at each of the four sampling sites because no additional snow was available to augment the melt water. Although both rain and snow were allowed to accumulate in the MVGB containers, approximately 77% of the precipitation over the entire sampling period occurred as snow, therefore each sample is assumed to represent a composite of snow that was deposited between collection periods.

2. Surface Water Sampling

Surface water was sampled in SCB and MVGB to determine the contribution of new snowmelt being discharged from the basins. In SCB, Sagehen Creek was sampled approximately every other month from February 2010 to August 2011. On August 28, 2010,

six locations along a 5 km reach of lower Sagehen Creek (Figure 8A) were sampled to determine spatial changes in groundwater inflow. For each SCB surface water sampling event, a submersible pump was used to field filter approximately 20 L of water through a 0.45 micron high-capacity filter. For the MVGB study, surface water from 11 locations including Martis Lake (ML), Donner Creek (DC), Truckee River (TR), and eight locations along several tributaries that discharge into Martis Lake (MC01, MC05-MC08, WMC02, MMC03, MMC04) (Figure 8B) were collected periodically in 2012 by submerging and filling 5 gallon polyethylene containers. Approximately 20 L of water was collected for each event, and samples were field filtered through a 0.45 micron high-capacity filter. Surface water was sampled in SCB and MVGB to determine the contribution of new snowmelt being discharged from the basins. In SCB, Sagehen Creek was sampled approximately every other month from February 2010 to August 2011. On August 28, 2010, six locations along a 5 km reach of lower Sagehen Creek (Figure 8A) were sampled to determine spatial changes in groundwater inflow. For each SCB surface water sampling event, a submersible pump was used to field filter approximately 20 L of water through a 0.45 micron high-capacity filter. For the MVGB study, surface water from 11 locations including Martis Lake (ML), Donner Creek (DC), Truckee River (TR), and eight locations along several tributaries that discharge into Martis Lake (MC01, MC05-MC08, WMC02, MMC03, MMC04) (Figure 8B) were collected periodically in 2012 by submerging and filling 5 gallon polyethylene containers. Approximately 20 L of water was collected for each event, and samples were field filtered through a 0.45 micron high-capacity filter.

3. Groundwater Sampling

A perennial spring in SCB (Figure 8A) was sampled four times from 2010 to 2011 to provide a snapshot of $^{35}SO_4$ activity in SCB groundwater. The spring was sampled at less frequent intervals compared to Sagehen Creek due to limited access and the difficulty of sampling. In MVGB, 12 production and irrigation wells (wells A to I, K, N, O) and one cistern (J) (Figure 8B) were periodically sampled from January to September 2012. Production and irrigation wells were equipped with a sampling spigot while a submersible pump was used to collect groundwater from the cistern. Three perennial springs in MVGB (springs X, Y, and Z) were sampled on October 29, 2012 using a submersible pump. Similar to surface water sampling, 20 L of water was collected for each spring and groundwater sample. Prior to analysis, all samples were filtered through a 0.45 micron high-capacity filter.

4. Laboratory Analysis

Recovery of $^{35}SO_4$ was achieved using a batch method technique summarized in Urióstegui *et al*. (2015) and Chapter II. Since natural concentrations of SO_4 are low in Sierran surface waters and groundwater, a carrier (100 mg of ^{35}S-free SO_4 added as dissolved Na_2SO_4) was added to ensure effective recovery of sulfate in the sample. Samples were analyzed on an ultra-low level liquid scintillation spectrometer at the Lawrence Livermore National Laboratory in Livermore, California. $^{35}SO_4$ activities are reported in mBq/L. The minimal detectable activity (MDA) ranged from 0.3 to 2.8 mBq/L due to variations in counting efficiencies, background count rates, sample volumes, and time that elapsed between sample collection and analysis. One sigma counting errors were typically less than 0.3 mBq/L. Reproducibility of the measurements were evaluated through

comparison of field duplicates using the relative error ratio (RER), with RER values at or below 3.0 being considered reproducible.

Concentrations of SO_4, as well other anions, were determined in the samples collected from February 2010 to July 2012 by ion chromatograph on a Dionex model DX500 at BC Laboratories, Inc. in Bakersfield, California. Surface water and groundwater samples collected from September 2012 to October 2012 were analyzed at the Lawrence Livermore National Laboratory in Livermore, California, using a Metrohm Model 881 ion chromatograph.

5. Quantification of New Snowmelt Contribution

In snow dominated Sierra Nevada mid-elevation basins such as SCB and MVGB, the majority of precipitation falls as snow during the winter and completely melts by mid-summer. Snowmelt in Western mountains is a more efficient recharging agent than rain, even when snow constitutes a relatively small portion of the total precipitation (Earman *et al*., 2006). When groundwater is mainly derived from annual snowmelt, new snowmelt containing $^{35}SO_4$ can be treated as an annual pulse input to the groundwater basin. Determining the activity of ^{35}S in this pulse is not straight forward. The half-life of ^{35}S (87.5 days) is sufficiently short that significant decay will occur over the course of a snow season. Melting and recharging snow (as well as samples of accumulated snow) will contain both recent snow with high ^{35}S activity and old snow with lower ^{35}S activity. Furthermore, $^{35}SO_4$ activity of fresh snow changes from one snowfall event to another over the season as demonstrated by the MVGB snow composites (see below).

The bulk input of snow $^{35}SO_4$ activity to the SCB groundwater and surface water was assumed to initiate at the onset of snowmelt (t_0), which was define as the day after peak

41

snow water equivalence (SWE; April 7, 2010 for winter 2009/2010, and April 2, 2011 for winter 2010/2011). Due to data gaps at the SCB weather station during the study period, complementary meteorological data was obtained from SNOTEL #539 located in an adjacent basin to the north of SCB (Figure 8A). This SNOTEL station is located at 2135 m, which is approximately the mean elevation of SCB.

The percent of new snowmelt (PNS) in SCB groundwater and surface water was determined by:

$$PNS_t = \frac{A_{GW,SW}}{A_{SNOW}} * 100$$

(2)

where PNS_t is the percent of new snowmelt (PNS in %) in groundwater (GW) or surface water (SW) on collection date t; $A_{GW,SW}$ = groundwater or surface water $^{35}SO_4$ activity (mBq/L) on collection date t, with the mean activity reported for field duplicates; A_{SNOW} = mean snow $^{35}SO_4$ activity (mBq/L) on t_0, decay corrected to date t. For SCB, A_{SNOW} on t_0 (April 7, 2010) for winter 2009/2010 was assumed to be the average $^{35}SO_4$ activity for the February 13, 2010 full depth snow composites; in winter 2010/2011, A_{SNOW} on t_0 (April 2, 2011) was the average $^{35}SO_4$ activity for the March 5, 2011 full depth snow composites.

Although groundwater and surface waters in SCB is primarily derived from winter snowpack, runoff and shallow subsurface flow from precipitation or melt events that occur outside of the primary snowmelt period of spring to early summer may increase the $^{35}SO_4$ activity in surface water, particularly during baseflow conditions. The PNS for surface waters and groundwater collected from t_0 through September 31st (water year day 365) assumes an A_{SNOW} $^{35}SO_4$ activity of t_0 decay corrected to the collection date t; however, waters collected from October 1st (water year day 1) to t_0 of the following winter are not

42

decay corrected because precipitation and short melt events during this low-flow period

could increase the $^{35}SO_4$ activity leading to an overestimation of the PNS in surface waters

and shallow groundwater.

This study was expanded to MVGB in 2012 with higher-frequency snow sampling in

winter 2011/2012 allowing for greater confidence in the snow end member $^{35}SO_4$ activity.

Mean $^{35}SO_4$ activity was determined using a volume-weighted approach in which snow

$^{35}SO_4$ activity at four snow sampling locations is expressed as:

$$S_t = \frac{\sum_{i=1}^{4} a_i P_i}{P_{Total}} \tag{3}$$

where S_t is the volume-weighted mean snow $^{35}SO_4$ activity (mBq/L) for a given site decay

corrected to groundwater or surface water collection date t; a = snow $^{35}SO_4$ activity (mBq/L)

for the snow sampling event i =1 to 4 decay corrected to date t; P = precipitation amount (m)

deposited between snow sampling events (Table 7). For example, $P_{i=2}$ represents the total

precipitation that fell between time i=1 (January 25, 2012) and i=2 (February 24, 2012).

MVGB daily precipitation data was available from SNOTEL #834 near MVGB site S11

(Figure 8B) and was used for all four snow sampling locations.

Table 7. MVGB precipitation from SNOTEL #834. The precipitation amount that fell
during the sampling period represents 77% of the total precipitation during water year
2012.

Sample	Collection Date	Sampling Period	Precipitation (m)	Amount of Total Precipitation (%)*
P1	25-Jan-2012	05-Nov - 25-Jan	0.16	33
P2	24-Feb-2012	26-Jan - 24-Feb	0.02	4
P3	04-Apr-2012	25-Feb - 04-Apr	0.25	51
P4	02-May-2012	05-Apr - 02-May	0.06	13
P Total			0.49	

*Amount of total precipitation that fell during sampling period (05-Nov-2012 to 02-May-2012).

The volume-weighted mean snow activity for the entire basin was determined by:

$$A_{SNOW} = \frac{\sum_{i=1}^{4} S_i}{S_{Total}}$$

(4)

where A_{SNOW} = decay corrected mean snow $^{35}SO_4$ activity (mBq/L) for snow sampling sites

n=1 to i. Similar to SCB, the PNS in MVGB groundwater or surface water the was

calculated using Equation (2).

E. Results and Discussion

1. Snowpack End Member

Concentrations of SO_4 in SCB snowpack were consistently ≤0.5 mg/L, which is typical

of precipitation measurements in the Sierra Nevada (e.g. Williams and Melack, 1991, 1997;

Williams $et\ al.$, 1993; Chorover $et\ al.$, 1994; Meixner $et\ al.$, 1998). MVGB snow composites

also had generally low SO_4 concentrations of <0.3 mg/L in January and February 2012;

higher concentrations in May 2012 may be due to less solute dilution resulting from a

decrease in storm size (Williams and Melack, 1997).

The $^{35}SO_4$ activity of SCB snowpack ranged from 5.5±0.3 to 12.4±0.3 mBq/L (Table 8),

with an average activity of 8.3±0.1 and 7.4±0.2 mBq/L for winters 2009/2010 and

2010/2011, respectively. The SCB snowpack $^{35}SO_4$ activity are similar to values reported for

snowpack in high-elevation basins in the Rocky Mountains 13.1±0.5 to 25.0±1.7 mBq/L

(Sueker $et\ al.$, 1999, Michel $et\ al.$, 2000, Michel $et\ al.$, 2002). The $^{35}SO_4$ activity for the

higher-frequency MVGB snow composites varied between 1.1±0.5 and 52.9±3.4 mBq/L,

with the May 2, 2012 sampling event having the highest activity. Increasing MVGB snow

$^{35}SO_4$ activity from the winter to the late spring (Figure 9) may be due to stratosphere-to-

troposphere exchange during the spring and summer, which increases the depositional flux

of cosmogenic ^{35}S. Warming of air masses during the spring and summer months results in convective heating and downward transfer of aerosols into the troposphere, with peak stratosphere-to-troposphere exchange of cosmogenic radionuclides such as beryllium-7 occurring in the spring and summer at middle-latitudes, especially at high elevations (Brost *et al*., 1991; Feely *et al*., 1989).

Table 8. Sulfate concentrations and average $^{35}SO_4$ activity with 1σ counting uncertainties for SCB (Sites S01-S08) and MVGB (Sites S09-S12) winter snowpack.

SCB Site ID	Collection Date	SO$_4$ (mg/L)	$^{35}SO_4\pm1\sigma$ (mBq/L)	MVGB Site ID	Collection Date	SO$_4$ (mg/L)	$^{35}SO_4\pm1\sigma$ (mBq/L)
S01	13-Feb-2010	0.5	9.0±0.3	S09	25-Jan-2012	0.2	10.2±0.3
S02	13-Feb-2010	0.3	9.3±0.3	S10	25-Jan-2012	0.3	12.6±0.3
S02	13-Feb-2010	0.3	12.4±0.3	S11	25-Jan-2012	0.2	10.5±0.3
S03	13-Feb-2010	0.3	5.9±0.3				
S03	13-Feb-2010	0.3	7.8±0.3	S09	24-Feb-2012	<0.1	11.0±0.7
S04	13-Feb-2010	0.3	5.5±0.3	S10	24-Feb-2012	<0.1	1.1±0.5
				S11	24-Feb-2012	<0.1	2.8±0.5
S05	09-Jan-2011	<0.1	8.2±0.6	S12	24-Feb-2012	3.3	15.1±0.6
S05	09-Jan-2011	<0.1	6.8±0.6				
				S09	04-Apr-2012	3.1	17.7±0.6
S06	05-Mar-2011	0.2	5.9±0.4	S10	04-Apr-2012	<0.1	26.9±0.7
S06	05-Mar-2011	0.2	10.0±0.5	S11	04-Apr-2012	<0.1	11.9±0.5
S07	05-Mar-2011	0.2	10.4±0.5	S12	04-Apr-2012	4.1	25.4±0.6
S04	05-Mar-2011	0.2	5.9±0.4				
S04	05-Mar-2011	0.2	6.5±0.4	S09	02-May-2012	9.2	34.0±0.8
S08	05-Mar-2011	0.2	6.7±0.4	S10	02-May-2012	3.2	41.9±1.2
S08	05-Mar-2011	0.2	6.1±0.4	S11	02-May-2012	1.4	30.9±1.2
				S12	02-May-2012	5.1	52.9±3.4
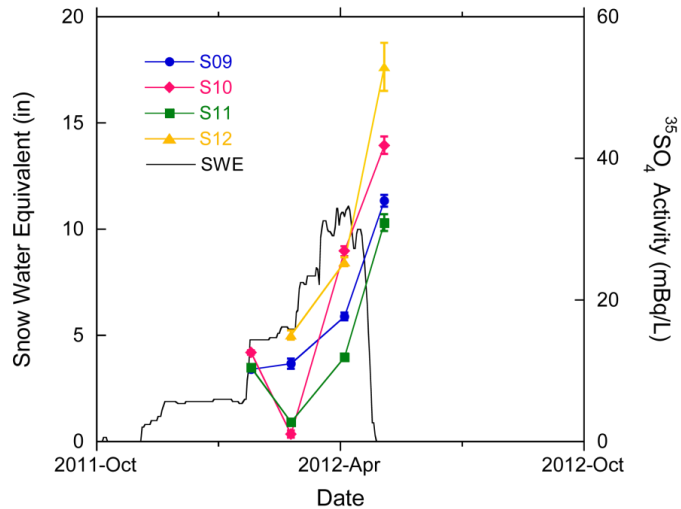
Figure 9. $^{35}SO_4$ activities for MVGB snow collected during winter 2011/2012 (January 25, February 24, April 4, and May 5). Error bars represent 1σ counting uncertainties.

2. Conservative Behavior of Sulfate in Surface Water and Groundwater

The model calculation of PNS from $^{35}SO_4$ activity assumes the sulfate is not reduced or exchanged during recharge and transport. Biogeochemical processes such as mineral weathering and ion exchange control the mobility of solutes in mountain basins. In SCB and MVGB, the majority of the groundwater and surface water samples had SO_4 concentrations that were within the range of <0.1 to 5.0 mg/L detected for most snowmelt samples. Mean groundwater ages plotted versus SO_4 concentrations for springs and wells in both SCB and MVGB reveal a minimal trend between groundwater apparent age and SO_4 concentrations (Figure 10). Rademacher *et al*. (2001) did note a trend between major cations and residence time in SCB spring water indicating that water rock interactions are occurring in the subsurface, however, this evidence supports the assumption that chemical weathering in these basins has little influence on stream SO_4 hydrochemistry at these sites. Based on the minimal trend between groundwater age and SO_4 concentrations and the limited SO_4

46

adsorption capacities found in other high-elevation Sierra Nevada catchments (Williams *et al.*, 2001), sorption of $^{35}SO_4$ in SCB and MVGB soils is not expected to affect the transport of $^{35}SO_4$ in these groundwater basins.

Figure 10. Groundwater apparent age versus SO_4 concentration for SCB and MVGB springs and wells. MVGB groundwater ages plotted at 50 years with an arrow to the right represent ages of >50 years and are not included in the calculation of the correlation coefficient. The low correlation coefficient observed for both SCB (R^2= 0.26) and MVGB (R^2= 0.12) suggests a minimal trend between groundwater apparent age and SO_4 concentrations. Groundwater apparent age data were obtained from Manning *et al.* (2012) and Segal *et al.* (2014).

Due to the capacity of vegetation and soils have the capacity to retain anions such as SO_4^{2-}, a decoupling of $^{35}SO_4^{2-}$ from the hydrologic flow path would complicate the interpretation of the new snowmelt fraction in surface water and groundwater determined by the ^{35}S tracer method. For example, SO_4^{2-} exchange in the soil zone is expected to have little effect on the total concentration of SO_4^{2-}; however, the SO_4^{2-} reaching the groundwater system or surface water would have a lower ratio of ^{35}S activity to SO_4^{2-} concentration, resulting in a smaller calculated percent new snow relative to the actual percent new snow.

A simplified SO_4 mass balance provided in Appendix A revealed a net export of SO_4 from SCB, which may be due to higher atmospheric SO_4 loading from previous decades or organic matter mineralization in the soil zone. While SO_4 may be immobilized in the soil zone or vegetation, accurate constraints to the biogeochemical cycling of SO_4 requires additional data such as stable isotopic analysis of SO_4 ($^{34}SO_4/^{32}SO_4$) to quantify the extent of biogeochemical cycling in the basin.

3. Sagehen Creek Basin: New Snowmelt Contribution to Surface Water and Groundwater

Time series measurements of $^{35}SO_4$ activities in Sagehen Creek collected from SCB site SC02 were between 0.0 ± 0.1 and 1.5 ± 0.9 mBq/L, with the exception of one sample collected August 24, 2010 and one collected August 7, 2011 that did not have detectable $^{35}SO_4$ activity (Tables 9 and 10). RER values of 0.0 to 2.2 indicate good reproducibility between sample duplicates. Calculated PNS values ranged from 0.2 ± 6.6 to $14.0\pm3.4\%$. For WY2010, the highest PNS was observed soon after the onset of snowmelt, with PNS increasing from 4.1 ± 1.6 to $14.0\pm3.4\%$ from February to April 2010 in response to snowmelt recession (Table 9, Figure 11). While stream discharge continued to increase in May 2010, PNS decreased to $4.8\pm2.7\%$. As streamflow receded in late spring and early summer, PNS in streamflow was consistently <15%, with no significant difference observed between the high-flow conditions of May 2010 ($4.8\pm2.7\%$) and baseflow conditions in August 2010 ($8.4\pm4.0\%$). These results suggest that while new meltwater is discharging into the stream via overland flow and/or shallow subsurface flowpaths during both high-flow and baseflow conditions, streamflow is primarily derived from groundwater recharged during previous winters.

Table 9. Sulfate concentrations, $^{35}SO_4$ activity, and the percent of new snowmelt (PNS) for SCB surface water from site SC02 and groundwater from Spring #11. For field duplicates, mean activity of the two measurements is reported and used to calculate PNS. Uncertainties are propagated $\pm1\sigma$ counting errors.

Date Collected	SO_4 (mg/L)	$^{35}SO_4$ (mBq/L)	Duplicate $^{35}SO_4$ (mBq/L)	RER	Reported $^{35}SO_4$ (mBq/L)	Snow $^{35}SO_4$ (mBq/L)[a]	PNS (%)
Surface water WY2010							
13-Feb-2010	1.2	0.4±0.2	0.3±0.2	0.3	0.3±0.1	8.3±0.1	4.1±1.6
25-Apr-2010	0.3	0.5±0.2	1.5±0.4	0.7	1.0±0.2	7.2±0.1	14.0±3.4
23-May-2010	0.3	0.3±0.2	NA	--	0.3±0.2	5.8±0.1	4.8±2.7
27-May-2010	0.3	0.3±0.1	NA	--	0.3±0.1	5.6±0.1	5.1±2.5
27-Jun-2010	NA	0.3±0.2	NA	--	0.3±0.2	4.4±0.1	7.5±3.9
30-Jul-2010	NA	0.4±0.1	NA	--	0.4±0.1	3.4±0.1	10.9±4.1
24-Aug-2010	0.2	ND[b]	0.2±0.1	--	0.2±0.1	2.8±0.0	8.4±4.0
Surface water WY2011							
06-Nov-2010	<0.1	0.6±0.1	0.9±0.1	2.1	0.8±0.1	8.3±0.1	9.1±1.1
12-Dec-2010	<0.1	0.6±0.1	0.6±0.1	0.0	0.6±0.1	8.3±0.1	6.9±0.9
05-Mar-2011	0.2	0.8±0.3	1.4±0.3	1.4	1.1±0.2	8.3±0.1	12.9±3.0
22-Apr-2011	0.3	1.2±0.3	0.4±0.2	2.2	0.8±0.3	6.3±0.1	12.3±4.2
08-Jun-2011	0.3	0.2±0.2	0.8±0.2	2.1	0.5±0.2	4.3±0.1	10.8±5.5
22-Jul-2011	0.2	0.0±0.1	0.2±0.1	1.4	0.1±0.2	3.1±0.1	3.5±5.3
07-Aug-2011	<0.1	ND[b]	0.0±0.2	--	0.0±0.2	2.7±0.1	0.2±6.6
Spring #11							
24-Aug-2010	<0.1	0.3±0.1	0.0±0.1	2.1	0.2±0.3	2.8±0.0	6.2±9.9
06-Mar-2011	0.2	0.1±0.3	ND[b]	--	0.1±0.3	8.3±0.1	0.8±3.5
08-Jun-2011	0.3	ND[b]	0.2±0.2	--	0.2±0.2	4.3±0.1	5.7±3.9

[a] Average decay corrected snow $^{35}SO_4$ activity for the given sample collection date
[b] Sample not incorporated into the reported $^{35}SO_4$ activity or calculated PNS
NA= Not Available
ND= Not Detectable
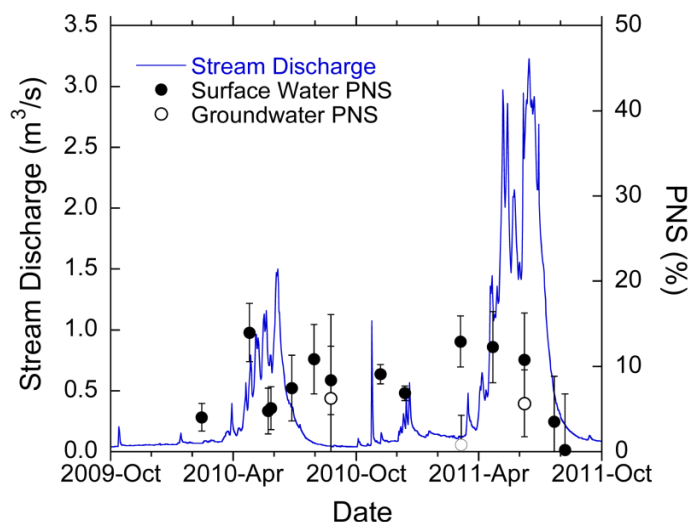
Figure 11. Sagehen Creek stream discharge and time series measurements of percent new snowmelt (PNS) in Sagehen Creek and SCB groundwater measured from Spring #11. Error bars represent propagated ±1σ counting errors. Stream discharge data from USGS National Water Information System.

To determine spatial variability of new snowmelt contribution to streamflow along Sagehen Creek, six sites were sampled along a 5 km reach on August 28, 2010 (Figure 8A). The average $^{35}SO_4$ activity for the six sites (0.1±0.1 mBq/L to 0.3±0.1 mBq/L) was not significantly different during this baseflow period, with PNS being <15% (Table 10). The low PNS throughout the reach is consistent with estimated groundwater input to streamflow using a numerical model based on $\delta^{18}O$ and CFC-12 concentrations for samples collected on August 28, 2010 at the same six sites (Earman *et al.*, 2015; Gleeson *et al.*, unpublished data). The lowest PNS calculated in this study observed at Site SC04, which is located about 2 km downstream in the transect and is the site with the highest modeled groundwater input based on $\delta^{18}O$ and CFC-12 concentrations (Gleeson *et al.*, unpublished data). While the calculated groundwater inflows varied significantly through the reach, total groundwater

input was 76% of the total flow, with the remaining 24% being derived from recent precipitation (Earman *et al*., 2015).

Table 10. Sulfate concentrations, $^{35}SO_4$ activity, and the PNS for surface water collected on August 28, 2010 from six sites along a 5 km reach Sagehen Creek. Site SC01 is located furthest downstream while site SC06 is furthest upstream. The average decay corrected snow endmember activity on August 28, 2010 was 2.8±0.0 mBq/L. Uncertainties represent propagated ±1σ counting errors.

Site ID	Distance Downstream (km)	SO_4 (mg/L)	$^{35}SO_4$ (mBq/L)	Duplicate $^{35}SO_4$ (mBq/L)	RER	Reported $^{35}SO_4$ (mBq/L)	PNS (%)
SC01	4.8	0.2	0.4±0.2	0.0±0.1	1.8	0.2±0.3	7.3±11.5
SC02	3.8	0.2	0.2±0.1	0.4±0.1	1.4	0.3±0.1	12.4±4.1
SC03	3.0	0.2	0.1±0.2	0.1±0.1	0.0	0.1±0.1	4.9±3.9
SC04	2.1	0.4	0.1±0.1	NA	--	0.1±0.1	4.0±4.8
SC05	1.2	<0.1	0.2±0.1	0.0±0.1	1.4	0.1±0.3	4.8±12.4
SC06	0	<0.1	0.3±0.2	0.2±0.1	0.4	0.2±0.1	8.3±4.4

NA= Not Available
RER= Relative Error Ratio

Similar trends of consistently low PNS in Sagehen Creek was observed throughout WY2011, despite total precipitation increasing from 0.67 to 1.22 m (82% increase) and peak SWE increasing from 0.47 to 0.89 m (53% increase) from WY2010 to WY2011. Prior to the onset of snowmelt in WY2011, the average $^{35}SO_4$ activity for streamflow in March 2011 was 1.1±0.2 mBq/L resulting in 12.9±3.0% PNS (Table 9, Figure 11). The June 8, 2011 sampling event during the peak flow period was collected within one week of the peak discharge for WY2011 (3.23 m^3/s on June 15, 2011), and PNS for this sampling event was 10.8±5.5%. During streamflow recession in July and August 2011, $^{35}SO_4$ activities declined and PNS values were 3.5±5.3 and 0.2±6.6%, respectively (Table 9). Minimal inter-annual variability of PNS in stream discharge suggests that even during a year with significantly

above average precipitation, such as the 50% above average precipitation in WY2011, Sagehen Creek stream discharge is dominated by deeper groundwater flowpaths that were recharged in previous winters.

In contrast to hydrologic models predicting that groundwater discharge to streams is inversely correlated to streamflow due to snowmelt runoff, interflow filling stream channels, and elevating stream head (Huntington and Niswonger, 2012), the trend of decreasing PNS during high flow suggests that groundwater discharge was not suppressed during the high-flow period of WY2010 or WY2011, and that overland flow and shallow subsurface flow was minimal relative to significant melt water storage and displacement of groundwater derived from previous winters.

Using the times series measurements of $^{35}SO_4$ activity and calculated PNS during the high-flow period, a hydrograph separation provides an estimate of the volumetric contribution of new snowmelt to stream discharge and groundwater recharge. The high-flow period of April to July (AMJJ) represents 79% of the total annual discharge from Sagehen Creek for WY2010 and 84% of the total discharge for WY2011, with the larger snowpack in WY2011 resulting in approximately three times the AMJJ discharge ($16.5 \times 10^6 \, m^3$) compared to WY2010 ($5.4 \times 10^6 \, m^3$) (Figure 12, Table 11). During AMJJ, new snowmelt (as defined by PNS calculated from $^{35}SO_4$ activities) contributes $8.0 \pm 0.3\%$ of total stream discharge in WY2010 and $9.9 \pm 0.5\%$ in WY2011. The difference between total annual precipitation and total stream discharge during AMJJ represents groundwater recharge, evapotranspiration (ET), and runoff outside of AMJJ season.

Based on the 27 km^2 area of SCB, SNOTEL #539 precipitation data, average daily ET of 1.4 to 1.8 mm/day (Markstrom *et al*., 2008; Tague and Peng, 2013), and the calculated new

snowmelt discharged in streamflow during AMJJ, the annual precipitation recharged to the groundwater system was between 0 and 21% in WY2010 and 41% in WY2011. These recharge values should be interpreted as maximum values since new snowmelt was observed in stream discharge outside of the AMJJ period. Assuming a specific yield of 0.08 to 0.15 and ET rate of 1.8 mm/day for SCB (Markstrom *et al*., 2008), the equivalent change in groundwater storage would be between 0 m for WY2010 and 3.4 to 6.3 m for WY2011 (Table 11). Based on the linear relationship between actual evapotranspiration and precipitation in SCB reported in Tague and Peng (2013), ET rates were estimated to be 1.4 mm/day for WY2010 and 1.8 mm/day for WY2011, resulting in a change in groundwater storage of 1.0 to 1.8 m for WY2010 and 3.4 to 6.3 m for WY2011 (Table 11).
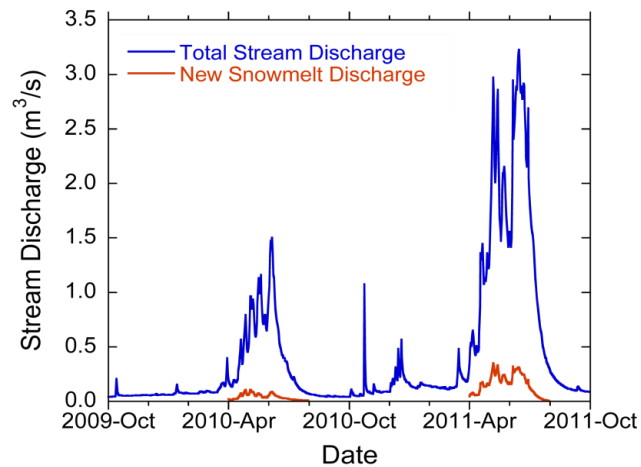
Figure 12. Hydrograph separation of Sagehen Creek discharge derived from new snowmelt during the primary discharge period of April, May, June, and July. The orange line is the contribution of new snowmelt to the total stream discharge based on the calculated PNS.

Table 11. Summary of Sagehen Creek discharge derived from new snowmelt for the primary snowmelt period of April, May, June, and July (AMJJ) and estimated change in groundwater storage.

Water Year	Total Annual Precipitation		AMJJ Total Discharge (m³)	AMJJ New Snowmelt	
	(m)	(m³)[a]		Discharge (m³)	% of Total Discharge
2010	0.7	1.8×10^7	5.4×10^6	$4.3 \times 10^5 \pm 0.2 \times 10^5$	8.0 ± 0.3
2011	1.2	3.3×10^7	16.5×10^6	$16.3 \times 10^5 \pm 0.9 \times 10^5$	9.9 ± 0.5

Water Year	Markstrom *et al.* (2008)		Tague and Peng (2013)	
	Groundwater Recharge (m³)[b]	Change in Storage (m)[c]	Groundwater Recharge (m³)[b]	Change in Storage (m)[c]
2010	1.2×10^5	0	3.9×10^6	1.0 - 1.8
2011	1.4×10^7	3.4 - 6.3	1.4×10^7	3.4 - 6.3

[a] Based on SCB drainage area of 27 km²
[b] Groundwater recharge is determined by $R = T_p - S_{AMJJ} - ET$; where R is groundwater recharge, T_p is total annual precipitation, S_{AMJJ} is the new snowmelt discharged from the basin in AMJJ, and ET is the annual evapotranspiration. Markstrom *et al.* (2008) report an average daily ET for SCB of 1.8 mm/day, while Tague and Peng (2013) estimate ET to be 1.4 mm/day for WY2010 and 1.8 mm/day for WY2011.
[c] Change in storage is the equivalent change in groundwater head based on the calculated annual groundwater recharge assuming an specific yield of 0.08 to 0.15 (Markstrom *et al.*, 2008).

Groundwater discharge collected from Spring #11 provides further insight into storage of new snowmelt in the aquifer. The $^{35}SO_4$ activity did not vary significantly between the three sampling events, which covered both baseflow and high-flow conditions. Based on $^{35}SO_4$ activity of 0.1 ± 0.3 to 0.2 ± 0.3 mBq/L during low-flow and 0.2 ± 0.2 mBq/L during high-flow, the PNS in groundwater was between 0.8 ± 3.5 and $6.2 \pm 9.9\%$ (Table 9, Figure 11). The presence of new snowmelt in SCB groundwater is supported by a recent integrated groundwater tracer and modeling study which concluded that groundwater discharge from springs is best characterized by a bimodal mixture of <1 year old water and water recharged after 1950 (Manning *et al.*, 2012).

The minimal PNS in both surface waters and groundwater throughout this study period indicate that there is substantial recharge of new snowmelt is occurring in SCB on a seasonal basis, and SCB has a relatively large groundwater storage capacity.

4. Martis Valley Groundwater Basin: New Snowmelt Contribution to Surface Water and Groundwater

In MVGB, tritium concentrations measured during WY2012 from the same wells sampled in this study suggests a pervasive component of young recharge (<50 years old) in most groundwater samples collected in multiple seasons (Segal *et al*., 2014). $^{35}SO_4$ activity in groundwater collected from 12 wells screened at a wide range of flow depths (Figure 8B, Table 12), one cistern, and three springs provides a more complete understanding of new snowmelt contribution to groundwater recharge in MVBG basin.

Table 12. Summary of well elevation and screen depth for MVGB wells.

Well ID	Well Type	Elevation (m asl)	Top (m bgs)	Bottom (m bgs)
A	Production	1753	82	274
B	Irrigation	1796	76	274
C	Production	1820	140	415
D	Production	1783	85	338
E	Production	1823	38	183
F	Production	1791	27	122
G	Production	1770	87	283
H	Production	1796	30	313
I	Irrigation	1797	15	61
J	Cistern	2073	-	-
K	Production	1783	66	244
N	Production	1832	46	274
O	Production	1830	43	274

m bgs= meters below ground surface

For the December 2011/January 2012 and June 2012 sampling events, all groundwater samples had measureable $^{35}SO_4$ between 1.0 ± 0.2 mBq/L (well E, June 2012) and 3.2 ± 0.3 mBq/L (well N, June 2012) resulting in PNS estimates of $8.4\pm2.2\%$ and $28.1\pm5.2\%$, respectively (Table 13, Figure 13). These results indicate that there is a component of new snowmelt contributing to the groundwater system throughout the winter and spring seasons, which was also observed for groundwater sampled in SCB. The generally low PNS in both shallow and deep wells in June 2012 suggests that immediately following the primary snowmelt period of April to May the majority of the groundwater (>60%) is derived from snowmelt recharged during previous winters.

Table 13. Sulfate concentrations, $^{35}SO_4$ activity, and calculated PNS for MVGB groundwater and surface water. Errors are propagated ±1σ counting errors.

Site ID	Date Collected	SO$_4$ (mg/L)	^{35}SO$_4$ (mBq/L)	PNS (%)
Wells				
A	19-Jun-2012	6.6	1.2±0.2	10.2±2.2
B	19-Jun-2012	15	1.2±0.2	10.7±2.6
C	19-Jan-2012	0.5	1.3±0.2	12.1±2.7[d]
C	19-Jun-2012	2.3	1.8±0.2	15.2±3.1
C	05-Sep-2012	2.8[a]	ND	<9[b]
D	19-Jan-2012	0.4	1.3±0.2	11.4±2.5[d]
D	19-Jun-2012	1.5	1.7±0.3	14.9±3.2
D	05-Sep-2012	1.4[a]	ND	<11[b]
E	19-Jan-2012	14	1.8±0.2	16.6±3.4[d]
E	19-Jun-2012	14	1.0±0.2	8.4±2.2
F	19-Jun-2012	0.9	2.0±0.3	17.3±3.5
F	05-Sep-2012	1[a]	ND	<11[b]
G	19-Jan-2012	4	1.2±0.2	11.0±2.5[d]
G	19-Jun-2012	3.9	1.7±0.2	14.2±2.7
G	05-Sep-2012	3.2[a]	ND	<8[b]
H	20-Dec-2011	3	1.5±0.2	13.8±3.1[d]
H	19-Jun-2012	3.4	1.9±0.2	16.3±3.0
H	05-Sep-2012	5[a]	ND	<11[b]
I	20-Jun-2012	2.7	1.9±0.2	16.3±3.2
I	05-Sep-2012	2.4[a]	0.7±0.2	10.8±3.7
J	20-Dec-2011	0.4	1.7±0.3	15.1±3.4[d]
J	20-Jun-2012	<1	2.2±0.3	19.2±3.6
J	06-Sep-2012	0.6[a]	ND	<8[b]
K	20-Dec-2011	19	1.8±0.3	15.9±3.5[d]
K	20-Jun-2012	15	1.5±0.3	13.2±3.4
N	19-Dec-2011	0.6	2.5±0.3	22.5±4.4[d]
N	20-Jun-2012	0.9	3.2±0.3	28.1±5.2
N	06-Sep-2012	1.0[a]	0.3±0.3	5.0±4.1
O	19-Dec-2011	0.6	1.9±0.3	17.2±3.7[d]
O	20-Jun-2012	1.1	2.2±0.2	19.4±3.5
O	06-Sep-2012	1.2[a]	ND	<8[b]
Springs				
X	29-Oct-2012	0.5	0.4±0.2	2.8±1.3[c]
Y	29-Oct-2012	1.3	0.6±0.3	3.7±2.0[c]
Z	29-Oct-2012	0.5	0.4±0.2	2.5±1.2[c]
Surface water				
MC01	25-Jan-2012	6.6	2.4±0.2	21.5±4.1
MC01	24-Feb-2012	5.3	ND	<14[b]
MC01	04-Apr-2012	3.5	1.6±0.4	9.8±3.3
MC01	02-May-2012	1.3	0.5±0.3	2.8±1.9
MC01	21-Jun-2012	1.0	1.8±0.2	15.3±3.1
WMC02	19-Jan-2012	1.2	1.6±0.2	14.3±2.9[d]
MMC03	24-Feb-2012	6.8	0.6±0.6	5.5±6.1
MMC03	02-May-2012	5.3	0.5±0.3	3.2±2.0
MMC03	09-Jul-2012	5.1	2.7±0.4	27.6±5.5

Site ID	Date Collected	SO$_4$ (mg/L)	^{35}SO$_4$ (mBq/L)	PNS (%)
MMC04	09-Jul-2012	<1.0	0.9±0.2	8.7±2.7
MC05	16-Aug-2012	0.8[a]	1.2±0.2	16.7±3.4
MC06	21-Jun-2012	0.8	2.0±0.2	17.6±3.3
Surface water				
MC07	09-Jul-2012	<1.0	0.9±0.2	8.9±2.5
MC08	16-Aug-2012	0.7[a]	0.8±0.2	10.3±3.2
ML	16-Aug-2012	1.2[a]	1.2±0.3	16.5±3.8
DC	21-Jun-2012	<1.0	2.5±0.2	22.0±3.9
DC	09-Jul-2012	1.2	0.9±0.3	8.6±2.9
TR	20-Dec-2011	1.4	2.2±0.3	19.9±4.3[d]
TR	21-Jun-2012	1.2	2.4±0.2	20.9±3.7
TR	09-Jul-2012	1.8	0.9±0.2	9.2±2.8
TR	16-Aug-2012	1.5[a]	1.1±0.2	15.4±2.9

[a] Sulfate concentration measured on LLNL ion chromatograph.

[b] Reported PNS value is based on the minimal detectable activity (MDA) for samples that had ^{35}SO$_4$ activities at or below background. MDA values varied between 0.5 to 0.6 mBq/L due to variations in counting efficiencies.

[c] Calculated PNS is based on the volume-weighted mean activity for MVGB snowpack decay corrected to the onset of snowmelt for WY2012, April 8, 2012 (15.7±3.2 mBq/L).

[d] Calculated PNS is based on the average snowpack activity for January 25, 2012.

ND= Not Detectable
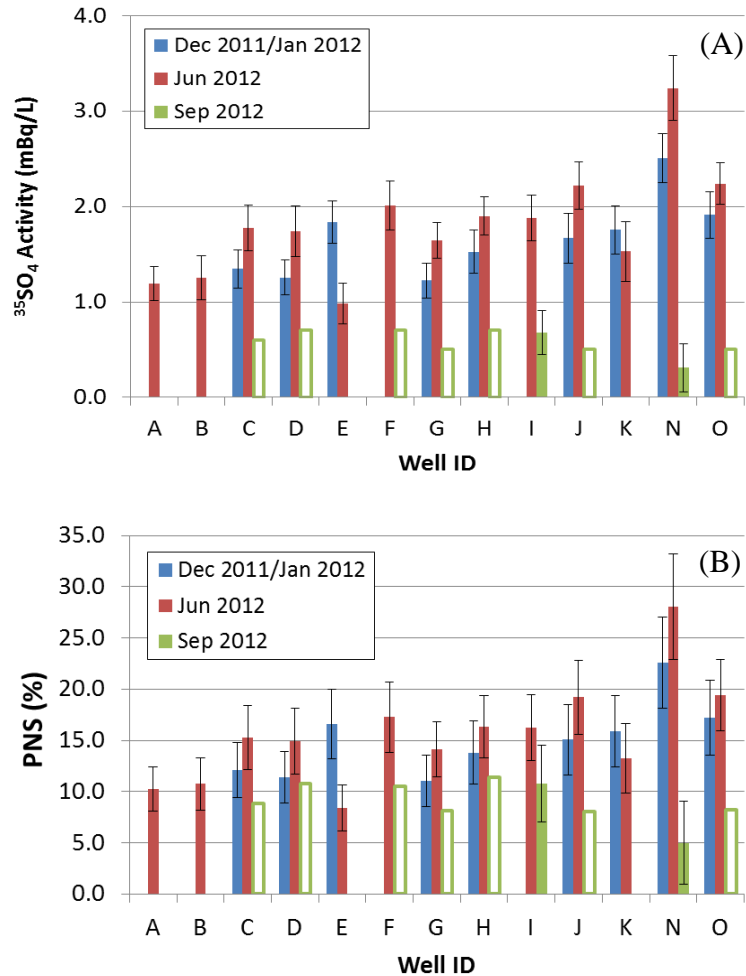
Figure 13. (A) $^{35}SO_4$ activities for 12 MVGB wells and one cistern (well J) sampled in December 2011/January 2012, June 2012, and September 2012. Open bars for September 2012 represent minimal detectable activities for samples that are at or below detection limits. (B) PNS for groundwater sampled in December 2011/January 2012, June 2012, and September 2012. Error bars are propagated 1σ counting errors.

In September 2012, only wells I and N had detectable $^{35}SO_4$ activities (Table 13), with wells C, D, F, G, H, J, and O having $^{35}SO_4$ activities at or below background levels. The largest activity of 0.7±0.2 mBq/L was observed for well I, which is the shallowest well that is likely receiving a component of water from nearby Donner Creek. Segal *et al.* (2014) reported an anomalously high noble gas recharge temperature calculated for well I in

September 2012, which the authors concluded was the result of mixing of local groundwater with water from Donner Creek during this period. Groundwater sampled from springs in October 2012 also had measurable $^{35}SO_4$ activities, indicating that groundwater derived from new snowmelt is a component of the shallow aquifer system in the fall.

For the nine wells sampled in both June and September 2012, groundwater $^{35}SO_4$ activity and subsequent PNS was significantly lower in September compared to June (Figure 13B). The apparent depletion of the new snowmelt fraction from spring to summer could be due to pumping from an age-stratified aquifer, natural discharge of new snowmelt via shallow flowpaths to streams and rivers, or mixing within the aquifer with groundwater derived from previous winters. Younger $^3H/^3He$ groundwater ages in June 2012 relative to September 2012 provide additional evidence for the depletion of a young groundwater component from spring to summer (Segal *et al*., 2014). Seasonal variability in the young (<50 year old) groundwater source (Segal *et al*., 2014) and a general shift to older $^3H/^3He$ groundwater ages from June to September may be due to a decrease in the component of new snowmelt component that was identified in this study. The unique data set of $^{35}SO_4$ activity from various depths in the groundwater aquifer and MVGB surface waters provides insight into recharge and transport of new snowmelt in the basin.

Time series measurements of $^{35}SO_4$ activity along Martis Creek, Middle Martis Creek, and West Martis Creek reveal a similar trend as that observed in SCB with an inverse correlation between PNS and stream discharge. Daily stream discharge is not available for these streams; however, a USGS stream gauge at nearby Donner Creek indicates that for WY2012, peak flows in the basin occurred from April to May 2012, and baseflow conditions were established by early August 2012. For the most frequently sampled sites

MC01 and MMC03, the $^{35}SO_4$ activity in the stream was <6% during the high-flow period of May 2012 (Table 13; Figure 14A). PNS increased significantly as stream discharge declined in late June and August; however, PNS was consistently <30% for the multiple sampling events. Surface water samples collected from June to August 2012 from ML, DC, and TR also indicate minimal contribution of new snowmelt in surface water (PNS <26%; Figure 14B).
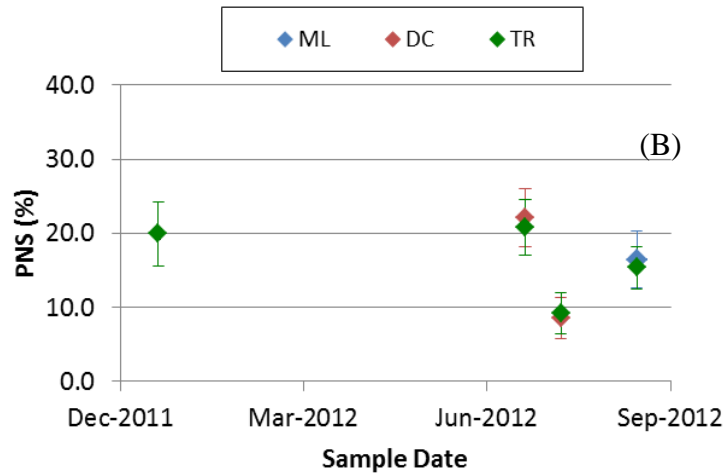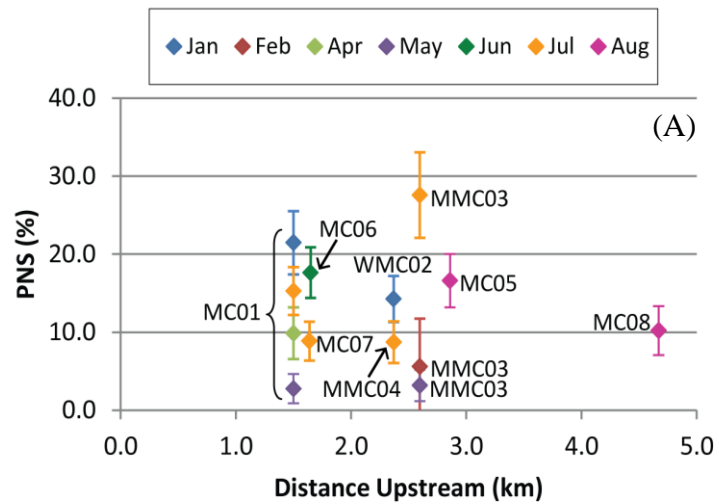
Figure 14. (A) PNS versus distance upstream from Martis Lake for surface water collected in WY2012 from along Middle Martis Creek (MMC03 and MMC04) and Martis Creek (MC01 and MC05-MC08). (B) PNS for surface water sampled from Martis Lake (ML), Donner Creek (DC), and Truckee River (TR). Error bars represent propagated $\pm 1\sigma$ counting errors.

To investigate spatial variability of new snowmelt being discharged to the stream, PNS values are plotted versus the distance upstream from Martis Lake in Figure 14A. In July 2012, the PNS for site MMC03 was 27.6±5.5%, which was significantly higher than the PNS at site MMC04 (8.7±2.7%) and MC07 (8.9±2.5%) (Figure 14A). In August 2012, the

PNS determined for the furthest upstream site, MC08, was 10.3±3.2%, which is similar to the PNS measured in July at sites MMC04 and MC07. A study using radon-222 (^{222}Rn) activity to identify groundwater influx into streams in MVGB found minimal groundwater contribution to streamflow for downstream sites MC01, WMC02, MMC03, and MMC04 in July 2012 (DeRubeis, 2013), with a secondary survey in August 2012 showing higher groundwater contribution at the MC08 upstream sampling site. Significantly higher PNS observed at site MMC03 also indicates that groundwater influx at this site is lower compared to site MC08. Although spatial variability in PNS is generally minimal along the 4 km reach, the significant increase over relatively short (<0.5 km) distances is useful in constraining groundwater discharge derived from old and new meltwater over a short study reach.

F. Conclusions

^{35}SO$_4$ is a useful intrinsic tracer that can answer questions regarding the recharge, storage, and transport of precipitation on <1 year timescales. In snow-dominated basins, the amount of snowmelt rapidly discharged from the basin during the primary snowmelt period provides insight into groundwater recharge and storage from seasonal snowmelt, which is useful for evaluating groundwater vulnerability to climate change and may lead to better surface/ground water numerical models.

This study successfully utilized ^{35}SO$_4$ to quantify the percent new snowmelt in groundwater and surface waters. A key finding was that despite large inter-annual variations in snowpack volume in SCB, new snowmelt had minimal direct contribution (PNS <15%) to Sagehen Creek stream discharge. In both basins, the low PNS in surface flows (PNS <30%) during the high-discharge period indicates that the majority of the seasonal snowmelt is

either recharging the groundwater aquifer or being stored in the soil and lost via evapotranspiration. Minimal PNS in groundwater sampled from springs or wells in both basins suggest that the groundwater reservoirs are relatively large in order to accommodate significant storage of annual snowmelt. While significant annual recharge in MVGB is consistent with a large storage capacity that would be expected for a basin of this size, the significant annual recharge from snowmelt in the smaller SCB was not expected. The implications of these findings are that the hydrogeologic system in SCB and MVGB could respond to climate change in a two-phase manner; 1) rapid responses in stream and spring discharge due to annual variability in precipitation, and 2) more gradual declines in discharge over decades due to reduced groundwater recharge resulting from declining snowpack. A test of this idea could be made now as a result of the prolonged drought these basins are currently experiencing.

As precipitation patterns continue to shift in the Sierra Nevada, the underutilized $^{35}SO_4$ tracer method will be a valuable tool for identifying how groundwater recharge processes may change under a changing climate by identifying the storage and transport of new snowmelt on short (<1 year) timescales. In addition to providing information on the relative size and storage capacity of the groundwater reservoir of a given basin, $^{35}SO_4$ may be a valuable scoping tool to identify which basins may be more vulnerable to the changing climate. Basins with shallow groundwater reservoirs are expected to have high contributions of new snowmelt in surface flows due to their limited storage capacities, and therefore would likely be the most affected by climate change.

IV. Quantifying Groundwater Travel Time near Managed Aquifer Recharge Operations using ^{35}S as an Intrinsic Tracer

A. Abstract

Identifying groundwater retention times near managed aquifer recharge (MAR) facilities is a high priority for managing water quality, especially for operations that incorporate recycled wastewater. To protect public health, California guidelines for Groundwater Replenishment Reuse Projects require a minimum 2 to 6 month subsurface retention time for recycled water depending on the level of disinfection, which highlights the importance of quantifying groundwater travel times on short time scales. This study developed and evaluated a new intrinsic tracer method using the naturally occurring radioisotope sulfur-35 (^{35}S). The 87.5 day half-life of ^{35}S is ideal for investigating groundwater travel times on the <1 year timescale of interest to MAR managers. Natural concentrations of ^{35}S in water as dissolved sulfate (^{35}SO$_4$) were measured in source waters and groundwater at the Rio Hondo Spreading Grounds in Los Angeles County, CA, and Orange County Groundwater Recharge Facilities in Orange County, CA. ^{35}SO$_4$ travel times are comparable to travel times determined by well-established deliberate tracer studies. The study also revealed that ^{35}SO$_4$ in MAR source water can vary with season and therefore careful characterization of ^{35}SO$_4$ is needed to accurately quantify groundwater travel time.

B. Introduction

Growing demands on groundwater resources makes the practice of artificially recharging underground aquifers increasingly important for supplementing water supply. In populated, semi-arid regions such as Southern California, replenishing groundwater basins using

reclaimed water provides a safe and drought resistant source for managed aquifer recharge (MAR). Water quality concerns are raised when recycled wastewater is a portion of MAR source waters. Understanding flow characteristics of recharged water near MAR operations is critical for protecting public and environmental health.

Water quality and numerical modeling studies near MAR operations have demonstrated that subsurface retention time is an important hydrologic parameter for natural removal of potential contaminants (e.g., Fox and Makam, 2009; Laws *et al*., 2011). Based on the time dependent degradation and inactivation of many contaminants in the subsurface by natural attenuation processes (e.g. Yates and Yates, 1987; Fox *et al*., 2001; Drewes *et al*., 2003; Hiscock and Grischeck, 2002; Laws *et al*., 2011), collectively known as soil aquifer treatment (SAT), current California regulations for Groundwater Replenishment Reuse Projects (GRRP) require minimum subsurface retention times for recharge water prior to extraction for potable use (California Division of Drinking Water, 2015). For MAR facilities that apply recycled municipal wastewater, the California Division of Drinking Water (DDW) recommends tracer experiments to quantify minimum retention times of no less than 2 months if the minimum pathogen removal is achieved in an above ground advanced treatment process. If tertiary treated recycled water is surface spread, the minimum retention time is 6 months.

Many common deliberate (intentionally introduced) and intrinsic (existing in the environment) hydrologic tracers utilized to investigate subsurface flow characteristics are either unable to resolve subsurface travel times on <1 year timescales or require significant field and laboratory effort. For example, shallow groundwater dating techniques using well established intrinsic tracers such as tritium/helium-3 (T/^{3}He), krypton-85 (^{85}K) and

chlorofluorocarbon (CFC) dating methods typically have uncertainties of ±2 years, which is too large to effectively determine travel time on the <1 year timescale of interest to MAR managers and regulators. Deliberate (or intentionally introduced) tracer methods such as the non-reactive, synthetic sulfur hexafluoride (SF_6) gas and noble gas isotopes of xenon (^{124}Xe and ^{136}Xe) have been used near MAR facilities (Moran and Halliwell, 2003; Clark *et al*., 2004; McDermott *et al*., 2008). A major disadvantage to the application of deliberate tracers is the significant field and laboratory effort necessary to develop sufficient data for robust breakthrough curves and to ensure that the tracer patch does not pass nearby monitoring wells without detection. Another significant limitation of deliberate hydrologic tracer experiments is that results are specific to hydrogeologic conditions and pumping regime at the time of the experiment. Furthermore, SF_6, which has been the principal deliberate tracer for determining groundwater retention times near MAR facilities in California (e.g., Gamlin *et al*., 2001; Clark *et al*., 2004, 2005; Avisar and Clark, 2005; McDormett *et al*., 2008) is now regulated because it is a strong greenhouse gas (IPPC, 1996). Current alternatives to SF_6, such as noble gas tracer studies are impractical due to high analytical costs and long analysis times despite progress being made on a new noble gas membrane inlet mass spectrometry (NG-MIMS) system (Visser *et al*., 2013). Due to the effort and timescale limitations of current tracer techniques, the development of new tracer methods that require minimal field and laboratory work, and that can resolve subsurface retention times on timescales of <1 year, will improve MAR management and safe use of recycled water for augmenting local water supplies.

This study developed and evaluated a new groundwater tracer technique to quantify subsurface travel times near MAR facilities using the naturally-occurring radionuclide

sulfur-35 (^{35}S), which is found in water as dissolved sulfate (^{35}SO$_4$). The new method was evaluated by comparing ^{35}SO$_4$ travel times to those determined with deliberate tracer experiments at two southern California field sites: the Rio Hondo Spreading Grounds (RHSG) in Los Angeles County (McDermott *et al*., 2008; Clark, 2011), and the Orange County Water District (OCWD) Groundwater Recharge Facility in Orange County (e.g., Gamlin *et al*., 2001; Clark *et al*., 2004; 2014).

C. ^{35}S as a tracer for groundwater travel time

The 87.5-day half-life of ^{35}S is ideal for investigating groundwater travel time up to 1.2 years (5 half-lives), which is the short timescale of interest to MAR managers and regulators. ^{35}SO$_4$ has been employed in hydrologic studies as an intrinsic tracer for SO$_4$ and groundwater for over two decades in high-elevation (mountain) basins (Cooper *et al*., 1991; Sueker et al., 1999; Michel *et al*., 2000; Shanley *et al*., 2005; Urióstegui *et al*., submitted); however, dilution of atmospherically-derived ^{35}SO$_4$ with anthropogenic SO$_4$ (i.e. that is SO$_4$ containing no detectable ^{35}S) in low-elevation regions of large river basins is expected to lower the specific activity of ^{35}SO$_4$ in SO$_4$. The ratio of ^{35}S to SO$_4$ may also decrease due to radioactive decay during transport downstream, or from input of ^{35}S-dead SO$_4$ from different reservoirs (soil zone, minerals, and biota). Since water in MAR facilities using recycled water is likely to have high SO$_4$ concentrations and low ^{35}S activity, a new analytical method (Urióstegui *et al*., 2015; Chapter II) was used in order to achieve accurate measurements of ^{35}SO$_4$ in these waters.

D. Travel time calculation

Under a simplified piston flow model at an MAR surface spreading facility, a deliberate or intrinsic tracer is incorporated into the source water above ground prior to recharge. Based on ideal tracers being non-reactive and not sorbing readily to the aquifer material, they are recharged and transported through the aquifer at the mean groundwater velocity. Tracer input functions in this study were empirically defined using the $^{35}SO_4$ activity of MAR surface water in spreading ponds. The subsurface travel time of water was calculated using the following decay equation:

$$t = \frac{(1/\lambda)}{ln(N_o/N)} \tag{5}$$

where t is the subsurface travel time in years, λ is the decay constant for ^{35}S (2.894 yr^{-1}), and N_o/N is the activity ratio of the $^{35}SO_4$ activity in the source water (N_o) and in the well (N) in mBq/L. Equation 5 does not account for subsurface dilution of young water (<1.2 year subsurface travel time) with older water (>1.2 year subsurface travel time), therefore the calculated subsurface travel time represents a maximum travel time because dilution of young recharge water with older groundwater would mimic radioactive decay and lower the $^{35}SO_4$ activity, resulting in an artificially long calculated subsurface travel time. The assumption made in Equation 5 of negligible dilution of young with old water is more appropriate for narrow screened shallow wells located near the infiltration basins then for longer screened productions wells located further down gradient, which likely mix groundwater of different ages (Manning *et al*., 2005; McDermott *et al*., 2008). Equation 5 also assumes conservative transport of $^{35}SO_4$ with no sorption or sulfate reduction. When considering $^{35}SO_4$ activity alone (i.e. not normalized to sulfate concentration), the effect of

sorption or sulfate reduction would be the same as mixing with older water in that the calculated subsurface travel time would be longer than the true subsurface travel time. $^{35}SO_4$ should behave as a conservative anionic complex and not experience significant sorption or reduction in oxic, near-neutral groundwaters.

E. Study sites

The RHSG and OCWD MAR sites are located in the same groundwater basin in southern California; however, due to a political divide along the Los Angeles County-Orange County line, the RHSG are situated in the Central Basin and the OCWD MAR facilities are in the Orange County Coastal Plain (Figure 15). In the northern regions of the basin, the RHSG are located in the Montebello Forebay and the OCWD MAR facilities are located within the Santa Ana Forebay. The Montebello Forebay is operated by the Los Angeles County Department of Public Works (LACDPW) and managed by the Water Replenishment District of Southern California (WRD). The facility is composed of the RHSG and San Gabriel Spreading Grounds (SGSG), with the RHSG consisting of 20 shallow (<4 m deep) infiltration basins that cover 3.1 km^2 (Figure 15). Additional basins are created in the San Gabriel River by inflating rubber dams; however, river recharge does not occur in the concrete-lined Rio Hondo River.

Artificial recharge at the Montebello Forebay began in 1938. In 1962, the Los Angeles County Sanitation Districts (LACSD) began providing tertiary-treated recycled wastewater for artificial recharge via gravity flow through river channels or pipes to the spreading basins. The 30-year average annual recharge at Montebello Forebay Spreading Grounds is 1.5×10^8 m^3 or 1.2×10^5 AF, which includes local water, imported water, and recycled water (WRD, 2015). As a drought relief measure, the regulatory limit of recycled water to

be recharged at Montebello Forebay Spreading Grounds was increased from 35% to 45% over a 10-year running average (WRD, 2015).

In the Santa Ana Forebay, natural recharge occurs primarily by direct percolation of Santa Ana River (SAR) water through highly permeable sands and gravels along the river. Since 1936, the OCWD has been artificially recharging various source waters along the SAR Channel in Anaheim, CA, including imported water from the Colorado River Aqueduct and State Water Project, SAR base flow, and SAR storm flow. In addition to the SAR channel, OCWD operates two dozen surface spreading basins at the OCWD MAR facilities that cover 6 km^2 of wetted area and range in depth from 2 m to 50 m (Figure 15). In 2008, OCWD began recharging recycled wastewater supplied by the OCWD Groundwater Replenishment System (GWRS) via a 21-km pipeline to Miller and Kraemer Basins. GWRS water is purified using a three-step advanced treatment process consisting of microfiltration, reverse osmosis and ultraviolet light with hydrogen peroxide disinfection. Annual recharge at the OCWD MAR facilities is 3.5×10^8 m^3 (2.8×10^5 AF) (Hutchinson, 2013), with GWRS supplying 15% of the total source water recharged by OCWD.
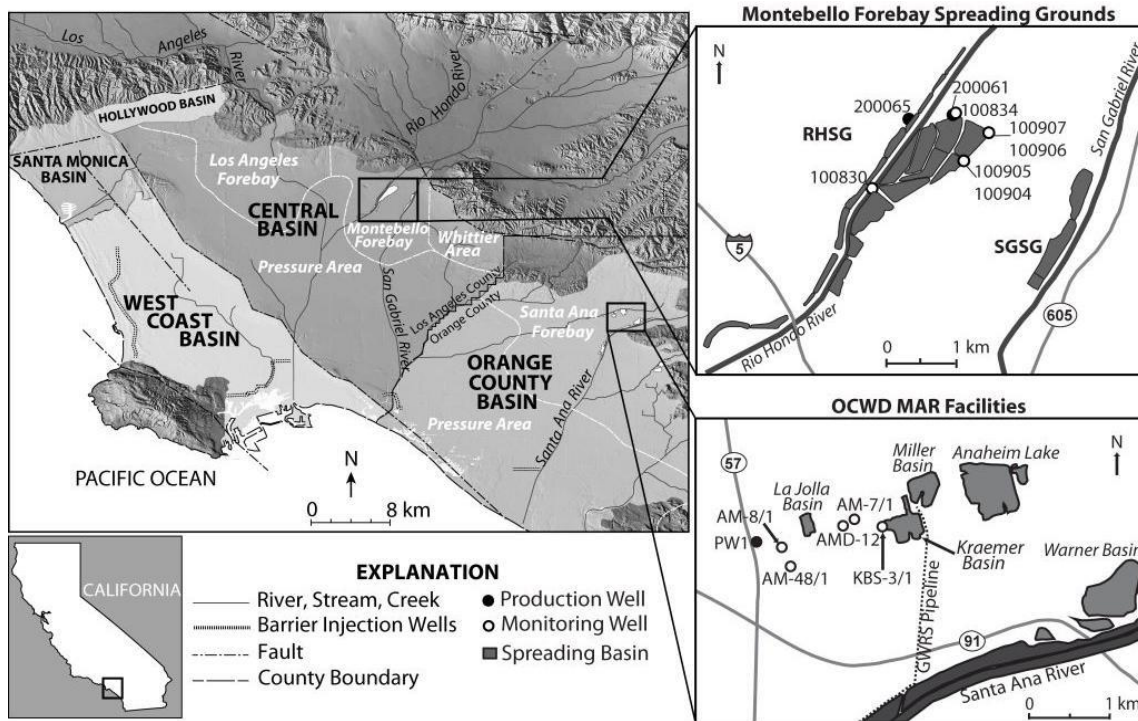
Figure 15. Location of RHSG and OCWD MAR Facilities in southern California and maps showing spreading basins and wells sampled in this study

F. Methods

1. Field Sampling

Surface water and groundwater from RHSG and OCWD MAR facilities were collected from 2010 to 2012 as part of routine monitoring at these sites. For each $^{35}SO_4$ sample, 20 L of water were field or laboratory filtered into polyethylene containers using a 0.45 micron high-capacity filter. At RHSG, six monitoring wells (100830, 100834, and 100904 to 100907) and two production wells (200061 and 200065) were sampled from January 2010 to February 2012 (Figure 15). Four of the six monitoring wells in Figure 15 occur in pairs; wells 10094 and 100906 are deep relative to 100905 and 100907 (Table 14). Surface water

from the RHSG was collected from an infiltration basin on the northern end of the spreading grounds on two sampling events: January 31, 2010 and June 2, 2010.

At the OCWD MAR study area, six monitoring wells, one production well, five infiltration basins, and SAR surface flows were sampled from December 2010 through December 2012 (Figure 15). Multiple depths were sampled at well AMD-12, with well AMD-12/1 screened at a shallower depth relative to AMD 12/2 (Table 14). On April 6, 2012, GWRS water was collected from two points along the transmission pipeline: immediately post-treatment at the Fountain Valley treatment facility and the discharge into Miller Basin. A rainwater sample collected on February 25, 2011 in Orange, CA, approximately 6 km south of the OCWD MAR facilities, provides a measure of the $^{35}SO_4$ activity of locally-derived precipitation.

Table 14. Screen depths for monitoring and production wells sampled in this study

Well ID	Well Type	Distance from Pond (m)	Depth to Top of Screen (m bgs)	Depth to Bottom of Screen (m bgs)
RHSG				
100830	Monitoring	43	16	28
100834	Monitoring	31	18	35
100904	Monitoring	3	24	27
100905	Monitoring	3	8	18
100906	Monitoring	5	23	26
100907	Monitoring	5	7	15
200061	Production	18	67	122
200065	Production	77	73	107
OCWD				
AM-7/1	Monitoring	130	64	69
AM-8/1	Monitoring	1250	82	87
AM-48/1	Monitoring	1250	82	91
AMD-12/1	Monitoring	525	101	107
AMD-12/2	Monitoring	525	149	158
KBS-3/1	Monitoring	<100	24	27
PW1	Production	1670	123	150

2. Laboratory Analysis

Recovery of $^{35}SO_4$ was achieved using the batch method technique described in Urióstegui *et al*. (2015) and Chapter II. Between 3 and 20 L were processed for each sample to obtain a desired 500 to 1500 mg of SO_4. For low-SO_4 samples containing ≤5 mg/L, a carrier (100 mg of ^{35}S-dead SO_4 as dissolved Na_2SO_4) was added to ensure effective recovery of sulfate in the sample. Results are yield-corrected based on the gravimetric recovery of $BaSO_4$ and decay-corrected to the sample collection date. One sigma counting errors were typically <2.0 mBq/L. The uncertainty reported for the calculated $^{35}SO_4$ travel times are the propagated one sigma counting errors based on the decay of ^{35}S.

Sufate concentrations for groundwater and surface waters at both study sites were determined by ion chromatography following EPA 300.0 method (Plaff, 1993). RHSG samples were analyzed on a Dionex model DX500 instrument at BC Laboratories, Inc. in Bakersfield, California. The OCWD MAR samples were analyzed on a Dionex ICS 3000 instrument at the OCWD Water Quality Laboratory in Fountain Valley, California.

G. Results and Discussion

1. Rio Hondo Spreading Grounds

RHSG surface water had $^{35}SO_4$ activities of 26.9±1.8 mBq/L on January 31, 2010 and 7.5±1.4 mBq/L on June 02, 2010. The higher activity in January is likely due to an increase in the contribution of recent storm water runoff to the spreading basin following a series of precipitation events during winter 2009/2010. Since ^{35}S is atmospherically produced, recent storm water runoff is expected to have higher concentrations of ^{35}S relative to other source components (e.g. recycled or imported water). Furthermore, because the majority of the

recharge at the RHSG typically occurs from late fall to early spring (Figure 16), the January

2010 $^{35}SO_4$ activity (26.9±1.8 mBq/L) was assumed to be the input end-member. This end-

member value was used to calculate the subsurface travel time using Equation 5.
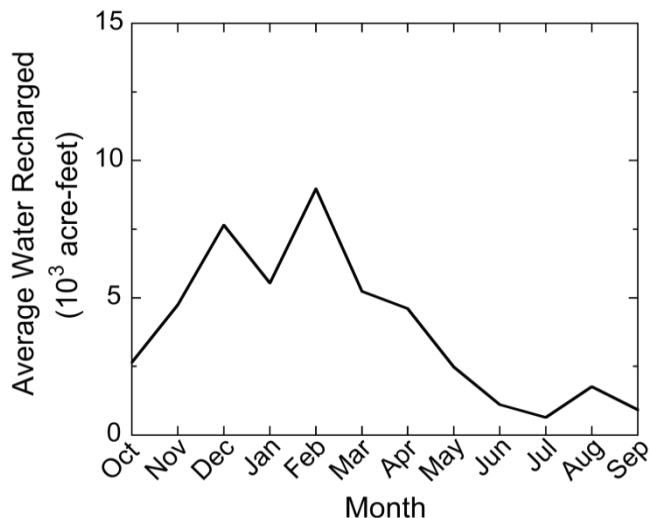
Figure 16. Average monthly water recharged at the RHSG from water year 2008-2009 to
2012-2013. The majority (79%) of the recharge occurs from late fall to early spring
(November to April) (LACDPW, 2013).

Time series measurements of $^{35}SO_4$ activities in groundwater ranged from 0.7±0.5

mBq/L to 21.1±1.7 mBq/L with the exception of the sample collected from 100905 on

February 23, 2012, which had non detectable $^{35}SO_4$ activity that resulted in a calculated

travel time of >41 weeks (Table 15). For the samples having measurable $^{35}SO_4$ activity,

calculated subsurface travel times were between 4±2 and 66+24/-10 weeks (Table 15, Figure

17). The calculated travel times represent maximum travel times because no correction was

made for mixing of young (<1.2 year old) recharge water with old (>1.2 year old)

75

groundwater within the wells. Actual travel times could be shorter if mixing occurs between these two components because dilution of young with old groundwater would appear as radioactive decay, resulting in an overestimation of groundwater travel time. Negligible mixing was assumed for the monitoring wells, which were all located at shallow depths near the infiltration basins; however, dilution at production wells should be considered because longer screened wells located further down gradient of the infiltration basins are likely to be a mixture of groundwater of different ages (McDermott *et al.*, 2008). For example, assuming no dilution at production well 200061, $^{35}SO_4$ activities resulted in travel times of 36+11/-7 weeks on March 29, 2011 and 47+16/-8 weeks on February 23, 2012. Under a mixing scenario containing a 1:5 dilution of young with old groundwater, travel times to well 200061 are 7+11/-7 and 18+17/-9 weeks for March 29, 2011 and February 23, 2012, respectively. However, both interpretations indicate that a component of recently recharged water (<1.2 yr) is produced at this well.

Assuming an end member $^{35}SO_4$ activity of 26.9±1.8 mBq/L for water recharged at the RHSG, seasonal differences in $^{35}SO_4$ travel times were observed for the monitoring wells, particularly for the two monitoring wells with the most robust data set: 100830 and 100834. For example, the three shortest $^{35}SO_4$ travel times for well 100834 occurred during the main recharge period of late fall to early spring for each water year: 20+4/-3 weeks on January 31, 2010; 10±2 weeks on March 28, 2011; and 4±2 weeks on February 23, 2012 (Figure 17). The steeper gradient due to enhanced recharge during periods of high recharge are likely driving shorter travel times to this well during the late fall to early spring period. For water year 2010 and 2011, well 100834 had longer travel times in the late spring to early summer (e.g., 43+10/-6 weeks on May 23, 2010 and 25±3 weeks on July 13, 2011). The groundwater

at well 100834 is approximately several months older in the late spring to early summer than groundwater sampled in the winter to early spring, which is expected under a simplified piston flow model.

Fewer measurements were made at the other RHSG wells; however, a similar trend of shorter travel times during the main recharge period followed by longer travel times several months later was observed for wells where multiple measurements were made within the same water year (100830, 100906, 100907: Figure 17). For example, the $^{35}SO_4$ travel time to well 100830 was 14+3/-2 and 17±3 weeks on March 24, 2011, which increased to 25+3/-2 weeks on July 13, 2011. Well 100907 had travels times of approximately 22+4/-3 weeks and 34+3/-2 weeks on the March 24, 2011 and May 23, 2011, respectively.

Table 15. Sulfate concentration, $^{35}SO_4$ activity, and subsurface travel time for groundwater collected at RHSG.

Well ID and Collection Date	SO$_4$ (mg/L)	$^{35}SO_4\pm1\sigma$ (mBq/L)[a]	$^{35}SO_4$ Travel Time$\pm1\sigma$ (weeks)[b]	Well ID and Collection Date	SO$_4$ (mg/L)	$^{35}SO_4\pm1\sigma$ (mBq/L)[a]	$^{35}SO_4$ Travel Time$\pm1\sigma$ (weeks)[b]
100830				100905			
24-Mar-2011	30	12.6±1.4	14+3/-2	13-July-2011	36	7.1±1.1	24±3
24-Mar-2011[c]	30	10.7±1.6	17±3	23-Feb-2012	67	ND	>41
13-Jul-2011	21	6.9±0.8	25+3/-2	100906			
15-Sep-2011	30	1.7±0.6	50+8/-5	23-May-2011	NA	4.0±0.9[d]	34+5/-4
04-Jan-2012	30	2.8±0.6	40±4	13-Jul-2011	25	3.8±0.8	35±4
23-Feb-2012	34	6.0±0.8	27±3	07-Jan-2012	21	1.6±0.5	51+7/-5
100834				23-Feb-2012	44	2.4±1.0	44+9/-6
31-Jan-2010	21	8.9±1.6[d]	20+4/-3	100907			
22-Apr-2010	106	3.3±1.1[d]	38+8/-5	24-Mar-2011	32	7.9±1.5	22+4/-3
23-May-2010	146	2.5±1.0[d]	43+10/-6	24-Mar-2011[c]	32	8.3±1.8	21+5/-4
28-Mar-2011	28	15.0±1.0	10±2	23-May-2011	22	4.1±0.5	34+3/-2
13-Jul-2011	32	6.5±1.0	25±3	07-Jan-2012	23	0.7±0.5	66+24/-10
04-Jan-2012	25	5.4±0.6	29±2	200061			
23-Feb-2012	70	21.1±1.7	4±2	29-Mar-2011	77	3.7±1.7	36+11/-7
100904				23-Feb-2012	56	2.0±1.2	47+16/-8
28-Mar-2011	29	12.0±1.3	15±2	200065			
28-Mar-2011	29	13.0±1.7	13+3/-2	24-Mar-2011	83	ND	>32
24-May-2011	22	10.3±0.6	17±2				
23-Feb-2012	66	2.5±1.5	42+16/-8				

[a] Reported error is 1σ counting error.

[b] Travel times calculated using 26.9±1.8 mBq/L end-member value. Reported error is the propagated 1σ counting error based on the decay of ^{35}S.

[c] Field duplicate

[d] Assumed 100% chemical yield

[e] Travel time for sample with non detectable $^{35}SO_4$ activity is calculated using the 2σ counting error.

NA= Not available
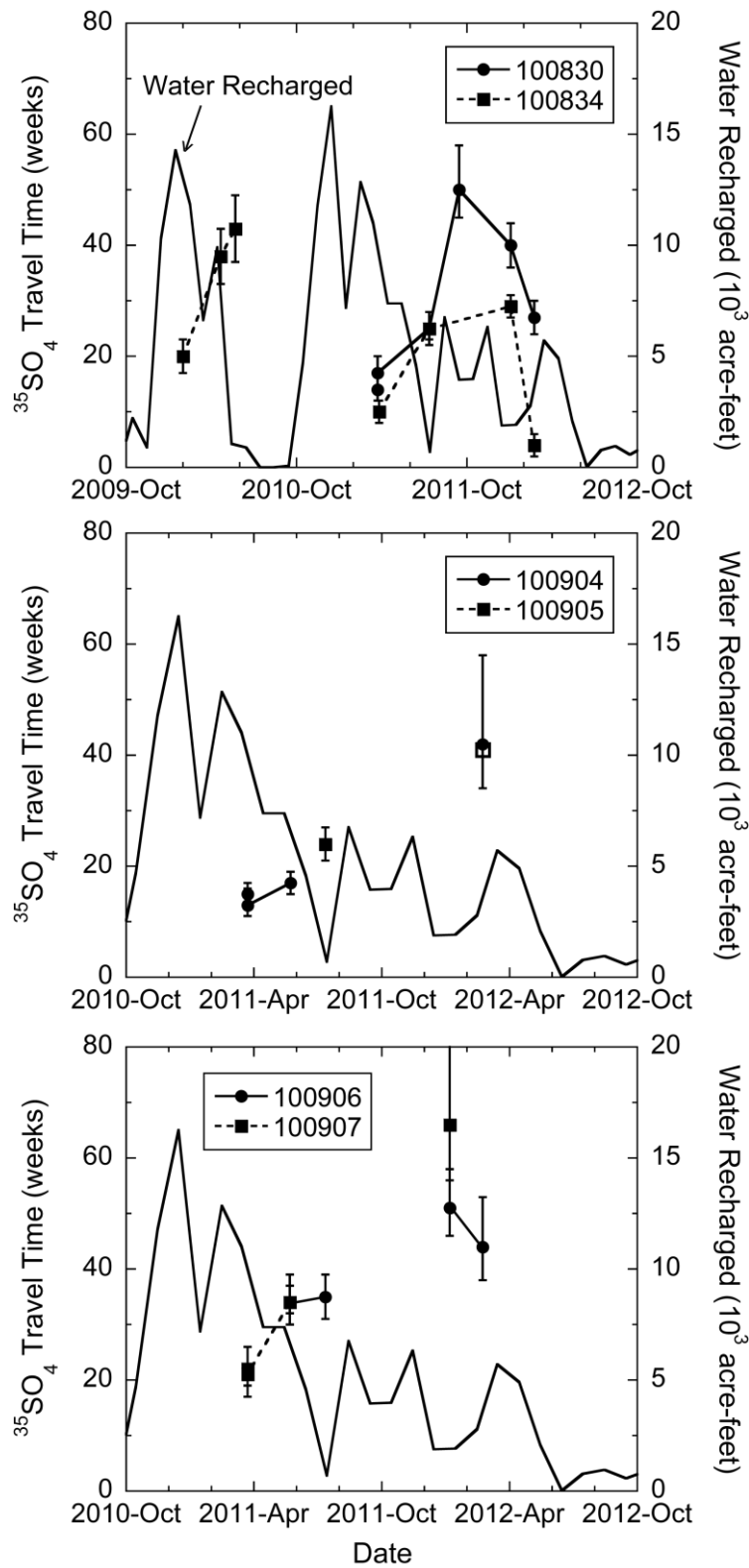
Figure 17. Time series of $^{35}SO_4$ travel times for monitoring wells and monthly recharge at RHSG. The February 23, 2012 sample collected from well 100905 had $^{35}SO_4$ activity below detection limit, therefore the open symbol represents a minimum travel time.

A deliberate tracer study using SF_6 gas that was initiated at the RHSG in January 2010 (Clark *et al*., 2011) provides a valuable opportunity to evaluate the $^{35}SO_4$ method. From a DDW perspective, deliberate tracers like SF_6 are more conservative compared to intrinsic tracer methods like $^{35}SO_4$. Given the less conservative nature of intrinsic tracers, DDW requires a multiplier of 1.5 to estimate travel time; a travel time of 6 months using deliberate tracer methods would be 9 months using intrinsic tracers.

It is important to consider that deliberate and intrinsic tracer experiments may measure different hydrologic conditions and give different travel times. With deliberate tracer experiments, a conservative tracer is applied during a discrete wetting event, thus the mean groundwater travel times (defined as passage of 50% of the tracer patch) are dependent on the hydrologic conditions during the pulse release. In contrast, the naturally occurring $^{35}SO_4$ tracer is applied intermittently during recharge events when the source water contains a fraction of recent (<1.2 year old) runoff. Although these different source functions likely result in different groundwater travel times, the SF_6 experiment provides a useful comparison to identify trends in the subsurface travel times of recharged water to nearby wells.

The shortest $^{35}SO_4$ subsurface travel time for a given well was selected for comparison with the mean SF_6 travel for that well because it represents the most conservative estimate that would be of interest to MAR managers. $^{35}SO_4$ travel times were within six weeks (1.5 months) of SF_6 travel times at three of the six monitoring wells: 100830, 100904, and 100906 (Table 16). Production wells 200061 and 200065 travel times were also in agreement for each tracer experiment indicating travel times of ≥36 weeks, suggesting that

dilution of recent recharge with older groundwater is not a significant factor in the calculation of $^{35}SO_4$ travel time.

Compared to the SF$_6$ deliberate tracer method, $^{35}SO_4$ as an intrinsic tracer provided reasonable estimates of subsurface travel times for the majority of the wells, but underestimated travel time to well 100834 while overestimating travel time to wells 100905 and 100907. Based on the seasonal trends observed for wells that were sampled frequently throughout the water year, monthly sampling of $^{35}SO_4$ in groundwater is recommended for future studies.

Table 16. Comparison of $^{35}SO_4$ and SF$_6$ subsurface travel times at RHSG.

Well ID	Collection Month-Year		Travel time (weeks)	
	$^{35}SO_4$	SF$_6$	$^{35}SO_4$[a]	SF$_6$[b]
100830	Mar-2011	Jun-2010	14±2	19
100834	Feb-2012	Jun-2010	4±2	18
100904	May-2011	May-2010	13±3	16
100905	July-2011	Apr-2010	24±3	13
100906	May-2011	Aug-2010	34±4	28
100907	Mar-2011	Mar-2010	21±4	6
200061	Mar-2011	Oct-2010	36±8	38
200065	Mar-2011	Jan-2012	47±22	>104

[a] $^{35}SO_4$ travel times are the shortest travel times measured for each well. Reported errors are propagated 1σ counting error.
[b] SF$_6$ travel times are the mean travel times derived from the center of mass (COM) arrivals to wells reported by Clark *et al.* (2011).

2. Orange County Groundwater Recharge Facilities

At the OCWD MAR site, $^{35}SO_4$ activity of surface waters from five infiltration basins and the SAR channel was 0.2 ± 0.7 to 28.4 ± 2.5 mBq/L, with the exception of four of the total 50 samples that had no detectable $^{35}SO_4$ activity (Table 17, Figure 18). Despite low $^{35}SO_4$ activity in post-treatment GWRS water (0.6 ± 0.1 and 0.7 ± 0.1 mBq/L), measurable $^{35}SO_4$ in the majority of samples collected from Miller and Kraemer Basins indicates a larger fraction of recent (<1.2 year old) water in the spreading ponds relative to GWRS water. Dry deposition of ^{35}S in SO_4 aerosols may also contribute to the higher activity in spreading ponds relative to GWRS water.

Compared to the $^{35}SO_4$ activity in local precipitation (20.7 ± 0.8 mBq/L), the lower $^{35}SO_4$ activity in the majority of OCWD MAR surface waters implies dilution of locally derived storm runoff with ^{35}S-dead water (e.g. imported water), and/or storage of recent runoff in surface reservoirs for >1.2 years prior to its delivery to the spreading basins. In fiscal year (FY) 2011-12 (July 2011 to June 2012), storm flow and local water made up less than 12% of the total source water to the groundwater basin (Hutchinson, 2013). Moreover, local average rainfall was 8.2 in for FY 2011-12 and 5.8 in in FY 2012-2013, which was more than 40% below the 50-yr average of 14.4 inches (Hutchinson, 2013; Hutchinson, pers. comm.). During these relatively dry water years, low inputs of storm flow/local water combined with high inputs of imported water and SAR base flow resulted in lower $^{35}SO_4$ activity in OCWD surface waters relative to local precipitation.

$^{35}SO_4$ activity in OCWD MAR surface water varies significantly by season (Figure 18) due to seasonal differences in recharge source water, with the exception of La Jolla Basin which had the lowest volume recharged during the study period (Figure 19). Higher $^{35}SO_4$

activity was generally observed in the early spring, likely due to a larger component or recent storm runoff in the spring months. For example, average $^{35}SO_4$ activity in Warner Basin increased from 4.1±0.9 on December 10, 2012 to more than 15 mBq/L in February and April 2013 (Table 17, Figure 18).

Table 17. Sulfate concentrations and $^{35}SO_4$ activity for OCWD MAR surface water and precipitation.

Sample ID and Collection Date	SO$_4$ (mg/L)	$^{35}SO_4\pm1\sigma$ (mBq/L)[a] Sample	Field Duplicate	Reported[c]
SAR				
06-Mar-2012	154	18.9±4.0	11.0±3.9	15.0±2.8
05-Jun-2012	168	ND	NA	ND
04-Dec-2012	89.8	5.3±1.1	3.2±1.0	4.3±0.7
05-Feb-2013	137	8.3±1.9	19.0±2.4	13.7±1.5
02-Apr-2013	133	16.2±1.7	NA	16.2±1.7
Warner Basin				
20-Mar-2012	122	15.4±2.1	NA	15.4±2.1
10-Dec-2012	117	1.5±1.2	6.6±1.3	4.1±0.9
04-Feb-2013	110	14.9±1.7	20.6±2.0	17.8±1.3
01-Apr-2013	125	22.0±1.8	NA	22.0±1.8
18-Jun-2013	142	6.9±3.6	5.0±4.1	6.0±2.7
La Jolla Basin				
10-Dec-2012	73.4	ND	0.3±0.8	0.3±0.8
04-Feb-2013	117	13.6±1.8	16.0±2.0	14.8±1.3
01-Apr-2013	215	16.0±2.3	15.0±2.3	15.5±1.6
Anaheim Lake				
06-Mar-2012	132	22.7±3.5	2.5±3.2	12.6±2.4
01-Oct-2012	27.1	6.0±0.6	5.9±0.6	6.0±0.4
05-Feb-2013	119	8.6±1.6	18.5±2.1	13.6±1.3
04-Jun-2013	160	3.9±4.1	8.3±4.5	6.1±3.0

Sample ID and Collection Date	SO$_4$ (mg/L)	$^{35}SO_4\pm1\sigma$ (mBq/L)[a] Sample	Field Duplicate	Reported[c]
Miller Basin				
20-Mar-2012	130	ND	NA	ND
06-Apr-2012	1.3	2.0±0.7[b]	0.8±0.6[b]	1.4±0.5
05-Jun-2012	1.3	0.4±0.7	0.2±0.7	0.3±0.5
25-Sep-2012	0.5	1.9±0.3[b]	1.7±0.3[b]	1.8±0.2
04-Dec-2012	0.6	0.6±0.2[b]	1.0±0.3[b]	0.8±0.2
02-Apr-2013	0.8	1.5±0.2	1.2±0.2	1.4±0.1
04-Jun-2013	4	1.7±0.6	2.2±0.6	2.0±0.4
Kraemer Basin				
20-Mar-2012	2.3	ND	NA	ND
05-Jun-2012	<0.5	0.3±0.6[b]	0.5±0.6[b]	0.4±0.4
10-Dec-2012	72.7	ND	NA	ND
05-Feb-2013	109	17.1±1.7	19.4±1.9	18.3±1.3
01-Apr-2013	188	28.4±2.5	11.1±2.0	19.8±1.6
Rain[d]				
25-Feb-2011	NA	19.9±1.1	21.4±1.2	20.7±0.8
GWRS TF[e]				
06-Apr-2012	1.1	0.6±0.1[b]	NA	0.6±0.1[b]
GWRS MB[e]				
06-Apr-2012	0.6	0.7±0.1[b]	NA	0.7±0.1[b]

[a] Reported error is 1σ counting error.
[b] Assumed 100% chemical yield.
[c] For field duplicates, the reported $^{35}SO_4$ activity is the average activity for the two samples.
[d] Rain sample was collected in the city of Orange, CA, from a location 6 km south of the OCWD MAR sites.
[e] GWRS water was sampled from two locations along the transmission pipeline: (1) water immediately post-treatment at the treatment facility in Fountain Valley (GWRS TF), and (2) GWRS discharge into Miller Basin (GWRS MB).
NA=Not Available
ND=Not Detectable

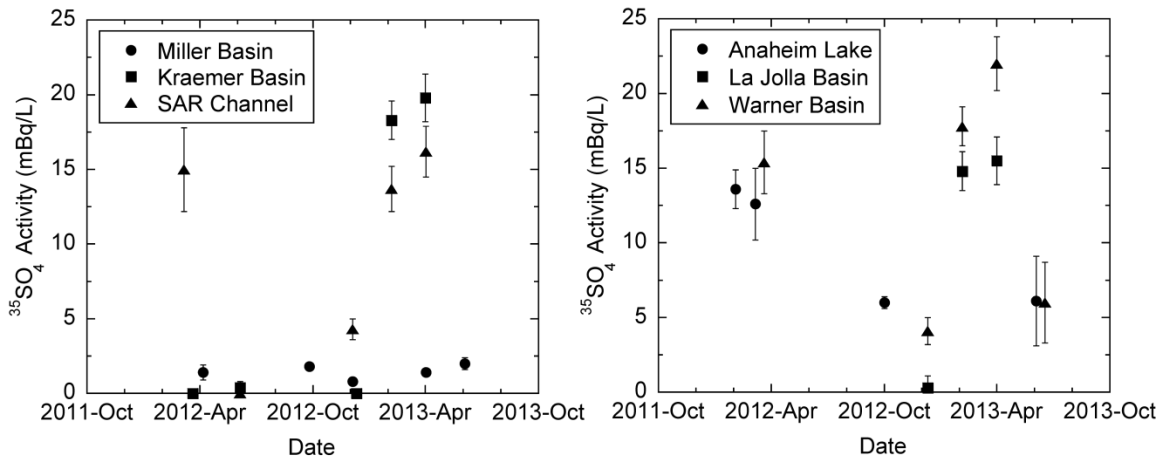**Figure 18.** $^{35}SO_4$ activities in surface water collected from OCWD MAR sites. Samples with non detectable activity are plotted as 0 mBq/L. Error bars represent 1σ counting errors.
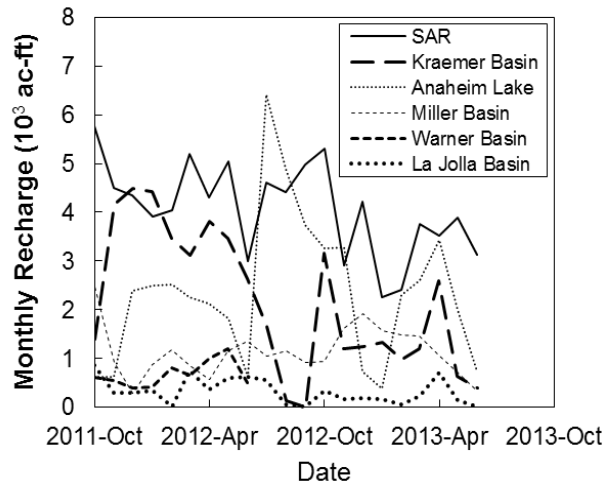
Figure 19. Total monthly recharge from October 2011 to June 2013 for the OCWD MAR spreading basins (Hutchinson, 2013). For Warner Basin, monthly recharge was available from October 2011 to June 2012.

Groundwater contours indicate that the general groundwater flow direction for the study area is in the west to southwest direction (Clark *et al*., 2004; 2014). Kraemer Basin is the nearest up-gradient spreading basin for monitoring wells AM-7/1, AM-12/1, AM-12/2, and KBS-3/1, and La Jolla Basin is the nearest up-gradient basin for wells AM-8/1, AM-48/1, and PW1. A deliberate tracer experiment conducted by Clark *et al*. (2004) demonstrated that all of the wells sampled in this study were hydraulically connected to Kraemer Basin. La Jolla Basin was put into operation in December 2007, and a second tracer study by Clark *et al*. (2014) in January 2008 demonstrated a similar trend in hydraulic gradients.

Since the average annual recharge at La Jolla Basin is less than 25% of the volume recharged at Kraemer Basin (Figure 20: 6.4 x 10^3 AF for La Jolla Basin and 2.9 x 10^4 AF for Kraemer Basin; Hutchinson, 2013), Kraemer Basin was assumed to be the main input source for all OCWD wells sampled in this study. Due to the highly variable monthly recharge at OCWD spreading basins during the study period (Figure 19), the input end-member was defined as the average $^{35}SO_4$ activity for Kraemer Basin for surface water samples that were above detection: 12.8±0.7 mBq/L.
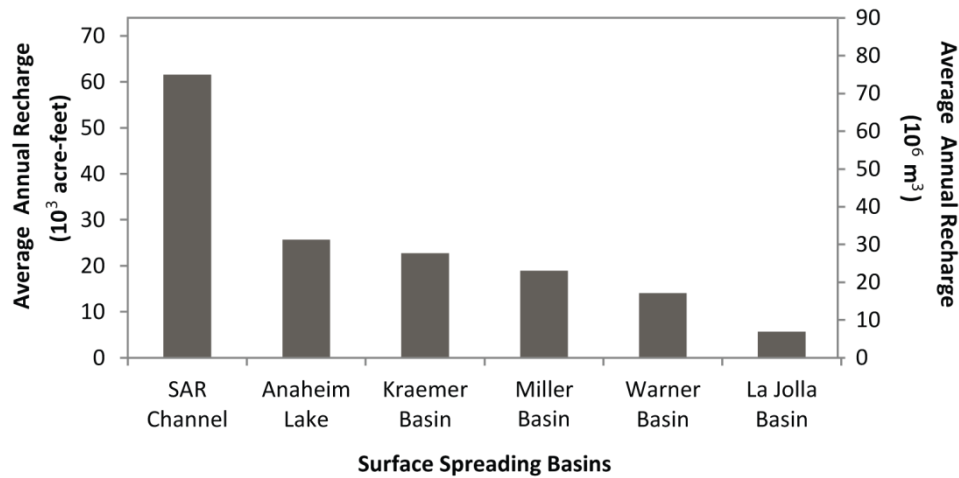
Figure 20. Average annual recharge for OCWD MAR spreading ponds. Reported values for SAR Channel, Anaheim Lake, Kraemer, and Miller are the 5-year average for July to June, 2007-2008 to 2011-2012. Since service to La Jolla Basin began in December 2007, the reported value for this basin is the 4-year average for July to June, 2008-2009 to 2011-2012 (Hutchinson, 2013). Miller Basin and Kraemer Basin receive GWRS water.

Based on the end-member value of 12.8±0.7 mBq/L, $^{35}SO_4$ groundwater travel times at OCWD were between 9±3 and >51 weeks (Table 18, Figure 21). A travel time could not be calculated for KBS-3/1 on February 05, 2013 because the groundwater $^{35}SO_4$ activity was larger than the input end-member. Time series measurements of groundwater travel times were seasonally variable, which may due to high variability in the source water end-member. For example, the $^{35}SO_4$ travel times for well AM-8/1 were between 11±2 and >51 weeks based on the input end-member of 12.8±0.7 mBq/L; however, assuming an end-member value of 19.8±1.6 mBq/L, which was the highest $^{35}SO_4$ activity observed for Kraemer Basin, the range of $^{35}SO_4$ travel times for well AM-8/1 increases to between 19±2 and >59 weeks. The increase in travel time of approximately 8 weeks (2 months) may explain some of the variability observed for the time series measurements of groundwater

travel times at the OCWD MAR site. These results highlight the need for careful

characterization of the input endmember at MAR sites where $^{35}SO_4$ activity in recharge

source water varies significantly by season.

Table 18. Summary of sulfate concentrations, $^{35}SO_4$ activities, and subsurface travel times for OCWD MAR groundwater.

Well ID and Collection Date	SO$_4$ (mg/L)	$^{35}SO_4 \pm 1\sigma$ (mBq/L)[a]			$^{35}SO_4$ Travel Time$\pm 1\sigma$ (weeks)[d]
		Sample	Field Duplicate	Reported[c]	
KBS-3/1					
13-Sep-2012	2.3	7.3±0.7[b]	NA	7.3±0.7[b]	10±2
10-Dec-2012	99.5	ND	NA	ND	>47[e]
05-Feb-2013	112	15.9±1.8	11.3±1.8	13.6±1.3	*
02-Apr-2013	177	5.4±1.8	NA	5.4±1.8	16+7/-5
AM-7/1					
21-Mar-2012	6.4	4.2±0.6	NA	4.2±0.6	20±3
22-May-2012	3.1	2.0±0.2[b]	2.2±0.6	2.1±0.3	33±3
25-Sep-2012	4.3	2.5±0.3	2.3±0.3	2.4±0.2	30±2
19-Nov-2012	2.4	1.4±0.2[b]	1.6±0.2[b]	1.5±0.1	39+2/-1
27-Feb-2013	17.3	4.5±0.4	3.4±0.5	4.0±0.3	21±2
16-Apr-2013	46.3	3.1±0.4	2.4±0.5	2.8±0.3	27±2
11-Jun-2013	53	1.7±1.4	1.5±1.4	1.6±1.0	38+18/-9
AM-8/1					
22-May-2012	58.9	1.7±0.6	1.0±0.6	1.4±0.4	40+6/-5
13-Sep-2012	34.2	7.0±0.7	NA	7.0±0.7	11±2
19-Nov-2012	26.1	ND	ND	ND	>51[e]
27-Feb-2013	15.7	3.0±0.4	2.8±0.3	2.9±0.3	27±2
16-Apr-2013	20.7	2.4±0.3	2.1±0.3	2.3±0.2	31±2
11-Jun-2013	21	2.6±0.8	2.5±0.8	2.6±0.6	29+5/-4
AM-48/1					
21-Mar-2012	86.3	ND	NA	ND	>24[e]
03-Oct-2012	36.8	ND	ND	ND	>42[e]
05-Feb-2013	25.2	3.9±0.5	4.2±0.6	4.1±0.4	21±2
04-Apr-2013	44.3	2.7±0.4	4.3±0.6	3.5±0.4	23±2
AMD-12/1					
21-Mar-2012	36.7	ND	ND	ND	>36[e]
22-May-2012	51.4	2.6±0.6	NA	2.6±0.6	29+5/-4
19-Nov-2012	52.5	ND	ND	ND	>43[e]
05-Feb-2013	17.9	2.9±0.3	3.8±0.5	3.4±0.3	24±2
16-Apr-2013	9.1	1.7±0.2	2.6±0.3	2.2±0.2	32±2
11-Jun-2013	4	1.6±0.5	1.9±0.6	1.8±0.4	35+5/-4

| Well ID and Collection Date | SO$_4$ (mg/L) | ^{35}SO$_4$±1σ (mBq/L)[a] | | | ^{35}SO$_4$ Travel Time±1σ (weeks)[d] |
		Sample	Field Duplicate	Reported[c]	
AMD-12/2					
21-Mar-2012	74	2.5±2.1	1.2±1.6	1.9±1.3	34+21/-9
26-Feb-2013	136	4.8±1.6	10.3±1.8	7.6±1.2	9±3
16-Apr-2013	142	ND	NA	ND	>30[e]
11-June-2013	108	3.2±2.7	10.1±3.2	6.7±2.1	12+7/-5
PW1					
04-Jun-2012	83.7	ND	NA	ND	>33[e]
10-Dec-2012	29.9	ND	ND	ND	>51[e]
04-Feb-2013	27.8	4.3±0.5	4.4±0.6	4.4±0.4	19±2
03-Jun-2013	26	2.7±0.9	2.8±0.8[b]	2.8±0.6	27+5/-4

[a] Reported error is 1σ counting error.

[b] Assumed 100% chemical yield.

[c] For field duplicates, the reported ^{35}SO$_4$ activity is the average activity for the two samples.

[d] Travel times calculated assuming 12.8±0.7 mBq/L as the ^{35}SO$_4$ input end-member. Reported error is 1σ counting error based on the decay of ^{35}S.

[e] Travel times for samples with non detectable activity are calculated using the 2σ counting error.

* Travel time undetermined due to a higher ^{35}SO$_4$ activity for groundwater relative to the source water end-member.
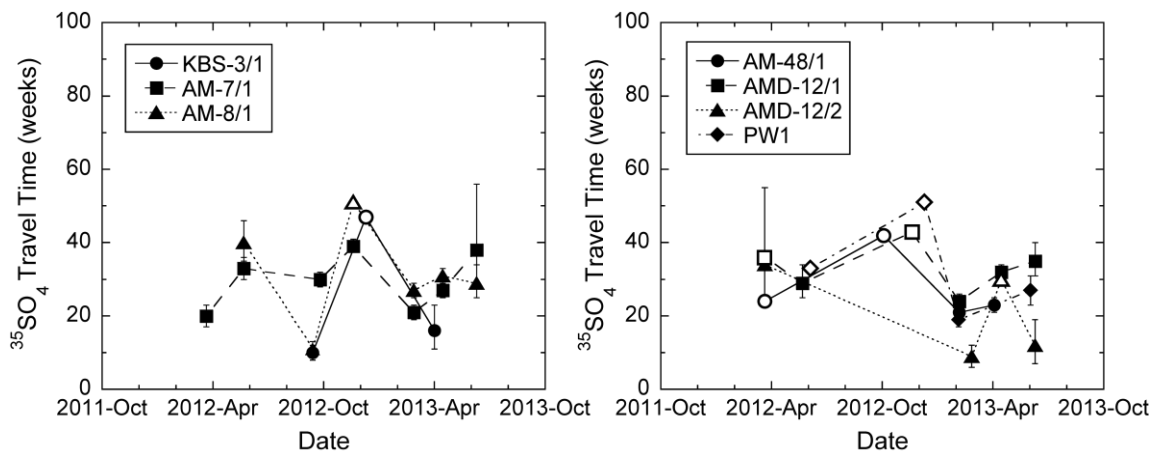
NA=Not Available

ND=Not Detectable

Figure 21. ^{35}SO$_4$ groundwater travel times from Kraemer Basin to down gradient wells. Open symbols represent sampling events that were below detection, therefore these values are interpreted as a minimum travel time.

Similar to the RHSG study, $^{35}SO_4$ groundwater travel times at OCWD are reasonable compared to those determined by a previous deliberate tracer study (Table 19). The shortest $^{35}SO_4$ travel times are within six weeks of mean SF_6 travel times for wells AM-7/1, AMD-12/1, and AM-48/1 (Table 19). The shorter $^{35}SO_4$ travel time to well AM-8/1 (11 ± 2 weeks) relative to SF_6 travel time (37 weeks) indicates that recharge to La Jolla Basin had a significant effect on travel time to this nearby, down gradient well.

Table 19. Comparison of groundwater travel times at OCWD MAR sites determined by $^{35}SO_4$ and SF_6 tracers.

Well ID	Collection Month-Year		Travel Time (weeks)	
	$^{35}SO_4$	SF_6	$^{35}SO_4$[a]	SF_6[b]
AM-7/1	Feb-2013	Jul-2008	21 ± 2	24
AM-8/1	Sep-2012	Sep-2008	11 ± 2	37
AMD-12/1	Feb-2013	Aug-2008	24 ± 2	31
AMD-12/2	Feb-2013	>Jan-2009	9 ± 3	>50
AM-48/1	Feb-2013	Jul-2008	21 ± 2	26
KBS-3/1	Sep-2012	-	10 ± 2	*
PW1	Mar-2012	-	19 ± 2	*

[a] $^{35}SO_4$ travel times are the shortest travel times measured for each well assuming an input end-member of 12.8 ± 0.7 mBq/L. Reported error is the propagated 1σ counting error.
[b] SF_6 travel times are the mean travel times to wells reported by Clark (2014).
*Incomplete breakthrough: center mass travel time is a minimum or could not be calculated.

H. Conclusions

This study successfully used the new analytical technique of Urióstegui *et al*. (2015) for measuring naturally-occurring $^{35}SO_4$ in the high SO_4 waters typical of MAR facilities. $^{35}SO_4$ activities in MAR groundwater and source waters collected from RHSG and OCWD MAR sites were successfully measured, and calculated travel times were reasonable compared to those determined by the well-established SF_6 and Xe-isotope deliberate tracer method at these sites. However, in some cases travel times were different.

$^{35}SO_4$ should be considered as new intrinsic groundwater dating tool with some considerations. Successful application of the $^{35}SO_4$ method at MAR sites is dependent on characterization of the $^{35}SO_4$ activities in MAR source waters and evaluation of mixing scenarios. MAR facilities using recycled water are likely to have high SO_4 concentrations and low ^{35}S activity. The lack of recent (<1.2 year old) water in MAR source waters limits the application of the $^{35}SO_4$ method due to consistently low $^{35}SO_4$ activity in recharge surface waters. For example, in order to quantify $^{35}SO_4$ subsurface travel times up to 9 months (3 half-lives) for piston flow transport of recharge water to nearby wells, $^{35}SO_4$ activity in source waters should ideally be 8 times above background count rates. Another factor affecting the application of the $^{35}SO_4$ method is potential dilution of recharge water with older groundwater. While considered at these study sites, the travel time comparisons between deliberate tracer experiments and $^{35}SO_4$ support the assumption that mixing of recharge water with older groundwater was not a significant factor; however, mixing scenarios should be investigated at other MAR sites as it will affect calculated travel times.

Careful characterization of the input function is important when determining the feasibility of using $^{35}SO_4$ as a natural tracer, especially for sites that incorporate significant

91

fractions of recycled water. Because $^{35}SO_4$ activity in MAR waters can vary significantly by season due to seasonal differences in recharge and well production, time series with a frequency of at least 1 month are recommended for the source water.

Unlike deliberate tracer studies that are dependent on the hydrologic conditions during the injection period (typically a few days to a few weeks), the $^{35}SO_4$ intrinsic tracer method is applied over a longer time period during each recharge season. If the $^{35}SO_4$ end-member is constrained for each season, the effect of varying recharge and pumping conditions on subsurface travel time can be quantified more easily by the $^{35}SO_4$ method than by conducting multiple deliberate tracer experiments.

$^{35}SO_4$ is underutilized as an intrinsic tracer technique in groundwater studies, and it can be a valuable tool in investigating the subsurface travel times on less than one year timescales at MAR sites where $^{35}SO_4$ activity is significantly above the detection limit.

V. Summary

Quantifying groundwater recharge and transport on short timescales of less than two years advances our knowledge of groundwater recharge mechanisms and storage capacities. This work demonstrates that $^{35}SO_4$ is a useful but underutilized tracer that can provide valuable insights into groundwater recharge mechanisms by resolving one-year timescales that cannot be achieved by common intrinsic tracer methods such as tritium/helium3 or dissolved noble gases.

Due to the inability of established techniques to analyze waters with moderate to high concentrations of SO_4, previous hydrologic studies utilizing $^{35}SO_4$ were limited to high-elevation basins and low-SO_4 waters. The new analytical method presented in Chapter II significantly advances measurement of naturally-occurring $^{35}SO_4$ in natural waters. The $^{35}SO_4$ method developed in Chapter II improved detection limits for low-SO_4 waters and expanded the analytical range of ^{35}S to high-SO_4 waters, allowing the technique to be applied to a wider range of environmental samples.

In the Sierra Nevada study (Chapter III), $^{35}SO_4$ in Sagehen Creek Basin and Martis Valley Groundwater Basin indicated significant annual groundwater recharge from snowmelt, and that recent (<1 year old) snowmelt represents only a small fraction of the larger aquifer system. The study suggests that as snowpack in the western U.S. continues to decline due to climate change, impacts to streamflow and springs may occur over two phases: 1) rapid responses in discharge due to annual variability in precipitation, and 2) more gradual, long-term declines in discharge in response to declining groundwater recharge. Using $^{35}SO_4$ in evaluating the vulnerability of water resources under a changing

climate shows the value of the technique. The data provided by $^{35}SO_4$ studies may be useful for advancing surface/ground water numerical models in watersheds.

In the MAR study (Chapter IV), $^{35}SO_4$ was successfully measured in high-SO_4 source waters and groundwater at two southern California MAR facilities, and calculated $^{35}SO_4$ groundwater travel times were reasonable at both study sites compared to earlier deliberate tracer experiments, which are considered by regulators as the preferred method for establishing compliance with the GRRP rules. The successful application of $^{35}SO_4$ method in high-SO_4 MAR systems was possible due to increased sample loading capacity and improved detection limits for ^{35}S; however, careful characterization of the $^{35}SO_4$ activity in source waters is recommended, especially if a significant component of source water is reclaimed water or imported water that has aged for than one year. The results highlight the value of ^{35}S in quantifying groundwater residence times on one-year timescales, and therefore it is a powerful new technique available to hydrologists, modelers, and water resource managers.

Future $^{35}SO_4$ studies in low-SO_4 systems, such as the Sierra Nevada, would benefit from the development of an *in-situ* sampler capable of processing large volumes of water in the field to increase $^{35}SO_4$ recovery and processing efficiency. Collecting and analyzing more $^{35}SO_4$ would improve ^{35}S counting statistics by reducing the minimal detectable activity and counting error, leading to a significant improvement in the capability to detect recent recharge in groundwater systems.

References

Avisar D, Clark JF. 2005. Evaluating travel times beneath an artificial recharge pond using sulfur hexafluoride. *Environmental & Engineering Geoscience* **11**: 309-317.

Böhlke JK, Michel RL. 2009. Contrasting residence times and fluxes of water and sulfate in two small forested watersheds in Virginia, USA. *Science of the Total Environment* **407**: 4363-4377.

Brost RA, Feichter J, Heimann M. 1991. Three-dimensional simulation of [7]Be in a global climate model. *Journal of Geophysical Research: Atmospheres* **96**: 22423-22445.

Brothers LA, Dominguez G, Abramian A, Corbin A, Bluen B, Thiemens MH. 2010. Optimized low-level liquid scintillation spectroscopy of ^{35}S for atmospheric and biogeochemical. *PNAS* **107**: 5311-5316.

Brumm M, Wang CY, Manga M. 2009. Spring temperatures in the Sagehen Basin, Sierra Nevada, CA: implications for heat flow and groundwater circulation. *Geofluids* **9**: 195-207.

Busenberg, E., and L. N. Plummer (1992), Use of chlorofluoromethanes (CCl_3F and CCl_2F_2) as hydrologic tracers and age-dating tools: Example-The alluvium and terrace system of Central Oklahoma. *Water Resources Research* **28**: 2257–2283.

Busenberg, E., and L. N. Plummer (2000), Dating young groundwater with sulfur hexafluoride-Natural and anthropogenic sources of sulfur hexa-fluoride. *Water Resources Research* **36**: 3011–3030.

California Department of Water Resources, 2006. Martis Valley Groundwater Basin. http://www.water.ca.gov/pubs/groundwater/bulletin_118/basindescriptions/6-67.pdf (accessed Jun 2014).

—. 2014. Public Update for Drought Response: Groundwater Basins with Potential Water Shortages and Gaps in Groundwater Monitoring. http://www.water.ca.gov/waterconditions/docs/Drought_Response-Groundwater_Basins_April30_Final_BC.pdf (accessed Jan 2015).

—. 2015. California's Groundwater Update 2013: A Compilation of Enhanced Content for California Water Plan Update 2013. http://www.waterplan.water.ca.gov/topics/groundwater/index.cfm (accessed Jun 2015).

California Division of Drinking Water. 2015. DPH-14-003E Groundwater Replenishment Using Recycled Water; California State Water Resources Control Board, Division of Drinking Water: Sacramento, CA. http://www.cdph.ca.gov/services/DPOPP/regs/Pages/DPH14-003EGroundwaterReplenishmentUsingRecycledWater.aspx (accessed Sep 2015).

Chao TT, Harward ME, Fang SC. 1964. Iron or aluminum coatings in relation to sulfate adsorption characteristics of soils. *Soil Science Society of America Journal* **28**: 632-635.

Chorover J, Vitousek PM, Everson DA, Esperanza AE, Turner D. 1994. Solution chemistry profiles of mixed-conifer forests before and after fire. *Biogeochemistry* **26**: 115-144.

Clark ID, Fritz P. 1997. Environmental isotopes in hydrogeology, CRC Press/Lewis Publishers, Boca Raton, FL, 328 pp.

Clark JF, Hudson GB, Davisson ML, Woodside G, Herndon R. 2004. Geochemical imaging of flow near an artificial recharge facility, Orange County, CA. *Ground Water* **42**: 167-174.

Clark JF, Hudson GB, Davisson ML, Avisar D. 2005. Gas transport below artificial recharge ponds: Insights from dissolved noble gases and a dual gas (SF_6 and ^3He) tracer experiment. *Environmental Science and Technology* **39**: 3939-3945.

Clark JF. 2011. The 2010 Rio Hondo Tracer Experiment; Final Project Report; Water Replenishment District; Lakewood, CA.

Clark JF, Morrissey S, Dadakis J, Hutchinson A, Herndon R. 2014. Investigation of groundwater flow variations near a spreading pond with repeat deliberate tracer experiments. *Water* **6**: 1826-1839.

Cook PG, Herczeg AL. 2000. Environmental Tracers in Subsurface Hydrology, Kluwer Academic Publishers, Boston, MA, 529 pp.

Cooper LW, Olsen CR, Solomon DK, Larsen IL, Cook RB, Grebmeier JM. 1991. Stable isotopes of oxygen and natural and fallout radionuclides used for tracing runoff during snowmelt in an Arctic watershed. *Water Resources Research* **27**: 2171-2179.

Davis SN, Campbell DJ, Bentley HW, Flynn TJ. 1980. Ground-water tracers-A short review. *Ground Water* **18**:14-23.

DeRubeis E. 2013. Radon as a tracer of groundwater-surface water interaction in Martis Valley. Master's Thesis. California State University, East Bay.

Drewes JE, Heberer T, Rauch T, Reddersen K. 2003. Fate of pharmaceuticals during groundwater recharge. *Groundwater Monitoring & Remediation* **23**: 64-72.

Earman S, Campbell AR, Newman BD, Phillips FM. 2006. Isotopic exchange between snow and atmospheric water vapor: Estimation of the snowmelt component of groundwater recharge in the southwestern United States. *Journal of Geophysical Research* **111**: D09302.

Earman S, Dettinger M. 2011. Potential impacts of climate change on groundwater resources- A global review. *Journal of Water and Climate Change* **2**: 213-229.

Earman S, Clark J, Manning A, Pool D, Urióstegui S. 2015. Investigation of methods of potential value to monitor groundwater recharge in the mountains of California. Desert Research Institute Report.

Ekwurzel B, Schlosser P, Smethie Jr. WM, Plummer LN, Busenburg E, Michel RL, Weppernig R, Stute M. 1994. Dating of shallow groundwater: comparison of the transient tracers $^3H/^3He$, chlorofluorocarbons, and ^{85}Kr. *Water Resources Research* **30**: 1693-1708.

Engdahl NB, Maxwell RM. 2015. Quantifying changes in age distributions and the hydrologic balance of a high-mountain watershed from climate induced variations in recharge. *Journal of Hydrology* **522**: 152-162.

Feely HW, Larsen RJ, Sanderson, CG. 1989. Factors that cause seasonal variations in Beryllium-7 concentrations in surface air. *Journal of Environmental Radioactivity* **9**: 223-249.

Fox PK, Makam R. 2009. Surface area and travel time relationships in aquifer treatment systems. *Water Environment Research* **81**: 2337-2343.

Fox PK, Narayanaswamy A, Genz, A, Drewes JE. 2001. Water quality transformations during soil aquifer treatment at the Mesa Northwest Water Reclamation Plant, USA. *Water Science &Technology* **43**: 343-350.

Frisbee MD, Phillips FM, Campbell AR, Liu F, Sanchez SA. 2011. Streamflow generation in a large, alpine watershed in the southern Rocky Mountains of Colorado: Is streamflow generation simply the aggregation of hillslope runoff responses? *Water Resources Research* **47**: W06512.

Gamlin JD, Clark JF, Woodside G, Herndon R. 2001. Large-scale tracing of ground water with sulfur hexafluoride. *Journal of Environmental Engineering* **127**: 171-174.

Genereux DP, Hooper RP. 1998. Oxygen and hydrogen isotopes in rainfall-runoff studies: in Isotope Tracers in Catchment Hydrology (Kendall C, McDonnell JJ, eds), Elsevier Science, Amsterdam, p. 319-346.

Glynn PD, Plummer LN. 2005. Geochemistry and the understanding of ground-water systems. *Hydrogeology Journal* **13**: 263-287.

Hamlet AF, Mote PW, Clark MP, Lettenmaier DP. 2005. Effects of temperature and precipitation variability on snowpack trends in the western United States. *Journal of Climate* **18**: 4545–4561.

Heard AM, Sickman JO, Rose NL, Bennett DM, Lucero DM, Melack JM, Curtis JH. 2014. 20th century atmospheric deposition and acidification trends in lakes of Sierra Nevada, California, USA. *Environmental Science and Technology* **48**: 10054-10061.

Hiscock KM, Grischeck T. 2002. Attenuation of groundwater pollution by bank filtration. *Journal of Hydrology* **266**: 139-144.

Holmbeck-Pelham SA, Rasmussen TC, Fowler LA. 2000. Regulation of injected ground water tracers. *Ground Water* **38**: 541-549.

Hong Y, Kim G. 2005. Measurement of cosmogenic ^{35}S activity in rainwater and lake water. *Analytical Chemistry* **77**: 3390-3393.

Huntington JL, Niswonger RG. 2012. Role of surface-water and groundwater interactions on projected summertime streamflow in snow dominated regions: An integrated modeling approach. *Water Resources Research* **48**: W11524.

Hutchinson AS. 2013. 2011-12 Report on Groundwater Recharge in the Orange County Groundwater Basin; Orange County Water District: Fountain Valley, CA.

Knowles N, Dettinger MD, Cayan DR. 2006. Trends in snowfall versus rainfall in the western United States. *Journal of Climate* **19**: 4545-4559.

LACDPW., 2013. Water conserved information; Los Angeles County Department of Public Works. http://ladpw.org/wrd/spreadingground/watercon/ (accessed Aug 2013).

Lal D, Peters B. 1967. Cosmic ray produced radioactivity on the Earth. In *Handbuch der Physik*, Sittle K (ed): Springer, Berlin, p. 551–612.

Laws BV, Dickensen ERV, Johnson TA, Snyder SA, Drewes JE. 2011. Attenuation of contaminants of emerging concern during surface-spreading aquifer recharge. *Science of the Total Environment* **409**: 1087-1094.

Likens GE, Herbert Borman F, Hedin LO, Driscoll CT, Eaton JS. 1990. Dry deposition of sulfur: a 23-year record for the Hubbard Brook Forest ecosystem. *Tellus* **42:B**: 319-329.

Liu FJ, Williams MW, Caine N. 2004. Source waters and flow paths in an alpine catchment, Colorado Front Range, United States. *Water Resources Research* **40**: W09401

Manning AH, Solomon DK. 2005. An integrated environmental tracer approach to characterizing groundwater circulation in a mountain block. *Water Resources Research* **41**: W12412.

Manning AH, Solomon DK, Thiros SA. 2005. ^{3}H/^{3}He age data in assessing the susceptibility of wells to contamination. *Ground Water* **43**: 353-367.

Manning AH, Caine JS. 2007. Groundwater noble gas, age, and temperature signatures in an alpine watershed: Valuable tools in conceptual model development. *Water Resources Research* **43**:W04404.

Manning AH, Clark JF, Diaz SH, Rademacher LK, Earman S, Plummer LN. 2012. Evolution of groundwater age in a mountain watershed over a period of thirteen years. *Journal of Hydrology* **460**: 13-28.

Markstrom SL, Niswonger RG, Regan RS, Prudic DE, Barlow PM. 2008. GSFLOW— Coupled ground-water and surface-water flow model based on the integration of the Precipitation-Runoff Modeling System (PRMS) and the Modular Ground-Water Flow Model (MODFLOW-2005): U.S. Geological Survey Techniques and Methods 6-D1; 1-240.

Massmann G, Sultenfuss J, Dunnbier U, Knappe A, Taute T, Pekdeger A. 2008. Investigation of groundwater a residence times during bank filtration in Berlin: Multi-tracer approach. *Hydrological Processes* **22**: 788–801.

McDermott JA, Avisar D., Johnson T, Clark JF. 2008. Groundwater travel times near spreading ponds: Inferences from geochemical and physical approaches. *Journal of Hydrologic Engineering* **13**: 1021-1028.

Meixner T, Brown A, Bales RC. 1998. Importance of biogeochemical processes in modeling streams in two watersheds in the Sierra Nevada, California. *Water Resources Research* **34**: 3121-3133.

Michel RL, Campbell D, Clow D, Turk JT. 2000. Timescales for migration of atmospherically derived sulphate through an alpine/subalpine watershed, Loch Vale, Colorado. *Water Resources Research* **36**: 27-36.

Michel RL, Turk JT, Campbell DH, Mast MA. 2002. Use of natural ^{35}S to trace sulphate cycling in small lakes, Flattops Wilderness Area, Colorado, U.S.A. *Water, Air, and Soil Pollution: Focus* **2**: 15-18.

Moran JE, Halliwell MS. 2003. Characterizing Groundwater Recharge: A comprehensive Isotopic Approach. American Water Works Association Research Foundation Report 90941, pp. 199.

Mote PW. 2003. Trends in snow water equivalent in the Pacific Northwest and their climatic causes. *Geophysical Research Letters* **30**: 1601.

Mote PW, Hamlet AF, Clark MP, Lettenmaier DP. 2005. Declining mountain snowpack in western North America. *Bulletin of the American Meteorological Society* **86**: 39-49.

Novak M, Michel RL, Prechova E, Stepanova M. 2004. The missing flux in a ^{35}S budget for the soils of a small polluted catchment. *Water, Air, and Soil Pollution: Focus* **4**: 517-529.

Parfitt RL. 1978. Anion adsorption by soils and soil materials. *Advances in Agronomy* **30**: 1-50.

PerkinElmer. 2014. Application note: Liquid scintillation- Counting aquaous samples by LSC.

Phillips F, Castro M. 2003. Groundwater dating and residence-time measurements.: in Treatise on Geochemistry (Holland HD, Turekian KK, eds.), Vol. 5, Surface and Ground Water, Weathering, and Soils (Drever JI, ed.), Oxford University Press, Oxford, p. 451-497.

Plaff JD. 1993. Method 300.3: Determination of inorganic anions by ion chromatography; Technical Report Number; EMSL, Office of Research and Development; U.S. Environmental Protection Agency: Cincinnati, OH.

Plummer LN, Busenberg E, Bohlke JK, Nelms DL, Michel RL, Schlosser P. 2001. Groundwater residence times in Shenandoah National Park, Blue Ridge Mountains, Virginia, USA: A multi-tracer approach. *Chemical Geology* **179**: 93-111.

Priyadarshi A, Hill-Falkenthal J, Thiemens M, Zhang Z, Lin M, Chan C, Kang S. 2014. *Journal of Geophysical Research: Atmospheres* **119**: 4125-4135.

Quast KW, Lansey K, Arnold R, Bassett RL, Rincon M. 2006. Boron isotopes as an artificial tracer. *Ground Water* **44**: 453-466.

Rademacher LK, Clark JF, Hudson GB, Erman DC, Erman NA. 2001. Chemical evolution of shallow groundwater as recorded by springs, Sagehen basin; Nevada County, California. *Chemical Geology* **179**: 37-57.

Rademacher LK, Clark JF, Clow DW, Hudson GB. 2005. Old groundwater influence on stream hydrochemistry and catchment response times in a small Sierra Nevada catchment: Sagehen Creek, California. *Water Resources Research* **41**: W02004.

Reid SE, Mackinnon PA, Elliot T. 2007. Direct measurements of reaeration rates using noble gas tracers in River Lagan, Northern Ireland. *Water & Environment Journal* **21**: 182-191.

Schlosser P, Stute M, Doerr H, Sonntag C, Münnich KO. 1988. Tritium/^{3}He dating of shallow groundwater. *Earth and Planetary Science Letters* **89**:353-362.

Segal DC, Moran JE, Visser A, Singleton MJ, Esser BK. 2014. Seasonal variation of high elevation groundwater recharge as indicator of climate response. *Journal of Hydrology* **519**: 3129-3141.

Shanley JB, Mayer B, Mitchell MJ, Michel RL, Bailey SW, Kendall C. 2005. Tracing sources of streamwater sulfate during snowmelt using S and O isotope ratios of sulfate and ^{35}S activity. *Biogeochemistry* **76**: 161-185.

Singleton MJ, Moran JE. 2010. Dissolved noble gas and isotopic tracers reveal vulnerability of groundwater in a small, high-elevation catchment to predicted climate changes. *Water Resources Research* **46**: 1-18.

Singleton MJ, Moran JE, Visser A, Urióstegui SH, Segal DC, DeRubeis E, Esser BK. 2014 California GAMA Special Study: Climate Change Impacts to Recharge in a High-Elevation Groundwater Basin, Lawrence Livermore National Laboratory LLNL-TR-548931.

Stute M, Zheng Y, Schlosser P, Horneman A, Dhar RK, Datta S, Hoque MA, Seddique AA, Shamsudduha M, Ahmed KM, van Geen A. 2007. Hydrological control of As concentrations in Bangladesh groundwater. *Water Resources Research* **43**: W09417.

Sueker JK, Turk JT, Michel RL. 1999. Use of cosmogenic ^{35}S for comparing ages of water from three alpine-subalpine basins in the Colorado Front Range. *Geomorphology* **27**: 61-74.

Sylvester AG. 2008. Geology of the Sagehen Creek and Independence Lake Hydrologic Basins, Sierra and Nevada Counties, California. http://www.geol.ucsb.edu/projects/tahoe/Sagehen/welcomeSage.html (accessed January 2012).

Tague C, Peng H. 2013. The sensitivity of forest water use to the timing of precipitation and snowmelt recharge in the California Sierra: Implications for a warming climate. *Journal of Geophysical Research: Biogeosciences* **118**: 875-887.

Tanaka N, Turekian KK. 1991. Use of cosmogenic ^{35}S to determine the rates of removal of atmospheric SO_2. *Nature* **352**: 226-228.

Urióstegui SH, Bibby RK, Esser BK, Clark JF. 2015. Analytical method for measuring ^{35}S in natural waters. *Analytical Chemistry* **87**:6064-6070.

Urióstegui SH, Bibby RK, Esser BK, Clark JF. In Reveiw. Quantifying annual groundwater recharge and storage in the central Sierra Nevada using naturally-occurring [35]S.

Visser A, Singleton M, Hillegonds D, Velsko C, Moran JE, Esser BK. 2013. California GAMA Special Study: Rapid, Low-Cost Noble Gas Tracer Monitoring to Determine Travel Times at Recharge Operations. Lawrence Livermore National Laboratory LLNL-TR-534291, p. 40.

Viviroli D, Archer DR, Buytaert W, Fowler HJ, Greenwood GB, Hamlet AF, Huang Y, Koboltschnig G, Litaor MI, López-Moreno JI, Lorentz S, Schädler B, Schwaiger K, Vuille M, Woods R. 2011. Climate change and mountain water resources: overview and recommendations for research, management and policy. *Hydrology and Earth System Sciences* **15**: 471–504.

Wanninkhof R, Asher W, Weppernig R, Chen H, Schlosser P, Langdon C, Sambrotto R. 1993. Gas transfer experiment on Georges Bank using two volatile deliberate tracers. *Journal of Geophysical Research* **98**: 237-248.

Williams MW, Melack, JM. 1991. Precipitation chemistry in and ionic loading to an alpine basin, Sierra Nevada. *Water Resources Research* **27**: 1563-1574.

Williams MW, Brown AD, Melack JM. 1993. Geochemical and hydrologic controls on the composition of surface water in a high-elevation basin, Sierra Nevada, California. *Limnology and Oceanography* **38**: 775-797.

Williams MR, Melack JM. 1997. Atmospheric deposition, mass balances, and processes regulating streamwater solute concentrations in mixed-conifer catchments of the Sierra Nevada, California. *Biogeochemistry* **37**: 111-144.

Williams MR, Leydecker A, Brown AD, Melack JM. 2001. Processes regulating the solute concentration of snowmelt runoff in two subalpine catchments of the Sierra Nevada, California. *Water Resources Research* **37**: 1993-2008.

Winograd IJ, Riggs AC, Coplen TB. 1998. The relative contributions of summer and cool-season precipitation to groundwater recharge, Spring Mountains, Nevada, USA, *Hydrogeology Journal* **6**: 77–93.

WRD, 2015. Engineering Survey and Report, 2015; Water Replenishment District: Lakewood, CA, 2015. http://www.wrd.org/WRD_ESR_Final_Report_March_5_2015.pdf (accessed Aug 2015).

Yates MV, Yates SR. 1987. A comparison of geostatistical methods for estimating virus inactivation rates in ground water. *Water Research* **21**: 1119-1125.

Appendix A. Sulfate Mass Balance for Sagehen Creek Basin

Previous studies in the southern Sierra Nevada reported terrestrial neutralization of acidity present in precipitation, with solute mass balances indicating that terrestrial processes uptake atmospherically derived N and S (Williams and Melack, 1997). To determine the potential extent of biogeochemical cycling of SO_4^{2-} in this region, a simplified quantitative mass balance of SO_4^{2-} was performed for Sagehen Creek Basin (SCB).

Monthly SO_4^{2-} concentrations in wet deposition were available beginning in Water Year (WY) 2002 from a National Atmospheric Deposition Program (NADP) collection site CA-50 located near snow site S02 (see Figure 8A). Precipitation-weighted mean SO_4^{2-} concentrations for wet deposition varied between 0.01 and 1.59 mg/L, with a logarithmic curve being the best fit for the data (Figure 22). While no correlation was observed between SO_4^{2-} concentration and total precipitation (Figure 23), the higher SO_4^{2-} concentrations ($\geq$ 0.25 mg/L) occurred during months having monthly precipitation totals of < 20 cm, indicating a general dilution of SO_4^{2-} concentrations with increasing storm size.

Dry deposition has been identified as an important component of total S deposition in the Sierra Nevada and other high-elevation basins, supplying about 37% of the total S input (Williams and Melack, 1997; Likens *et al*., 1990). The average annual input of SO_4^{2-} derived from wet deposition was 1.86 x 10^2 kg, with the estimated bulk annual input of SO_4^{2-} being 2.55 x 10^2 kg when corrected for the contribution of dry deposition (Figure 24).

Sagehen Creek is the main tributary in SCB. Sulfate concentrations in Sagehen Creek water were measured by the USGS once or twice a month over a nine-year period (WY2006 to WY2014) from a sampling location near the USGS stream gauge at the base of the basin (see Figure 8A). Stream SO_4^{2-} concentrations were between 0.03 and 0.30 mg/L (Figure 25),

which is similar to the range of SO_4^{2-} concentrations for the majority of precipitation samples collected during WY2002 to WY2014. These results provide further evidence that minimum attenuation of SO_4^{2-} by adsorption-desorption is occurring in the basin, and that weathering of SO_4^{2-} minerals is minimal. Monthly SO_4^{2-} concentrations were stable throughout the water year; however, small pulses of higher-concentration SO_4^{2-} water in the stream ($\geq$0.2 mg/L) were observed during the early winter for WY2009 and WY2010, which may be due to solutes in snowpack becoming more concentrated during the melt season.

Average annual SO_4^{2-} output from the basin via Sagehen Creek was 5.80×10^2 kg (Figure 24), which suggests that more SO_4^{2-} is leaving SCB than is deposited on year to year basis. A possible explanation for the net export observed for WY2006 to WY2014 is an increase in SO_4^{2-} deposition in previous decades that is not captured in the short, twelve-year record examined in this simplified mass balance. For example, Heard *et al*. (2014) reported declining SO_4^{2-} concentrations in Sierra Nevada Lakes beginning in the early 1980s, which the authors attributed to emission reductions and lower SO_4^{2-} loading resulting from air quality regulations. A record of SO_4^{2-} deposition from 1982 to 2015 at the central Sierra Nevada NADP site CA-99 located in Yosemite Valley also revealed generally higher SO_4^{2-} concentrations from 1982 to 2006 compared to 2007 to 2015 (Figure 26). In SCB, apparent groundwater ages of springs ranged from <2 to 36 years (Rademacher *et al*., 2001; Manning *et al*., 2012), and the $^{35}SO_4^{2-}$ study described in Chapter III found that stream water is mainly derived from groundwater older than one year, indicating that groundwater flowpaths contributing to stream discharge may be derived from groundwater recharged prior to 2007. This older water with higher SO_4^{2-} loads could contribute to the overall net export of SO_4^{2-} from SCB.

In addition to net SO_4^{2-} export being potentially derived from SO_4^{2-} deposited in previous decades, organic matter mineralization may also contribute to the overall net export of SO_4^{2-}. Even after correcting for dry deposition, the mean input due to deposition is less than 45% of the export by the creek indicating that there must be another source of SO_4^{2-} within SCB.

While a net export of SO_4^{2-} may indicate minimal retention and immobilization of SO_4^{2-}, constraining the biogeochemical cycling SO_4^{2-} requires additional data such as stable isotopic analysis of SO_4 ($^{34}SO_4/^{32}SO_4$). To accurately quantify the extent of SO_4^{2-} immobilization by microbial processes and vegetation, stable isotopic composition of S in snowpack, groundwater, stream water, and vegetation would be valuable in future studies.
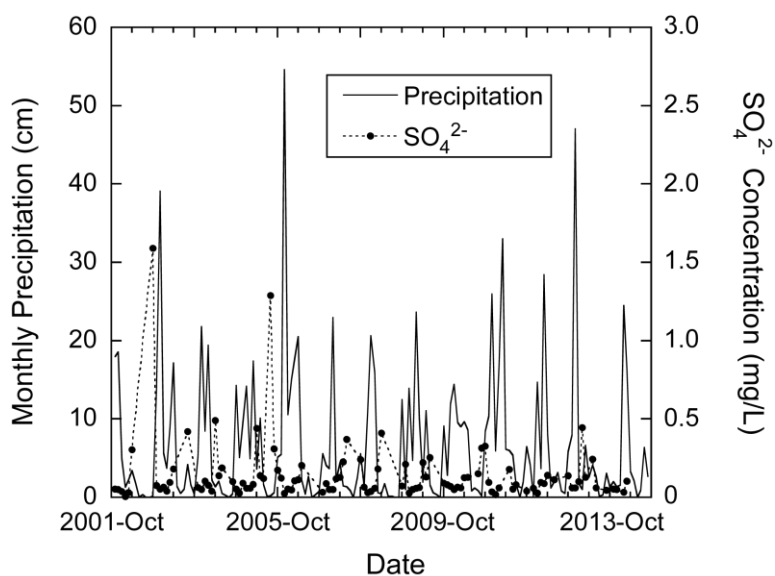

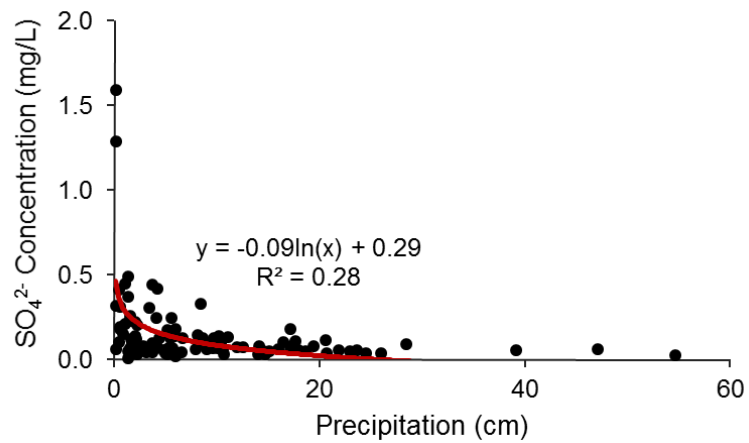**Figure 22.** Monthly precipitation totals and volume-weighted mean SO_4^{2-} concentration in precipitation for SCB from WY2002 to WY2014. Data source: NADP (http://nadp.isws.illinois.edu/data/sites/siteDetails.aspx?net=NTN&id=CA50).

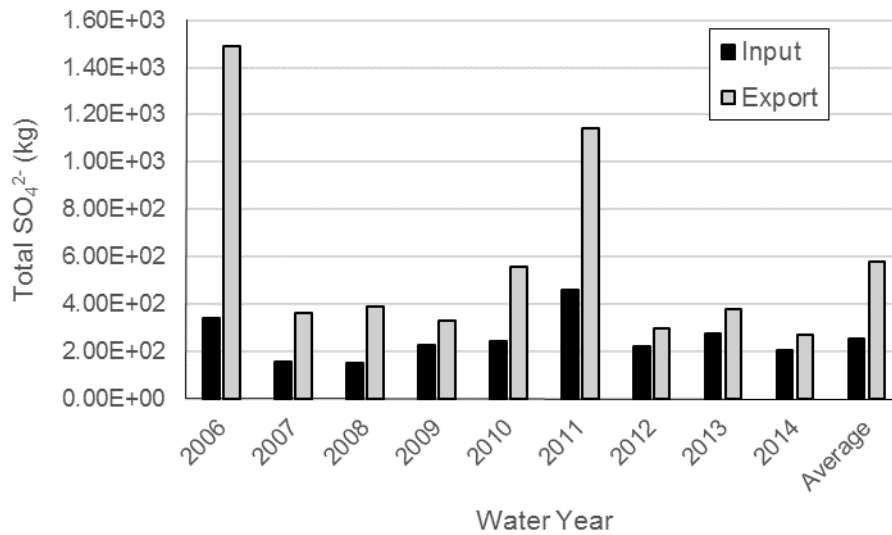**Figure 23.** Precipitation-weighted mean SO_4^{2-} concentration versus precipitation totals.

Figure 24. Annual input and export of SO_4^{2-} for WY 2006 to 2014. Input values are based on the bulk (wet + dry) deposition of SO_4^{2-}.
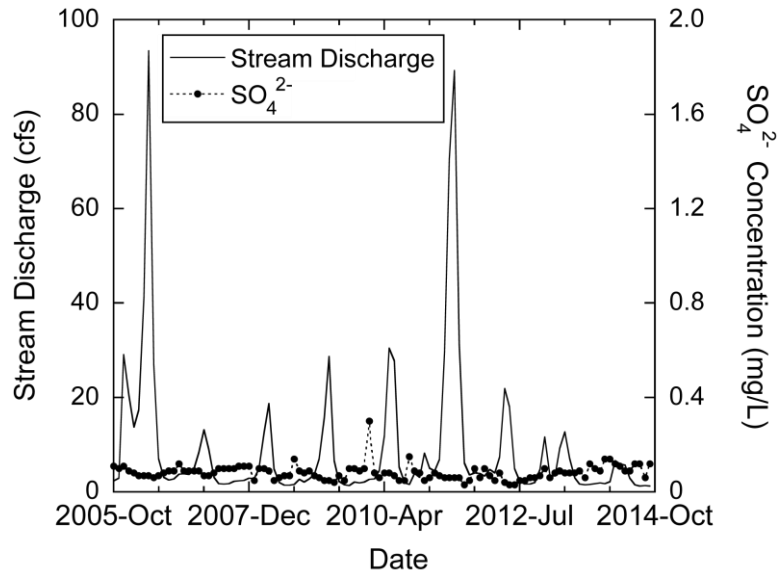
Figure 25. Time series of Sagehen Creek stream discharge and SO_4^{2-} concentration. Data source: US Geological Survey National Water Information System (http://waterdata.usgs.gov/ca/nwis/inventory/?site_no=10343500&agency_cd=USGS).
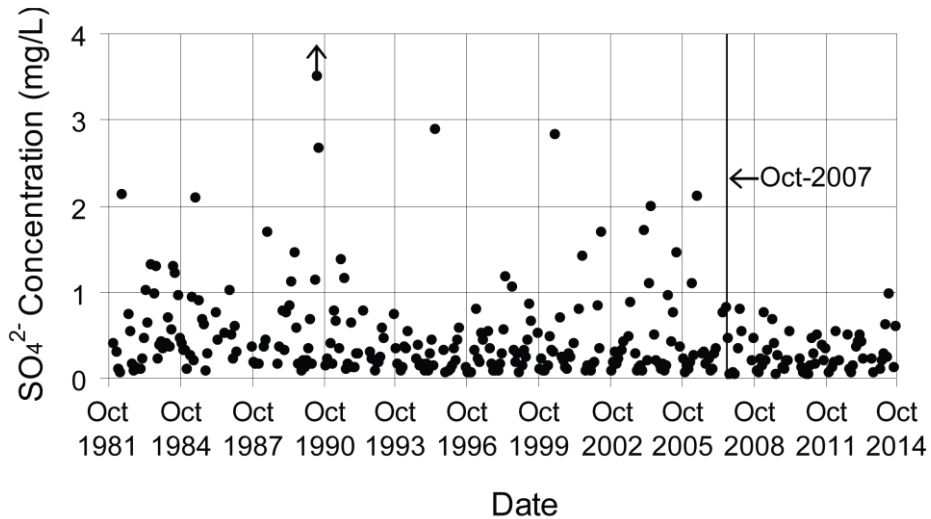

Figure 26. Monthly precipitation-weighted mean SO_4^{2-} concentration for NAPD site CA-99 in Yosemite Valley. The sample plotted with a vertical arrow is 14.1 mg/L. Data source: NADP (http://nadp.sws.uiuc.edu/data/sites/siteDetails.aspx?net=NTN&id=CA99).

105